Theses and Dissertations   Student Graduate Works

3-21-2013

An Inverse Kinematic Approach Using Groebner Basis Theory Applied to Gait Cycle Analysis

Anum Barki

Follow this and additional works at: https://scholar.afit.edu/etd

Part of the Optics Commons

AN INVERSE KINEMATIC APPROACH
USING GROEBNER BASIS THEORY
APPLIED TO GAIT CYCLE ANALYSIS

THESIS

Anum Barki

AFIT-ENP-13-M-02

DEPARTMENT OF THE AIR FORCE
AIR UNIVERSITY

AIR FORCE INSTITUTE OF TECHNOLOGY

Wright-Patterson Air Force Base, Ohio

AFIT-ENP-13-M-02

AN INVERSE KINEMATIC APPROACH USING GROEBNER BASIS THEORY

APPLIED TO GAIT CYCLE ANALYSIS

THESIS

Presented to the Faculty

Department of Engineering Physics

Graduate School of Engineering and Management

Air Force Institute of Technology

Air University

Air Education and Training Command

in Partial Fulfillment of the Requirements for the

Degree of Master of Science in Optical Science and Engineering

Anum Barki, BS

March 2013

AFIT-ENP-13-M-02

AN INVERSE KINEMATIC APPROACH USING GROEBNER BASIS THEORY

APPLIED TO GAIT CYCLE ANALYSIS

Anum Barki, BS

Approved:

_____   _____
Dr. Ronald F. Tuttle (Chairman)   Date

_____   _____
Dr. Kimberly Kendricks (Member)   Date

_____   _____
Lt Col Brian McBee (Member)   Date

_____   _____
Dr. Amy Magnus (Member)   Date

AFIT-ENP-13-M-02

Abstract

This research highlights the results obtained from applying the method of inverse kinematics, using Groebner basis theory, to the lower limbs of a human gait cycle to extract and identify gait signatures. Kinematics of the human body has been researched for a long time for clinical studies, sports, and human recognition. Over the years, human recognition has become an important task in applications such as security and surveillance. Studies in the past have shown that gait signatures can be extracted out of video and be used to identify individuals. The force protection issues of today, such as attacks by suicide bombers against military and civilian groups, have motivated a team at AFIT to research pattern recognition in the human gait cycle to identify an individual carrying a concealed load on his or her body. The research program called INSPIRE (Integration of a Sensor Package for Identifying Radical Extremists) set as its goal to identify gait signatures of human subjects and distinguish between subjects carrying a concealed load to those subjects without a load. This thesis focuses on studying the human gait cycle as well as methods used in identifying gait signatures. The main objective hearin is to model the movement of the lower extremities based on motion captured observations, in particular, foot placement and the joint angles for subjects affected by carrying extra load on the body. A method of inverse kinematics using Groebner basis theory is developed to a model of the lower extremities in order to determine all the solutions of the joint angles, given the position and orientation of the foot. The human gait cycle is captured and analyzed using an advanced optical VICON Motion capture system (passive infrared). The results obtained help build the gait database and augment INSPIRE algorithms to include a four degree of freedom model of the lower extremities.

iv

I dedicate my work and give special thanks to my lovely parents and my dear brother. Their unconditional support and love has really been appreciated throughout this research effort and I am grateful to have such a loving and caring family. I must also thank my wonderful friends who have given me their fullest support for the last few years.

Acknowledgements

I would like to express my sincere appreciation to my faculty advisor, Dr. Ronald Tuttle, for his guidance and support throughout the course of this thesis effort. The insight and experience was certainly appreciated. I would also like to thank my sponsor from the Signature Support Program for both the support and latitude provided to me in this endeavor. Furthermore, I thank my committee members, Dr. Kimberly Kendricks of Central State University for steering me to this project and seeing me through as well as Dr. Amy Magnus and Lt. Col Brian McBee for their support throughout this project.

Anum Barki

Table of Contents

List of Figures

List of Tables

AN INVERSE KINEMATIC APPROACH USING GROEBNER BASIS THEORY APPLIED TO GAIT CYCLE ANALYSIS

I. Introduction

1.1   Motivation

Terror attacks, such as suicide and car bombings, are becoming an increasing threat for Middle Eastern countries and it is reported as one of the major methods of spreading terror in such countries. Not only are there increasing threats for civilians, but U.S. coalition and warfighters are also facing this problem on a daily basis. The medical journal, The Lancet [24], published a study that documented civilian casualties from suicide attacks during the Iraq War from 2003 to 2010. The study documented over thirty thousand injured civilians and over twelve thousand civilian deaths caused by suicide bomb events. It also reported deaths of 200 coalition troops of which 175 were of the United States. The Iraq Body Count (IBC) [2], an online database, also documented reported deaths of Iraqi civilians from the first day of the Iraq war. Figure 1 highlights the average number of civilian deaths per day caused by terror attacks such as car and suicide bombs. The displayed statistics show that as of December 17, 2012 an average of 7.5 civilians died each day due to these terror attacks. Statistics much like the one presented here clearly show an increased threat to civilian and military personnel from suicide attacks.

The force protection issues of today, such as suicide bombers attacking civilians, police and military assemblies, as well as national security, are the principle motivations for the Center for Technical Intelligence Studies and Research (CTISR) at Air
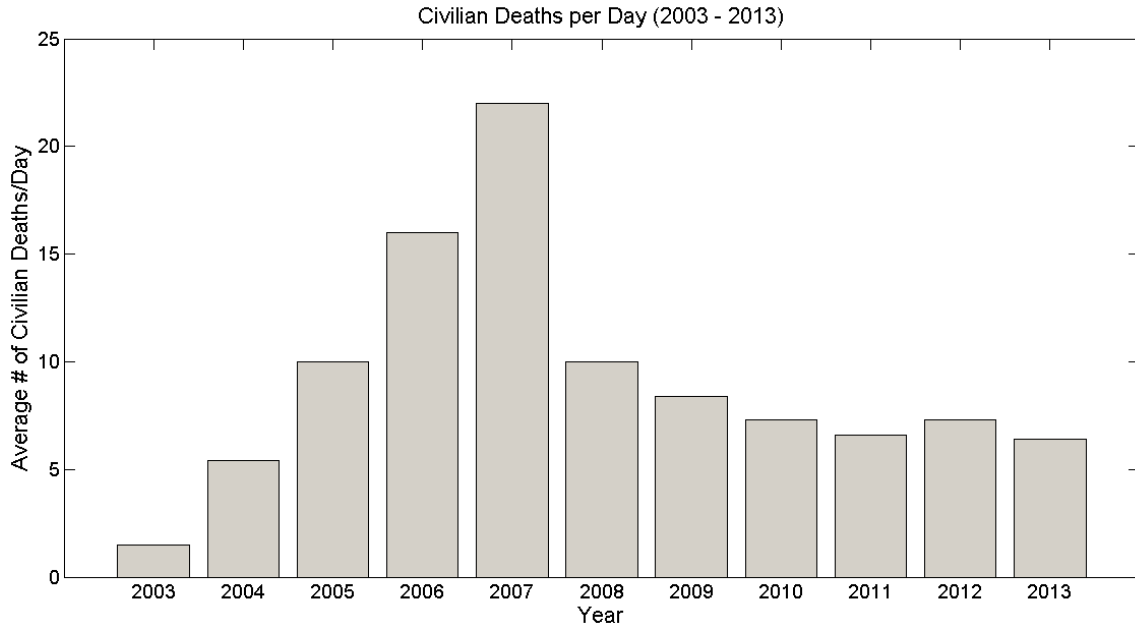
Figure 1. Civilian Deaths Caused by Car and Suicide Bombings in Iraq War. The statistics obtained show the average number of civilian deaths per day due to car bombs and suicide attacks in the Iraq War from 2003 to 2013. The graph shows an average number of 6.4 civilian deaths per day in the year of 2013.

Force Institute of Technology (AFIT) to investigate the biometrics of gait which will provide insight into the walking behavior of a potential suicide bomber.

1.2 Background

INSPIRE (Integration of a Sensor Package for Identifying Radical Extremists) is the project under which AFIT has been investigating human gait characteristics. The purpose of INSPIRE is to design a suicide bomber vetting system that is able to screen individuals 500 to 1000 feet away from a checkpoint. The goal of this project is to study human gait and its characteristics while an individual is carrying or concealing a bomb. The initial challenge of INSPIRE was to create a rich and robust database and extend the National Institute of Standards and Technology Human ID at a Distance gait program (HiD) that was started in 2000. The HiD program focused on human recognition by collecting outdoor gait data. It focused on covariate factors such

as lighting, footwear, apparel, surface conditions, and shadowing. In contrast, the INSPIRE project is to investigate gait variance and not Human ID.

INSPIRE database consists of video recordings of 100 subjects recruited from AFIT, Wright State University, University of Dayton, and Cedarville University. The database includes anatomical and demographic information of each subject such as: height, weight, race and ethnicity, measurements of lower and upper extremities, and injuries that might alter the subject's gait. The subject's gait was recorded as they walked a race track that consisted of a set of steps, catwalk, ramp and a flat grassy field as shown in Figure 2. The different parts of the race track added more gait dynamic variations, such as subjects' center of gravity, and allowed the researchers to observe the effects of different walking surfaces. The data was collected using two Canon GL2 cameras situated perpendicular to the race track and about 50 feet from the outside perimeter. A vest, weighing 3 to 5 kilograms, was used to simulate an improvised explosive device (IED) that would be worn by a potential suicide bomber. Each subject walked the circular race track four times: the first time with normal attire and no added weight or coat, the second time with the added vest and no overcoat, the third time with the vest situated around the waist along with a long overcoat to conceal the vest, and lastly with just the overcoat with no vest. Video of the volunteers navigating through the racetrack was collected and saved into the database.

Since the database was created, a number of investigations have been performed using the video recordings of the subjects. In 2012, Borel et al.[11] analyzed the existing database and investigated the lower back angle with loaded gait perturbation. From the weight distribution, 18 of the 100 subjects were chosen and back angle measurements were performed using two different approaches. The segmented videos of the subjects ascending and descending the steps as they walked with and without

Figure 2. INSPIRE Racetrack. The INSPIRE racetrack included a set of stairs, a crossover platform and a ramp. Exact location of the ramp is 28 feet from the left side of the building, 25 feet from the right side of the building, and 6 feet away from the building. The vertical dark markings, situated every 5 feet, were used for scaling purposes in the video analysis.

load were analyzed. Overcoat trials were excluded due to the low resolution of the video. The two methods, a customized MATLAB graphical user interface (GUI) and an ImageJ script, were created to calculate the lower back angle frame by frame, Figure 3. The points were drawn manually on the frame as the algorithms calculated the angles automatically. Lower back angle measurements varied from 0 to 40 degrees with respect to the horizontal. For most of the subjects, the results exhibited a greater angle in the lower back when the subjects ascended or descended the stairs without a vest. A few subjects exhibited little to no variation in back angle regardless of load and some subjects even showed a larger lower back angle while wearing a vest. Overall, the results revealed little variation in lower back angle measurement for with and without additional load. The authors concluded that due to the low image resolution, background noise, and obscuration by subject's arm no significant relationship could be determined.

Similarly, in 2010, Kendricks et al.[29] from Central State University and the team at AFIT analyzed the INSPIRE database to investigate arm and leg swing motion during the gait cycle. The goal of this analysis was to present an approach

Figure 3. MATLAB GUI and ImageJ. The MATLAB GUI (left) and the ImageJ (right) were both used to analyze the back angle and these interfaces calculated these angles for each trial frame by frame. Two vectors were drawn manually by the user and the angles between them were measured and recorded [11].

that utilizes the theory and algorithms of Groebner basis to solve for the inverse kinematic problem of the upper and lower extremity in the sagittal plane of motion. A detailed explanation on Groebner basis theory, the concepts of inverse kinematics, and sagittal plane motion follows in the theory section of this thesis. Captured video data was extracted, and developmental software was used to manually place markers on the joints of the upper and lower extremity, for a total of 100 points of the gait cycle. The joints consisted of shoulder, elbow and wrist for the upper extremity and hip, knee and ankle for lower extremity. This tool allowed the extraction of the joints' spatial coordinates at each frame. Due to low image resolution and noise in the INSPIRE race track database, supplementary VICON motion capture data was collected to analyze arm and leg swing motion. The researchers projected the motion of a linked structure, with three degrees of freedom (DOF), on the *(x,y)*-Cartesian coordinate plane as shown in Figure 4. In robotics and mechanics, DOF is defined as a combination of joint link pairs that define the configuration of a robotic system. In this orientation, a kinematic model was derived that demonstrated the motion of the upper and lower extremity. Using geometric analysis, kinematic equations were

5
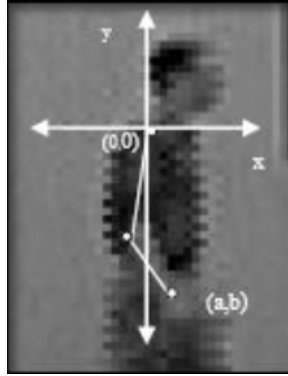
Figure 4. Upper Extremity Projection onto (x,y)-Plane. The upper extremity joints, including shoulder, elbow and wrist, were projected onto an (x,y)-Cartesian coordinate plane to analyze the motion of the linked structure contained 3 DOF. A kinematic model was then derived that demonstrated the motion of the upper extremity in the two dimensional sagittal plane of motion. This 3 DOF model could also be used for the lower extremity [29].

derived and Groebner basis algorithms were applied to analyze possible movements at each joint. The modeled equations were then applied to the captured spatial coordinates from each frame. The resulting model allowed the team to analyze wrist placement and the joint angles that constitute that motion in a normal gait and make comparisons with load bearing gait motion.

Kendricks et al.[30] then furthered their studies and focused on looking at flexion and extension angles of shoulder in 100 points of the gait cycle. The researchers conducted gait analysis on seven human subjects, ages 20-26 years of age, walking at their normal comfortable speed. Static and dynamic motion was captured using a 6-camera Motion Analysis system by Motion Analysis Corporation. The system allowed for extraction of spatial coordinates at the joint centers and the researchers were able to apply their two dimensional kinematic model derived from prior research discussed previously [29],[40]. The angles predicted varied from actual joint angle measurements with an average error or 23%. The authors concluded the error to be the cause of motion capture in only two dimensions, since the joints bend and rotate in the third dimension during the gait cycle.

6

1.3   Objective

The objective of this thesis project is to contribute to gait cycle analysis study by studying the extension and flexion movements of the lower extremity that constitute the gait of a human. Four important parameters that will be analyzed include extension and flexion at the hip and knee joints, plantar and dorsi flexion at the ankle joint and the placements of the foot. In order to analyze these parameters, a three-linked structure consisting of four DOF will be projected onto the *(x,y)*-Cartesian coordinate plane. The four DOF will represent the four parameters whereas the three links will signify the segments connecting the four parameters. Using the concepts of forward and inverse kinematics, discussed in Chapter 2, a math model of the lower extremity will be devised and a geometric approach will be utilized to derive equations that will explain the motion of the linked structure. Next, Groebner basis theory will be applied to the equations to analyze the joint angle movements in the lower extremity. The existing INSPIRE database will be extended to include indoor recordings of the human gait as captured by a motion capture system observing human subjects on an instrumented treadmill. A MATLAB GUI will be developed to analyze the data more accurately and efficiently. Extensive analysis will provide gait patterns of the lower extremity with a detailed comparison of gait variance among normal and load influenced gait. This research focuses on answering the following question: How are gait patterns, in specific joint angles of the lower extremity, of a person walking without any load different from gait patterns of that same person walking with an additional load strapped on the upper and mid-torso of the their body? In order to investigate this question, extensive background research on theory and similar concepts and techniques was completed and the findings are outlined in the following chapter.

II. Theory

2.1   Chapter Overview

This chapter of the thesis covers the theories used in this study. It is divided into five sections. The first section highlights the two defined kinematic problems and the different methods used in the research to solve for the inverse kinematic problem. The second section focuses on Groebner basis theory and how it is applied to solve for the inverse kinematic problem. The third section follows by providing a detailed explanation of the sagittal plane of motion and the research that provides substantial evidence as to why this thesis focuses on gait characteristics in that plane of motion. The fourth section provides an in-depth research on how gait patterns may or may not be affected when constrained to a treadmill. Finally, the last section concludes with an in depth investigation on the effects of load on gait cycle analysis.

2.2   The Kinematic Problem

Kinematics is a concept of classical mechanics that describes the motion of a body and its displacement without considering the causes of motion such as time, forces, and moments. The two types of kinematic problems, the forward and inverse, are widely known and used in the area of robot manipulators. An example of a human kinematic chain, Figure 5, consists of linked segments and joints that control the motion of such segments. This figure depicts, for example, an arm and a leg consisting of three segments and three joints. In robot kinetics, the end effector is known as the end of a linked structure that interacts with the environment, which in this case is the wrist or the foot. With the known joint parameters segment lengths, the ability to solve for the position and orientation of the end effector is known as the forward kinematic problem. In contrast, the inverse kinematic problem solves for the
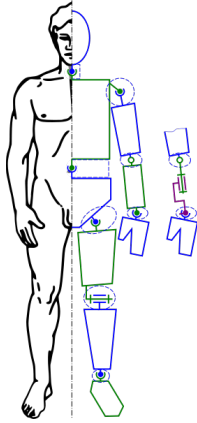
Figure 5. Human Skeleton as a Kinematic Chain. This representation shows a human skeleton as a kinematic chain that allows positioning using the kinematic problem. The upper extremity chain includes the shoulder, elbow and the wrist joint whereas the lower extremity consists of the hip, knee and the ankle joint. The hand and the foot are considered the end effector for this representation [18].

joint parameters with the known position and orientation of the end effector. The forward kinematic problem is straightforward and avoids complexity in deriving the equations. However, inverse kinematics can be more difficult and the solution to this problem can be computationally expansive and too time consuming for real time, as you are trying to find all possible joint configurations to reach a point in space. Recall that the objective of this research is to study lower extremity joint angles during the gait cycle to distinguish signatures of a potential suicide bomber. Therefore, inverse kinematics and its solutions will be further investigated in the following subsection.

Inverse Kinematic Solutions.

Due to its complex nature, inverse kinematics has widely been researched specifically in the area of robot manipulators. Many researchers have developed new algorithms that aim to simplify and solve for the inverse kinematic problem. Such algorithms can be classified as analytical or numerical methods. Analytical methods allow the user to find all possible solutions to the problem, whereas, the numerical methods converge to finding a single solution for the inverse kinematic problem.

Traditional methods such as closed form solutions and algebraic-elimination are categorized as analytical, while Newton-Raphson, optimization techniques, differential equation conversion, Jacobian Transpose, and Damped Least Squares can be considered numerical. In some cases, researchers have developed algorithms that combine the numerical and analytical methods, while others have moved to non-traditional methods such as the application of Groebner basis algorithms to solve for the inverse kinematic problem. The following paragraph will provide a brief overview of some of the mentioned algorithms and in turn explain the advantages and disadvantages of each.

The Newton-Raphson method is iterative in nature and has been widely used for solving inverse kinematic problems in robot manipulators [26]. This method can be problematic for robots consisting of higher degrees of freedom which will in turn produce highly nonlinear equations or singularities. The singularity problem arises when the target is unreachable and the arms of the linked structure jitter and oscillate when reaching for the target. Similarly, the pseudoinverse method [47] also has difficulties performing near singularities. In conclusion, these algorithms can cause the system to be ill-posed and result in a failed algorithm.

On the other hand, Wampler et al.[43] and Deo et al.[14] used an algorithm known as the damped least squares (DLS) method that more readily converges to a solution. This particular algorithm efficiently handles singularities by using a damping factor that controls the joint velocity vector and allows computation of redundant and non-redundant manipulators. Buss et al.[14] built on the damped least squares method and used a technique known as singular value decomposition [20] to solve for the inverse kinematic problem by looking at joint angles individually. Their proposed method is known as the selectively damped least squares method (SDLS) and it was tested on multibodies with multiple end effectors. The algorithm predicted how

much the angle moves in order for the end effector to reach the desired position and compared that to the real measured distance. The algorithm was compared to the Jacobian transpose [14], pseudoinverse, and the DLS method. The authors in this study concluded that SDLS was faster in determining target positions while the DLS method was faster at tracking within reach target positions and converging to a single solution.

Another solution to the inverse kinematic included a combined optimization technique, which was originally proposed by Wang et al.[44]. Unlike the Jacobian matrix, this method is not dependent on initial or singular configurations of the robot manipulator and is also independent of the robot's DOF. The authors tested their proposed combined method and compared it with individual working algorithms. These tests were conducted on different robotic arms to investigate the concern of singularities, joint limitations, continuous joint space trajectories, and how the algorithms performed with redundant manipulators. Their results showed that the proposed combined method was not dependent on initial and singular configurations of the manipulator. It handled boundary constraints more efficiently and was able to find multiple solutions to the inverse kinematic problem.

Efforts to use numerical and analytical methods together have also been researched to determine inverse kinematic solutions. Tolani et al.[42] developed a toolkit that models the inverse kinematic of the human arm or leg. This combination kit not only aids in solving the problem but also targets partial orientation and aiming problems. Time and accuracy of the developed algorithm was compared to traditional optimization and Jacobian routines using an open kinematic chain. The results concluded that numerical methods alone were not reliable for all the test and Jacobian and optimization methods failed with some applications due to local minima. Inverse Jacobian proved to be the slowest since it solves for an entire trajectory, instead of

the final posture of the arm. The proposed combined method was not developed on a starting posture and is repeatable. It is capable of operating with redundant systems and allows the user to explore multiple solutions to the inverse kinematic problem.

A modern algebraic approach, Groebner basis theory [28, 46], has also been used to solve the inverse kinematic problem in various robotic manipulators. This algorithm is applied to a given set of non-zero polynomial equations that are derived from joint geometry. This technique allows the user to obtain all the possible joint angle configurations that determine the position and orientation of the end effector. It can also be used with complex joint geometry, such as manipulators with higher DOF. The Denavit Hartenberg (D-H) Matrix method for solving inverse kinematic was compared to Groebner basis method and both algorithms were applied to the GMF Robotics A-10 Robot [28]. The research proved that the D-H method had difficulties producing results with joint geometry consisting of higher DOF, which would produce a higher number of polynomial equations. Also, the D-H method failed in producing all the possible solutions to the inverse kinematic problem. With Groebner basis algorithms, however, the computations do not depend on the number of polynomials in a set, but rather the defined term ordering of the monomials in the set. Therefore, Groebner basis is good for processing configurations that contain higher DOF. Table 1 summarizes the different solutions discussed above and highlights their advantages and disadvantages. This research will be using the Groebner basis approach; hence, the following section gives an overview of the Groebner basis theory and its algorithm.

Table 1. Advantages and Disadvantages of Different Inverse Kinematic Solutions

Method	Advantages	Disadvantages
Newton Raphson	Simple & straightforward	Iterative & slow computations
		Fails near singularities
		Converges to a single solution
		Fails with higher DOF systems
Algebraic Elimination	Operates up to 6 DOF	No guarantee for a solution
		Neither unique nor continuous
Optimization Techniques	Avoids matrix inversions	Fails for local minimum
		Not able to find global solutions
Jacobian Transpose	Fast for small structures	Fails near singularities
		Ill conditioned
Jacobian Inversion	Fast for small structures	Time consuming for higher DOF
	Real-time calculations	Fails near singularities
DLS/SDLS	Classifies singularities	Time consuming
	Multiple end effectors	Converges to a single solution
Denavit Hartenberg Matrix	Operates up to 7 DOF	Run-time error
		Not able to find all solutions
		Sometimes no solutions can be found
Groebner Basis Theory	Simple & straightforward	Run-time error
	Non-complex computations	
	Real-time calculations	
	Finds all possible solutions	
	Classifies singularities	

2.3 Groebner Basis Theory

Groebner basis theory, named after Bruno Buchberger, is mainly an algebraic algorithm that is applied to a given set of non-zero polynomials [13]. The computation of the algorithm produces a Groebner basis, which is a set of multivariate nonlinear polynomials having in common certain properties that allow simple algorithmic solutions for problems in mathematics, such as the inverse kinematics problem. The algorithm uses a specific order defined by the user and back substitution to find a solution to the variables in the set. To introduce this concept, consider a set F of polynomial equations such that $F \subset k[x_1, \ldots, x_n]$ and k represents a field of characteristic zero.

1. The set of polynomials F is *transformed* into another set of polynomials G.

2. The obtained set G bears *nice properties* (e.g. canonicality, elimination and syzygy property [37]) such that it is called a Groebner basis.

3. F & G generate the same ideal causing them to produce the same sets of solutions.

The Groebner basis Theory states that:

1. Due to the *nice properties* of G, problems that were difficult to solve in terms of F, are easy to solve with G.

2. There exists an *algorithm*, Buchberger's Algorithm, that transforms an arbitrary F into G.

3. The solutions obtained from G can be translated back to the solutions of F.

Our research will focus on Groebner basis algorithms over previously mentioned methods because we are interested in finding all the possible solutions to our inverse kinematics problem which can only be attained using the Groebner basis algorithms.

Also, we will be looking at higher DOF configurations in the lower extremities sagittal plane which will not only be difficult but time consuming to solve with matrix algebra and previously mentioned algorithms. This research will analyze joint angles of the lower extremity in a two dimensional plane and it will focus on the sagittal plane of the human body only. Investigations on human sagittal plane of motion were performed to justify this decision.

2.4   Sagittal Plane of Motion

The human body is categorized into three imaginary cardinal planes when viewed as an anatomical reference position: sagittal, coronal (frontal), and the transverse plane of motion, Figure 6. Each plane is a two-dimensional surface described by spatial coordinates of three non-linear points. Borghese et al.[12] proved that most of the walking dynamics occurs in the sagittal plane of motion, a vertical plane that divides the body into equal masses of left and right halves. The forward and backward movements of the body are considered to be sagittal plane movements, since they occur in that plane of motion. Similarly, jumping jacks and executing a cartwheel are frontal plane movements because they allow the body to move laterally [23]. According to the American Academy of Orthopedic Surgeons [34], the movements of the sagittal plane include flexion and extension. Arm swing, along with the motion of the opposing leg, is the natural motion observed in normal bipedal gait. It follows a specific pattern in which peak flexion occurs at the midpoint of the stride phase thereby concluding that arm swing motion is dominated by the sagittal plane of motion [49].

Modalities such as video and model based gait analysis have been used previously to justify analysis of gait in the sagittal plane. A video-based study by Krebs et al. [33] performed research in which the reliability of observational gait kinematics was

15
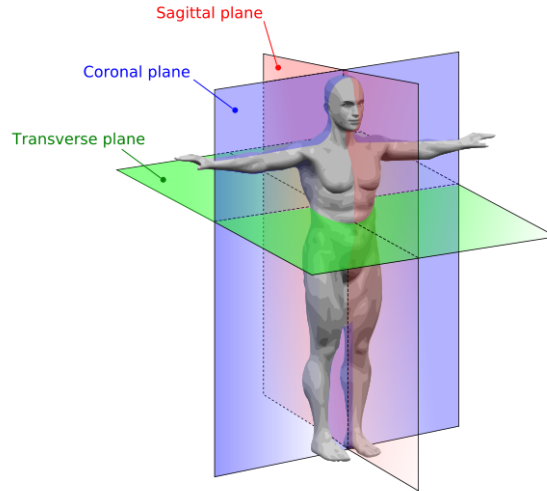
Figure 6. Planes of Motion. The human body consists of three planes of motion: Sagittal, Coronal, and the Transverse plane. The sagittal plane divides the body into equal parts of left and right causing extension and flexion to be part of that plane [5].

analyzed. Fifteen children with lower extremity disability were recorded and observed as they walked with an assisted orthotic system. Lower extremity and trunk of the subject was viewed in the sagittal, transverse and frontal plane of motion. Three individuals trained in observational gait analysis rated the gait and an agreement of an average of 67.5% was concluded between the raters. These ratings were based on previous pilot studies that were performed by researchers to determine the most accurate way of observational gait analysis [3, 4, 9, 17, 21]. Despite the low average, the analysis shows that ratings of the sagittal plane motion were more reliable than the ratings of the frontal and transverse plane. Sagittal plane analysis is more reliable because its axes of rotation are collinear to the observer's visual axis.

Similarly, a model-based study done by Kadaba et al.[27] proves that sagittal plane motion is more reliable at analyzing angles for larger joints, such as hip and knee. The research proposed a method of analyzing gait kinetics and kinematics to validate the repeatability of the captured data. The data was taken over the course of three days in which 40 subjects were tested three times each day. Three dimensional motion capture

system and reflective markers were used to examine motion at the pelvis, hip, knee and ankle. It was concluded from the kinematic data that intrasubject repeatability was more reliable in the sagittal plane of motion. Although the repeatability for joint angle motion in the transverse and frontal plane were reliable between same day testing, they proved to be poor for data that was taken on different days. This was mainly due to inconsistent marker placement. Overall, for joint angle motion, the sagittal plane proved to be less variable and more repeatable than frontal and transverse plane of motion. Similarly, Zhang et al.[50] performed a model-based study of gait in the sagittal plane of motion in which subjects were identified through video sequences based on their side view. The technique was proposed with a two-step approach: extraction of joint position trajectories using a five link biped model and recognition of the joint trajectories using Hidden Markov Models. In this model based study, the lower extremity was represented as trapezoids while the upper body was simplified by a silhouette without arms. The authors applied the proposed method to two sets of gait databases: University of South Florida (USF) Gait Challenge [35] and Carnegie Mellon University Motion of Body (CMU MoBo) [22] data set. The CMU MoBo data set consisted of 25 subjects walking on a treadmill at either a speed of slow or fast, and with or without an incline. USF gait challenge data set consisted of 75 subjects walking in an outdoor setting. After applying the proposed algorithms to the data sets, a recognition rate of 96% and 61% was achieved for CMU MoBo and USF Gait Challenge data sets, respectively. A lower recognition rate for the USF Gait Challenge data set was due to the great distance between the subject and the camera.

As mentioned in Chapter 1.3, the objective of this research includes expanding the gait database to include gait recordings using a treadmill. Gait analysis based on instrumented treadmill has been widely used in clinical research and it can offer

a number of potential advantages. The following section will attempt to produce research that has used an instrumented treadmill for gait analysis purposes and the results that were obtained. This will in turn substantiate the usage of this instrument for the purpose of this thesis.

2.5 Treadmill Gait Analysis

The instrumented treadmill is increasingly being used in clinical gait analysis because it can offer a controlled and convenient environment for testing. Many studies have been conducted that investigate whether kinematics and kinetics of gait on the treadmill are equivalent to overground locomotion. Riley et al.[36] studied the kinematics and kinetics of gait and compared overground and treadmill walking in healthy subjects. For their research, 26 subjects between the age of 18 and 35 were recruited and kinematic data was collected using a 10-camera VICON motion capture system. The subjects first walked a 15 meter overground path as data was collected. Their average speed was determined and the treadmill was set to that speed. The analysis of the research concluded that time-distance parameters between the treadmill and overground gait were very similar. There was no significant difference in the timing of gait cycle events. Most significantly, the kinematics such as joint parameters of the lower extremity, were very similar. Quantitatively, the differences in kinematic maximum and minimum values were less than two degrees, which the authors concluded was within the range of variability of the measure.

Similarly, Watt et al.[45] studied three dimensional kinematic and kinetic gait patterns of gait between overground and treadmill walking in elderly subjects. Eighteen subjects were recruited and gait parameters were compared. The results showed a reduced absolute kinematic maxima and minima for treadmill walking, which implies a larger range of motion for overground walking. The comparison also revealed

the adoption of quicker cadence and shorter stride lengths during treadmill walking. Because of the small differences observed between treadmill and overground walking kinematics, the authors suggest that instrumented treadmill use for research and training purpose is appropriate only if the subjects accommodate to the treadmill prior to data collection. Inexperience with the treadmill may contribute to the gait related changes that were detected in this study. As mentioned previously, the aim of this thesis is to determine and compare gait patterns that tend to be altered with the addition of extra load on the body. The following section summarizes some of the research conducted on gait and the effects observed due to additional load on the body. This will lay the groundwork for this thesis and give some insight as to what kind of gait behavior will be expected with load.

2.6 Effects of Load Carriage on Gait

Gait, manner of bipedal walking, consists of the stance and the swing phase, Figure 7. Stance phase, which accounts for 60% of the gait cycle, begins with initial foot contact and accounts for the entire period of time when that foot is in contact with the ground. The stance phase, which constitutes for about 40% of the gait cycle, begins with the toe off and accounts for the period of time when that foot is not in contact with the ground.
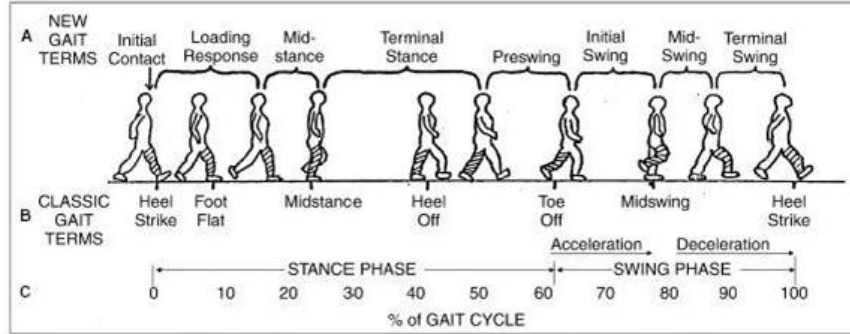
Figure 7. Gait Cycle. 100 percent of the gait cycle includes the stance and the swing phase. The stance phase begins with initial contact, heel strike, and ends with toe off. The swing phase begins at toe off and ends with the heel striking the ground [16].

Even though the physiological [32] and electromyographic [10, 19], effects of load on gait have been researched, there still is a lack of research on the kinetics and kinematics effects of load carriage. Researchers have reported that during load carriage, stance phase duration is unchanged while swing phase duration is decreased [19]. The dynamic effects such as ground reaction forces and lateral forces have also been researched extensively based on load carriage [31].

Tillbury-Davis et al.[41] investigated the kinetic and kinematic effects of increasing load carriage on the lower extremity. Military personal that carry load on a day-to-day basis were recruited for this study and changes to the lower limb were analyzed in the sagittal plane. The research concluded that loads up to 64% of an individual's body mass had very little effect on the sagittal plane of motion. The authors concluded that this pattern could have resulted from the individuals' daily task routine. The volunteers were all military personal, whose muscles have probably adjusted to carrying heavy loads on the body, making it difficult to distinguish any variance between the gait patterns. On the contrary, Kinoshita [31] investigated effects of different loads and carrying systems on gait and reported very significant results. The investigation was performed on ten healthy males that did not interact with carrying task on a daily basis. One particular kinematic analysis of joint angles

revealed greater knee flexion during load bearing gait. Similarly, Wittman et al.[48] and Knapik et al. [32] also addressed the question on whether significant load is distinguishable through visual analysis of gait. Both of the studies reported a decrease in swing phase with additional load causing the knee to have a greater flexion.

2.7 Scope

Using the kinematic concepts introduced in section 2.2 this research will aim to derive an inverse kinematic model which will consist of the lower extremity in the sagittal plane of motion. It will consist of four DOF which will include the extension/flexion at the hip and knee joint and dorsiflexion/plantarflexion at the ankle joint, with the foot being the end effector of the system. Due to the advantages it offers, Groebner basis theory will be used to solve for the inverse kinematic equations derived from the projection of the two dimensional model onto an *(x,y)*-Cartesian coordinate plane. The solutions to the inverse kinematics will give an insight to how the joint angles will behave with the known position of the end effector. This thesis will investigate load effects on gait using an instrumented treadmill. Chapter 3 of this document gives a detailed explanation of the methods of this research.

III. Methodology

3.1 Chapter Overview

This section of the thesis gives an overview of the methodology and it is divided into three sections. The first section gives a detailed explanation of how the lower extremity math model was derived and how the kinematic problem was applied to the motion of the lower limb. The second section highlights the application of the Groebner basis algorithm and the solutions obtained from its application. Lastly, the third section gives a validation to the derived inverse kinematic math model and the solutions obtained from applying the Groebner basis algorithms.

3.2 Lower Extremity Math Model

Investigation of lower extremity gait patterns in the sagittal plane of motion was the focus of this research. A two dimensional linked structure of the lower extremity is projected onto the (x,y)-Cartesian coordinate plane, Figure 8. The projection demonstrates the motion of a linked structure consisting of three segments, L_1, L_2, and L_3, three joints, θ_1, θ_2 and θ_3, and an end effector. The first joint is situated at the origin while the end effector is located at (x_4, y_4). Through simple geometric analysis and forward kinematics we can find the position of the end effector as

$$x_4 = L_3 \cos(\theta_3 + \theta_2 + \theta_1) + L_2 \cos(\theta_2 + \theta_1) + L_3 \cos \theta_1$$

$$y_4 = L_3 \sin(\theta_3 + \theta_2 + \theta_1) + L_2 \sin(\theta_2 + \theta_1) + L_3 \sin \theta_1.$$

Using trigonometric identities of addition and subtraction, the above equations were further simplified. Let $c_i = \cos\theta_i$ and $s_i = \sin\theta_i$ such that i = 1,2,3.
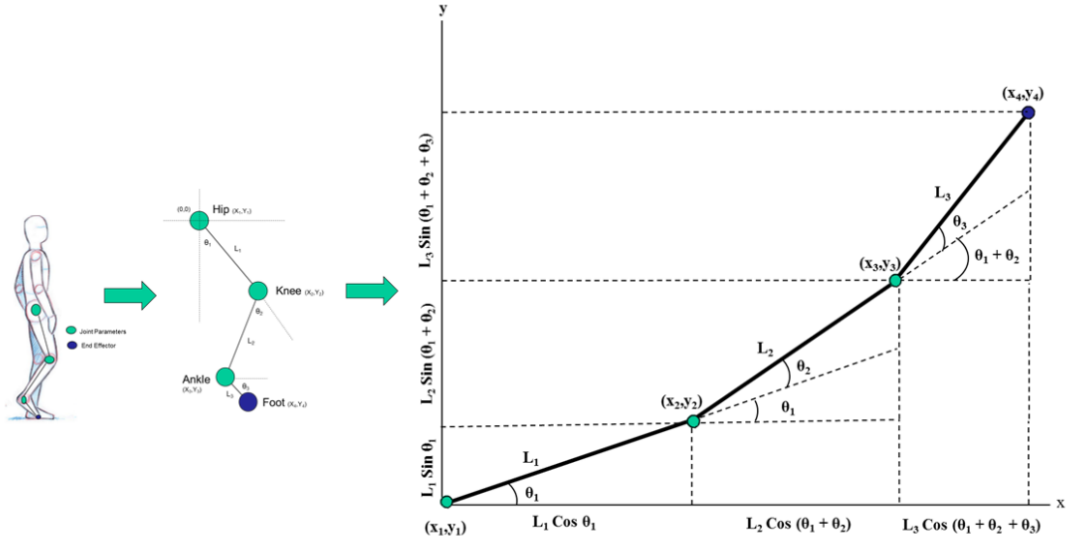
Figure 8. Two Dimensional Projection. Projection of a linked structure containing 4 DOF onto the (x,y)-Cartesian coordinate plane, with the first joint at the origin. Includes three joints and an end effector that interacts with the environment. The following is used to derived the inverse kinematic equations and also applied to the joints of the lower extremity.

$$x_4 = L_1c_1 + L_2c_1c_2 + L_3c_1c_2c_3 - L_2s_1s_2 - L_3c_3s_1s_2 - L_3c_2s_1s_3 - L_3c_1s_2s_3 \qquad (1)$$

$$y_4 = L_1s_1 + L_2c_2s_1 + L_3c_2c_3s_1 + L_2c_1s_2 + L_3c_1c_3s_2 + L_3c_1c_2s_3 - L_3s_1s_2s_3 \qquad (2)$$

$$\cos^2\theta_1 + \sin^2\theta_1 = 1 \rightarrow c_1^2 + s_1^2 = 1 \qquad (3)$$

$$\cos^2\theta_2 + \sin^2\theta_2 = 1 \rightarrow c_2^2 + s_2^2 = 1 \qquad (4)$$

$$\cos^2\theta_3 + \sin^2\theta_3 = 1 \rightarrow c_3^2 + s_3^2 = 1 \qquad (5)$$

Together we have a system of five equations with six unknowns: c_i and s_i. In order to make the system of equations computationally easier, the following equation was introduced to explain the first joint at the origin as

$$\sin\theta_1 = \frac{y_2}{L_1} \rightarrow s_1 = \frac{y_2}{L_1}. \qquad (6)$$

A software package was used to apply Groebner basis theory and algorithms to find a solution to the system of equations giving us now, an inverse kinematic model with a system of 6 equations and 6 unknowns.

3.3   Using MAGMA to Calculate Groebner Basis

MAGMA is a software package that is designed to solve problems in algebra, number theory and geometry. It is based on Unix-like and Linus based operating systems and can be run on Windows. This software package is produced and distributed by the Computational Algebra Group at the University of Sydney. The code detailed in Appendix A was entered into MAGMA and the following Groebner basis was calculate for our inverse kinematic model.

$$c3 + \frac{c1(L1*x4)}{L2*L3} + \frac{0.5\left(-L1^2 + L2^2 + L3^2 - x4^2 - y4^2\right) + y2*y4}{L2*L3} = 0 \qquad (7)$$

$$s1 - \frac{y2}{L1} = 0 \qquad (8)$$

$$c1^2 + \frac{-L1^2 + y2^2}{L1^2} = 0 \qquad (9)$$

$$s3 + \frac{a}{b}*s2*c1 + \frac{c}{d}*s2 + \frac{e}{f}*c1 + \frac{g}{h} = 0 \qquad (10)$$

$$c2 + \frac{i}{j}*s2*c1 + \frac{k}{l}*s2 + \frac{m}{n}*c1 + \frac{o}{p} = 0 \qquad (11)$$

$$s2^2 + \frac{q}{r}*s2*c1 + \frac{s}{t}*s2 + \frac{u}{v}*c1 + \frac{w}{x} = 0 \qquad (12)$$

where variables $a, b, c, ..., x$ are defined in Appendix C

The Groebner basis, Equations (7) - (12), are reduced further and solved for each unknown. Equation (8) is first solved to give one solution to s_1. Equation (9) is solved to give two solutions to c_1, positive and negative. The two solutions to c_1 are

24

then substituted into equation (7) which gives two solutions to c_3. Equation (12) is solved as a quadratic equation with the substitution of two solutions from c_1, therefore giving a total of four solutions to s_2. All solutions of s_2 and c_1 are then substituted into equation (10) and (11) producing four solutions to s_3 and c_2. Figure 9 outlines the summary of the solutions obtained. Inverse tangent $tan^{-1}(\theta_i) = \frac{sin(\theta_i)}{cos(\theta_i)}$ is applied to the obtained solutions and joint angles θ_1, θ_2 and θ_3 are found, producing two solutions for θ_1 and four solutions for θ_2 and θ_3. Recall the properties of Groebner basis from Chapter 2 stating that Groebner basis algorithms applied to the inverse kinematic sets of equations will aim to find all the solutions to that problem. The multiple solutions for a joint explain its behavior without any constraints added to the system. However, the equations above have only found partial solutions to the system of equations. Note, that variables (b, d, f, h, j, l, n, p, r, t, v, x) are all in the denominator of the rational terms in equations (7) - (12). In order to find *all* solutions, the system of equations would be analyzed again for cases where these variables would equal zero. Hence, additional solutions do exist, but for the purpose of this thesis, only the current solutions will be further explored. In order to specify which solution would work for the lower extremity in gait motion, the different solutions will be validated with pre-existing clinical lower extremity dataset. The validation will allow us to see which solution confirms as the true solution for our motion captured data.

3.4   Model Validation

To validate the inverse kinematic model, a dataset called Plug-In Gait (PIG) [6], containing lower extremity flexion and extension angles, was obtained from VICON Motion Capture System [7]. This dataset is VICON's conventional gait model that has been used widely in the research of clinical gait analysis. The data was collected by research engineers in a closed environment with VICON motion capture cameras
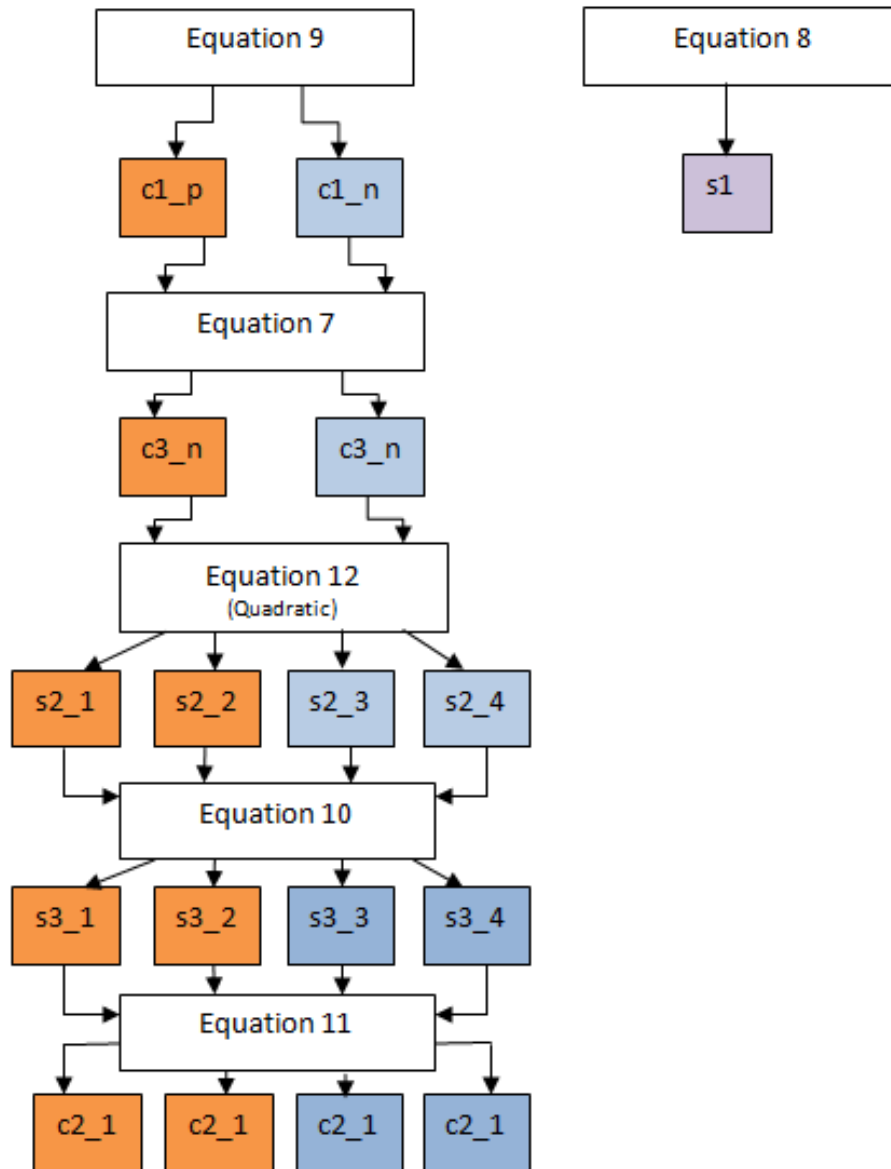
Figure 9. Groebner Basis Solution Flow Chart. The configuration shows the solutions obtained from each equation. Applying Groebner basis theorem to the system of equations produced one solution for s1, two solutions for c1 and c3 and four solutions for s2, s3, c2.

using retro-reflective markers that track and record the spatial coordinates of the markers and inturn provide the gait angles. The extracted measured angles of the hip, knee and ankle joints consisted of one full gait cycle. The angles, hip θ_1, knee θ_2 and ankle θ_3, were substituted into equation (1), (2) and (6) to find the spatial coordinates (x_4,y_4) and (x_2,y_2). These coordinates were then plugged into the reduced Groebner basis equations (7)-(12) and through back substitution, joint angles were determined and plotted against the original dataset. The results are summarized in Figure 10, 11, and 12. The accuracy of the predicted lower joint angles from the inverse kinematic (IK) model were verified against the measured PIG angles using the Root Mean Square Error Analysis (RMSE), see Table 2. The MATLAB code for calculating RMSE is highlighted in Appendix B of this document.
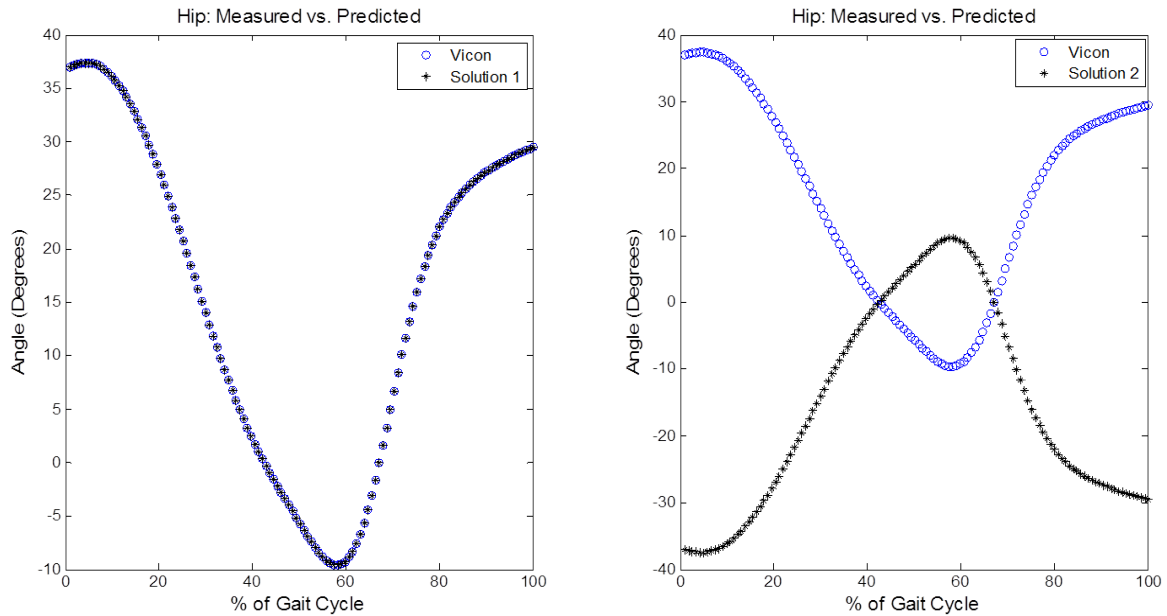
Figure 10. Validation of Hip Angle. Flexion and extension angles plotted for the PIG dataset vs the flexion and extension angles obtained from the Groebner basis algorithms. Two solutions were produced for θ_1 and the predicted data overlays the measured data in solution one. Solution two is a reflection upon the x-axis. This shows that the hip angle is 100% validated for at least one solution and the algorithm did not fail for the entire gait cycle.

27
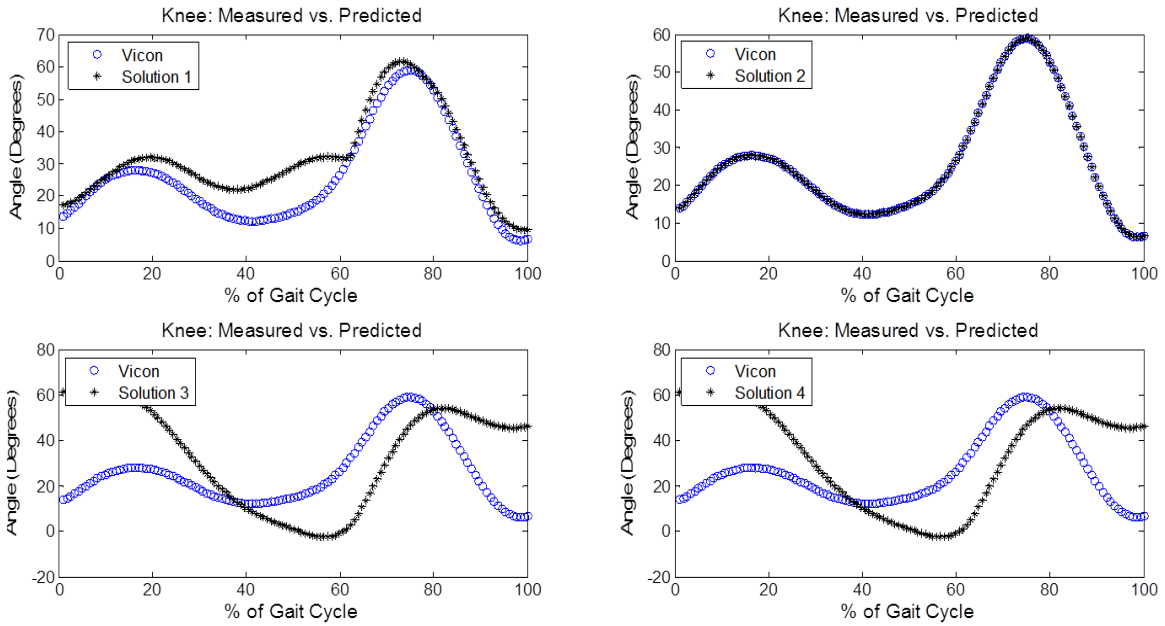
Figure 11. Validation of Knee Angle. Flexion and extension angles plotted for the PIG dataset vs the flexion and extension angles obtained from Groebner basis algorithms. Four solutions were produced for θ_2. Only solution 2 shows an overlay of the PIG dataset, showing that the knee angle is 100% validated and the algorithm did not fail for the entire gait cycle for that solution only.
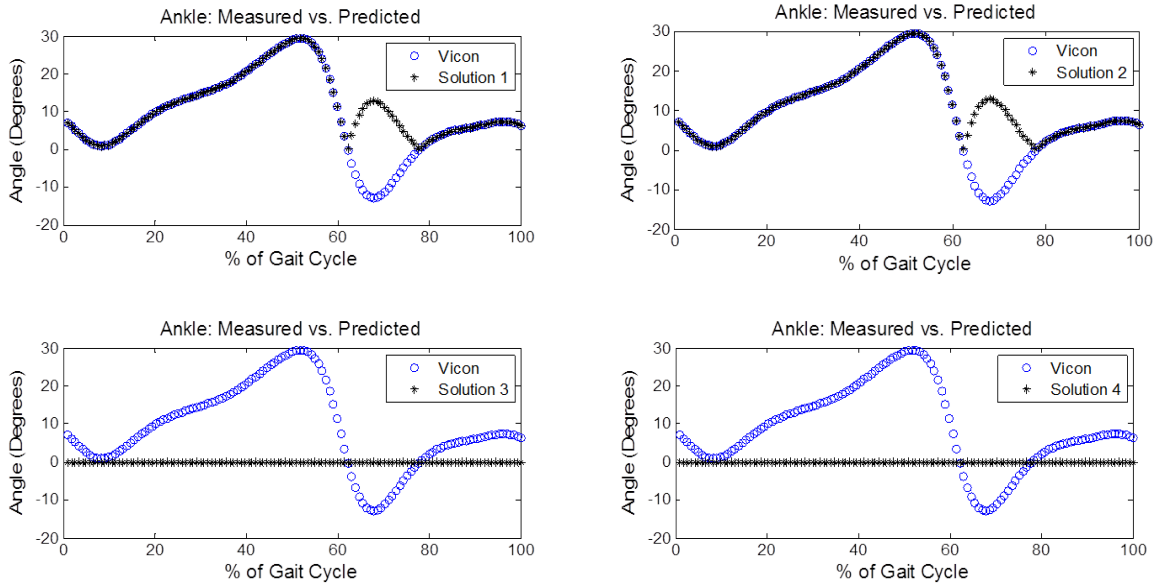
Figure 12. **Validation of Ankle Angle. Flexion and extension angles plotted for the PIG dataset vs the flexion and extension angles obtained from Groebner basis algorithms. Four solutions were produced for θ_3. None of the solutions are 100% validated, although, solution 1 and solution 2 are validated for the stance phase of the gait cycle. This shows that the algorithm has failed for the ankle's swing phase of the gait cycle.**

Table 2. RMSE Analysis between VICON's PlG (Measured) and IK Model (Predicted)

Measured	Predicted	RMSE (%)
Hip angle	Hip: Solution 1	0.000
	Hip: Solution 2	43.4634
Knee angle	Knee: Solution 1	6.806
	Knee: Solution 2	0.000
	Knee: Solution 3	63.522
	Knee: Solution 4	63.522
Ankle angle	Ankle: Solution 1	6.903
	Ankle: Solution 2	6.903
	Ankle: Solution 3	174.414
	Ankle: Solution 4	174.414

RMSE and graphical analysis shows an error of 0% for solutions 1 and 2 of the hip and knee angle, respectively. Solution 2 of the hip is a reflection upon the x-axis. None of the solutions for the ankle angle match the measured model. This result verifies that hip and the knee angle were verified for at least one solution, allowing us

to use those solutions for our captured gait motion data. The lowest RMSE value for the ankle angle was solution 1 and 2. Therefore, solution 1 for hip, solution 2 for the knee, and solution 2 for the ankle angle were used to finalize our inverse kinematic math model that describes the motion of the lower extremity in the sagittal plane of motion.

IV. Experiment

4.1 Equipment

The equipment used for this experiment included the VICON Motion Capture System [7] which consisted of the hardware, software and its accessories that offered the highest capture accuracy. The equipment also included a treadmill in a closed environment, to ensure complete capture of the gait cycle, and a load bearing vest that simulated a bomb vest.

VICON Motion Capture System.

Hardware.

VICON is an infrared marker-tracking system that offers millimeter resolution of three dimensional spatial displacements. The system used for this research consisted of ten VICON MX T160 infrared (IR) motion tracking cameras outfitted with IR optical filters and an array of IR LEDs, Figure 13. The cameras illuminate their respective field of view with harmless IR (thermal) light, and then capture the IR signals reflected off the subject's body with the aid of reflective markers. The markers arranged on the body reflect the IR radiation emitted by the LEDs while all other light is filtered, allowing the system to only recognize the markers of interest. The VICON system can deliver up to six degrees-of-freedom data using these reflective markers and high resolution cameras. It provides the researcher with the highest order of positional and angular frequency. After the capture, the images taken from the IR cameras can be used to reconstruct a three dimensional representation of the markers in virtual space, Figure 14. Reconstruction can allow the user to further extract the spatial coordinates and its displacements in an ASCII (Delimited) file format, which could be viewed and/or edited using Microsoft Office Excel workbook.

Figure 13. VICON Motion Capture Camera. T-series VICON motion capture camera, with millimeter resolution, was used to capture the spatial coordinates of the subject of interest (SOI). The markers situated on the SOI reflect the IR radiation emitted by the LEDs on the camera.

For this experiment, the VICON cameras were connected to a a PC workstation that consisted of a monitor and a central processing unit with Windows XP, and a data-station that consisted of VICON's MX bridge panel that had the ability to communicate between the cameras and the PC workstation.

Software.

VICON Nexus [38]was used to record and process the collected data. Nexus is a Life Sciences-specific software package that is compatible with the VICON's hardware mentioned previously. Nexus is capable of reducing the noise in the raw data which provides the researcher with the most accurate motion captures. The software package allows the user to vary the camera settings such as strobe intensity, gray-scale, threshold and minimum circularity ratio. Nexus offers built in plug-ins that allow for calibration of the VICON cameras, processing of the collected data, and exporting the desired data in a variety of file formats. For this experiment, the
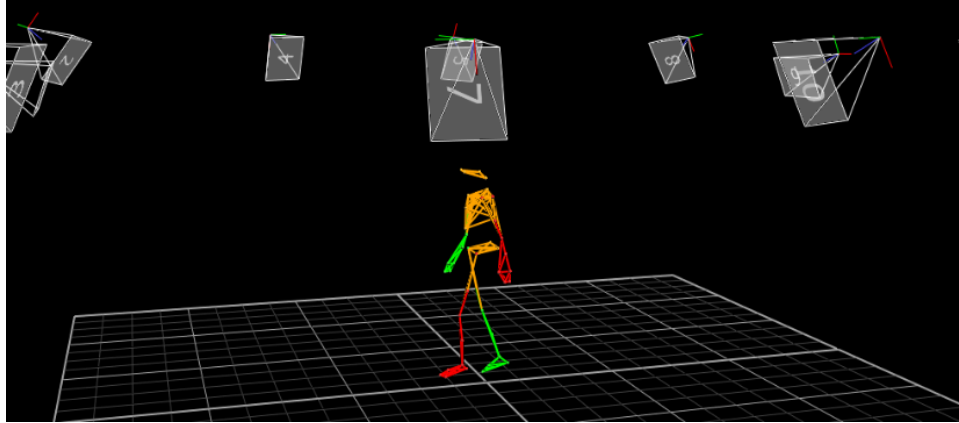
Figure 14. Three-Dimensional Reconstruction of Spatial Coordinates. 3D image extracted from VICON Nexus. The dots represent the markers' spatial coordinates and the lines connected to the dots represent the segments.

Nexus software was installed on a desktop computer with Windows XP.

Accessories.

Use of VICON motion tracking cameras necessitates subjects be outfitted with a set of light weight reflectors. These reflectors are small foam balls covered with a reflective tape. The VICON hardware and software collect the spatial coordinates of these reflective markers situated on the body. To capture the most accurate spatial data, VICON's Lycra body suit was used to capture the movement of the markers rather than the body to which the markers are attached. This includes loose clothing, which can greatly influence the results obtained as they would constantly move during the capture. Since this research focused on the lower extremity, only the pants of this suit was used, Figure 15

Instrumented Treadmill.

A Pro-Form ZT3 treadmill [8] was used in this experiment, Figure 16. This particular treadmill allowed the user to walk normally while staying in the same place, allowing for capture of at least 5 full gait cycles. The device offered an easy-to-use

Figure 15. Body Markers. VICON's retroreflective markers are precisely placed on the joints of the lower extremity. Marker #1 is placed on the hip joint near the femoral greater trochanter. Marker #2 is placed at the lateral condyles near the knee joint. Marker #3 is placed near the talocrural ankle joint. Marker #4 is placed laterally near the joint of the fifth metatarsal.

quick speed and quick incline controls to provide the most natural gait. It included an LCD window with priority display to allow the user to monitor their walking speed. The treadmill ran on a 1.5 CHP Mach Motor and had an 18 x 55 tread-belt with a weight capacity of up to 250 pounds [8]. A safety review was conducted on the treadmill, and it was approved by the Air Force Research Lab Institutional Review Board (IRB).

Simulated Bomb Vest.

A 6-pocketed vest was used to signify a suicide bombing vest and determine if a statistically significant difference can be identified between encumbered and un-encumbered, Figure 17. The pockets hold pouches of weights ranging from 1 to 5 pounds. The weights are made of lead because of its high density, low cost, and resistance to corrosion. The total combined weight of the vest and lead weights ranged from 1 to 26 pounds.

Figure 16. Instrumented Treadmill. Pro Form ZT3 treadmill offered a controlled and convenient environment for testing. This allowed the complete capture of the gait cycle while keeping the subject at a constant speed.

Figure 17. Simulated Bomb Vest. A 6-pocket vest was used to simulate an improvised explosive device (IED). Lead weights (top right) were inserted into the pockets to imitate the real weight of a suicide weight. The vest is worn over the head and situated on the abdominal area.
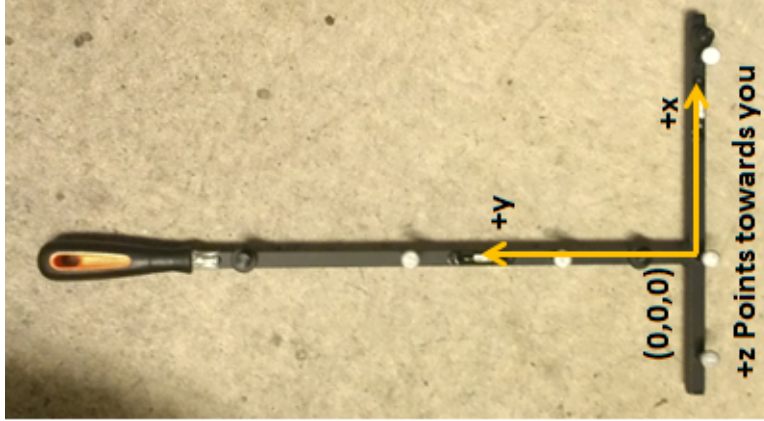
Figure 18. Calibration Wand. This 5-marker T frame not only aids in set-up and calibration of the VICON motion capture cameras, but also aids in setting the volume origin of the area in use. Visibility of the 5 markers from this wand allows the system to calculate the relative positions and orientations of the cameras and also linearizes them.

4.2 Experimental Setup

Calibration.

This is the single most important step in the preparation of the cameras, and must be performed regularly. The calibration allows the nexus software to calculate and orient the relative locations of all the cameras with respect to each other. With the recorded movements, calibration is responsible for processing these measurements to calculate the most accurate spatial dimensions. A calibration wand, Figure 18, was used for both the static and dynamic calibrations: static calibration calculates the volume origin whereas dynamic calibration linearizes the cameras and calculates their relative position and orientation.

Dynamic Calibration.

Using the VICON Nexus software, the cameras were pre-set with the following settings: strobe intensity = 0.6, camera gray-scale = Auto, threshold = 0.65, and minimum circularity ratio = 0.5. Before the dynamic calibration, visible noise was

36

removed from the captured volume. This noise included false reflections from equipment, floor, or any object present in the capture volume. White circular dots blinking or present in the 3D perspective view of Nexus, lets the user know of the exact location of the noise. The noise can also be masked if the user is not capable of physically removing it. The dynamic calibration was started with waving the 5-marker T-wand in the volume of interest. The wand was waved so the positions in the volume were covered in all orientations with variety of wand positions and waves. The wand was waived in the vertical figure of eight, vertical up and down and horizontal movements. When sufficient wave count determined by the Nexus software was achieved, the dynamic calibration was automatically stopped.

Static Calibration.

The calibration wand was placed on the floor in the center of the capture volume. A check was performed to make sure the cameras were only viewing the five markers on the calibration wand. A static measurement was taken by capturing 20 frames of the wand in a static position. This step set up the origin of the volume.

Pre-Measurements.

Marker Placement.

After a successful calibration, the participants were asked to change into the VICON Lycra body pants and the markers were attached to the bony prominence of the lower extremity, Figure 15. Marker 1 was placed on the hip joint near the femoral greater trochanter. Marker 2 was placed on the lateral condyles of the knee joint. Marker 3 was placed on the lateral side of the ankle on the lateral malleolus. Lastly, maker 4 was placed on the bony prominence of the fifth metatarsal. VICON's plug in gait (PIG), Helen Hays and the Cleavland Clinic marker sets were researched and

a Extensive research on proper marker placement and comparison of the different existing methods was done prior to creating this marker configuration [1].

Segment Lengths.

Segment lengths were determined by physical measurements. Segment 1, L1, was measured from the 1st to the 2nd marker. Segment 2, L2 was measured from the 2nd to the 3rd marker. Lastly, Segment 3, L3 was determined by measuring the distance between the 3rd and the 4th marker. The measurements were recorded in millimeters.

Average Walking Speed.

The average walking speed of a human is 3.5 miles per hour. Since this research utilizes the treadmill, average walking speed of the participants was determined prior to setting the speed on the treadmill. The participant was asked to walk a 30.5 feet long path as time was recorded. The average speed was determined by Equation (13). The participant was then asked to walk on the treadmill with the measured average speed for ten minutes. The participant had the ability to either stay with the measured speed or adjust it to their comfort level. Once the speed was determined, it was kept constant through the entire experiment. The consistent speed through out the experiment allowed us to measure joint kinematics without considering time. Recall from Chapter 2 the studies comparing the kinetics and kinematics of overground and treadmill influenced gait. The researchers from those studies concluded that the difference between overground and treadmill gait was non significant and using a treadmill for research and training purposes is appropriate only if the subjects accommodate to the walking speed of the treadmill. Therefore, for our experiment, the participants walked on the treadmill with their measured speed for ten minutes. This allowed them to accommodate to the measured speed and adjust it to their

comfort level. Regardless of the speed set on the treadmill, this research is concerned with measuring the joint angles of the lower extremity and how they are influenced by the additional load only.

$$\text{Average Walking Speed} = \frac{\text{Distance (miles)}}{\text{Time (hour)}} \tag{13}$$

Load Determination.

The participants were asked to weigh themselves using a measuring scale. The weight was recorded in pounds and the 10%, 15%, 20% of their body weight was determined until the percentage increased 26 pounds.

4.3   Gait Recordings

Twelve healthy subjects between 21-42 years of age were recruited for this study. Informed consent documents, approved by the Institutional Review Board (IRB), were signed by each subject. Participants were also asked to complete a medical screening questionnaire that would detail the physical conditions that could affect their gait. The collection of gait recordings for one participant consisted of one static and several dynamic trials. The subject was asked to stand in the center of the volume in a T-pose and static data were collected for 100 points. Next, the subject was asked to walk on the treadmill with their pre-determined walking speed. The subjects walked on the treadmill for 10 full gait cycles before their data were recorded. This procedure allowed the capture of normal gait which is generally attained after 10 full gait cycles. The data were recorded for 500 frames. The participants were then fitted with the vest situated on the abdominal and slightly overlapping the pelvic region. The vest was loaded with additional 10% of the participant's measured weight and gait patterns were again recorded as discussed above. Additional loads were added in increments

of 5%, without exceeding 26 pounds, and gait measurements were captured in the same manner. Table 3 summarizes the anatomical information and lists the number of trials conducted for each participant. The first trial for each subject was always a T-pose while the second trial was of the participant's normal gait without any additional load. The remaining trials for all the subjects were load influenced.

Table 3. Participant's Anatomical Data

Subject	Gender	Age	Height (in)	Weight (lb)	Speed (miles/hr)	L1 (mm)	L2 (mm)	L3 (mm)	Trials
1	M	28	72.0	145.0	3.60	445.50	457.20	152.40	4
2	M	27	69.0	160.0	2.30	406.40	406.40	152.40	4
3	M	24	67.0	181.0	2.60	406.40	406.40	127.00	3
4	M	28	76.0	219.0	2.70	414.02	508.00	149.86	3
5	F	23	69.0	144.5	3.00	406.40	406.40	152.40	4
6	F	25	64.5	132.0	2.50	469.90	330.20	127.00	4
7	M	31	64.0	123.5	2.50	408.30	408.30	126.50	5
8	M	23	70.0	176.0	2.10	482.60	406.40	165.10	4
9	F	24	62.0	115.0	2.80	381.00	378.46	124.46	5
10	M	21	73.0	189.0	3.20	457.20	431.80	139.70	3
11	F	42	62.0	150.5	2.90	381.00	378.46	124.46	4
12	F	21	66.5	113.5	2.70	431.80	444.50	114.30	5

4.4   Data Processing and Extraction

As the data was captured for each trial and each subject, the Nexus software collected the spatial coordinates into a database. The Nexus software then performed 3D reconstruction of the spatial coordinates recorded during each trail. Figure 19 shows a characteristic reconstruction. The markers were labeled accordingly, and segments were drawn to connect the markers. Using Nexus' built-in plug-in, unlabeled markers and trajectories were removed, and one full gait cycle was extracted in an ASCII (Delimited) file format. Each file contains the (xyz) coordinates of the four markers and their trajectories with respect to time. To facilitate the rendering of

gait cycle components, we created a MATLAB GUI to further process the data. See Appendix E for code details.
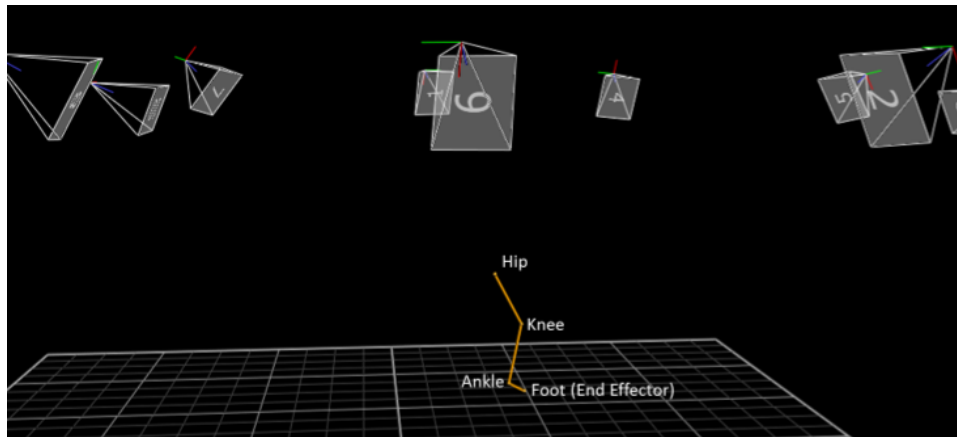
Figure 19. 3D Reconstruction of Lower Extremity. The collected data is called into the VICON's Nexus software where spatial coordinates are reconstructed and labeled. The markers of interest, hip, knee, ankle and foot, were labeled and marker positions and displacements were then extracted out to an excel file.

MATLAB GUI.

We created a Graphical User Interface (GUI) in MATLAB for processing the data faster and more accurately. Figure 20 shows a screen shot of the main window of the GUI. This interface allows the user to perform tasks interactively through different controls such as buttons. It performs tasks such as creating and customizing plots, and calculating the data. Each excel file, containing the (xyz) coordinates for each trial of each subjects, was processed using the GUI. First, the excel files with raw coordinate points was imported into the GUI. Recall that the origin for our lower extremity model was the coordinates of the hip joint. Therefore, after the trials were loaded into the interface, the program reset the origin and corrected the data points accordingly. The z axis coordinate was discarded since the model was derived in the two dimensional sagittal plane. The coordinates were set where the plane of motion was in the positive y direction in the (x,y)-Cartesian coordinate plane. The inverse kinematic model for the lower extremity which included the Groebner basis equations,
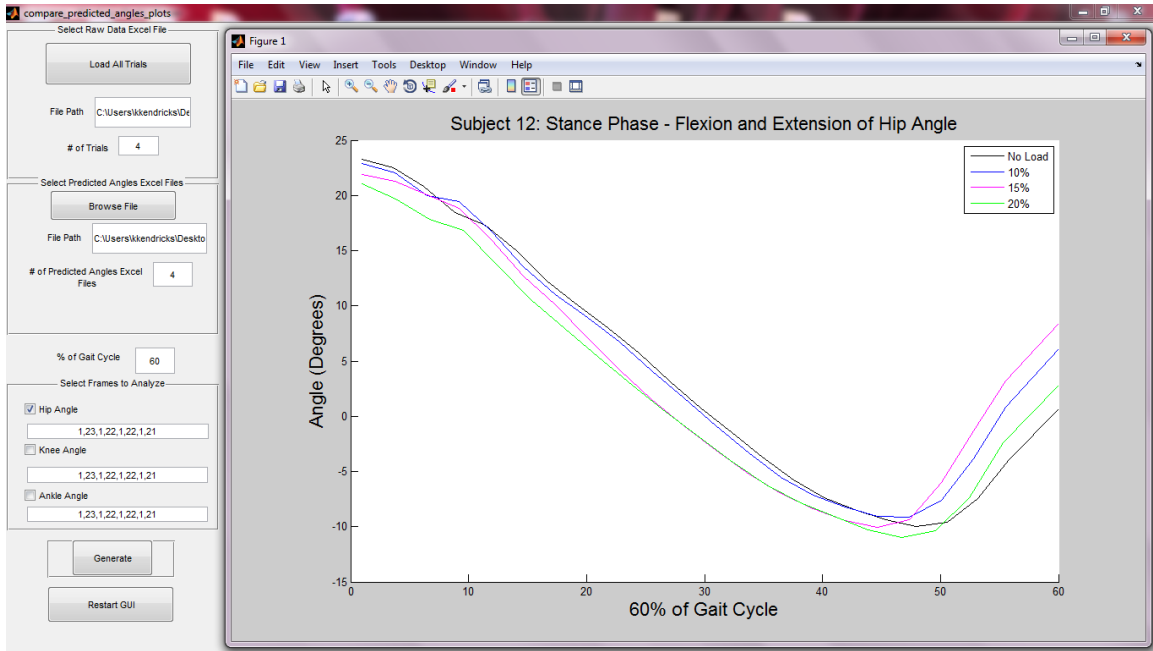
Figure 20. Graphical User Interface. GUI was created using MATLAB. This interface allowed us to process the data faster and more accurately. The excel files from the nexus software, containing (xyz) coordinates of the gait motion were imported into the GUI and predicted angles were calculated and graphed.

derived and verified in chapter 3, were pre-programmed into the GUI. Coordinates of the end effector (x_4, y_4), knee (x_2, y_2), and subject segment lengths, recorded in Table 3, were inputted into the equations, and respective joint angles were produced for each trial. The GUI interface produced an excel file for each trial, containing the joint angles, hip θ_1, knee θ_2, and ankle θ_3 for one full gait cycle. For every subject, their respective trials were graphed using the interface and the results are highlighted in the next chapter.

V. Data Analysis and Results

5.1 Chapter Overview

The objective of this research was to investigate lower extremity gait kinematic patterns, in specific joint angles of gait movement, in persons walking with and without extra load strapped on the upper and mid-torso of their body. The results and analysis presented in this chapter will show how the joint angles vary from the different scenarios. The results and analysis of the twelve subjects are presented in the following section.

5.2 Gait Joint Angles

The developed MATLAB GUI was able to produce a graphical representation of the subject's joint angles for the entire gait cycle. Figure 21, 22, and 23 show hip, knee, and ankle angles, respectively, plotted for all twelve subjects and for each trial. Trial 1 was excluded because it consisted of a static T-pose capture and did not actually contribute to the gait cycle joint analysis. Trial 2 for each subject consisted of one gait cycle without any load strapped on the body. The successive trials were of one gait cycle influenced by carrying extra load. The load was determined by the subject's body weight and Table 4 outlines the amount of weight each person carried with each trial. Due to the weight restrictions, not all subjects were able to walk with 15% and 20% additional load. The subjects were allowed to carry up to 26 pounds only.

Table 4. Weight (lbs) carried by each participant for their respective trials

Subject	10%	15%	20%
1	15	22	–
2	16	24	–
3	18	–	–
4	22	–	–
5	14	22	–
6	13	20	–
7	12	19	25
8	18	26	–
9	12	17	23
10	19	–	–
11	15	23	–
12	11	17	23
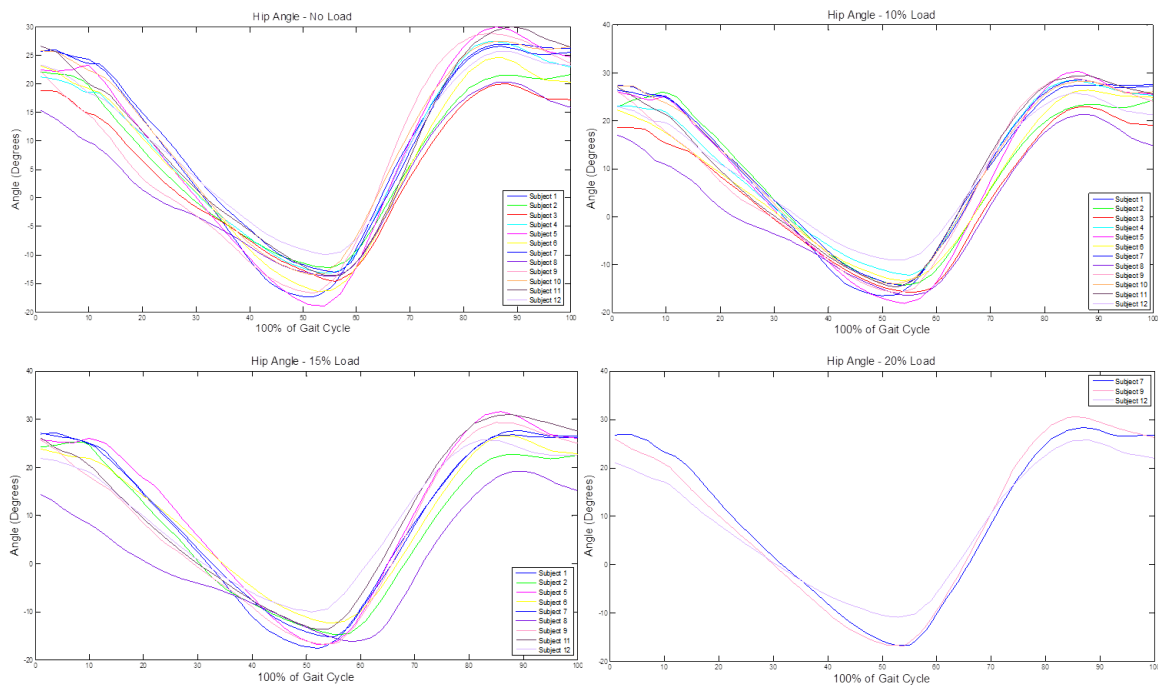
Figure 21. Hip Angle for Entire Gait Cycle. Hip joint angle plotted for each trial and for all 12 subjects: No Load top left, 10% Load top right, 15% bottom left, and 20% bottom right.

44
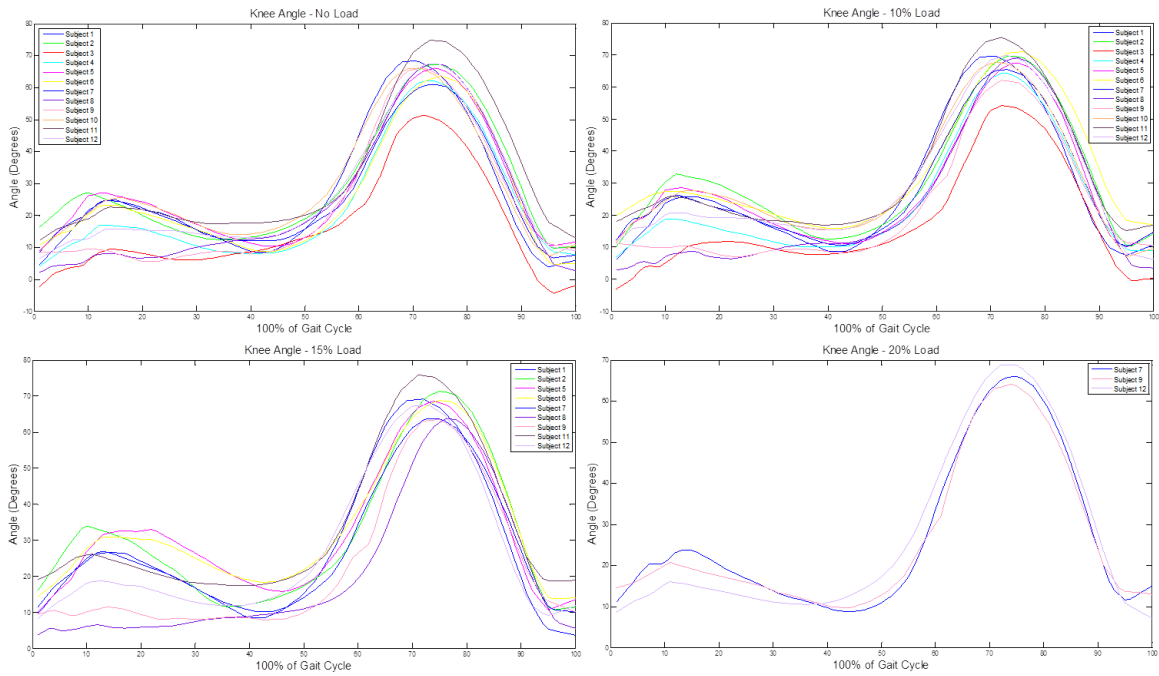
Figure 22. Knee Angle for Entire Gait Cycle. Knee joint angle plotted for each trial and for all 12 subjects: No Load top left, 10% Load top right, 15% bottom left, and 20% bottom right.
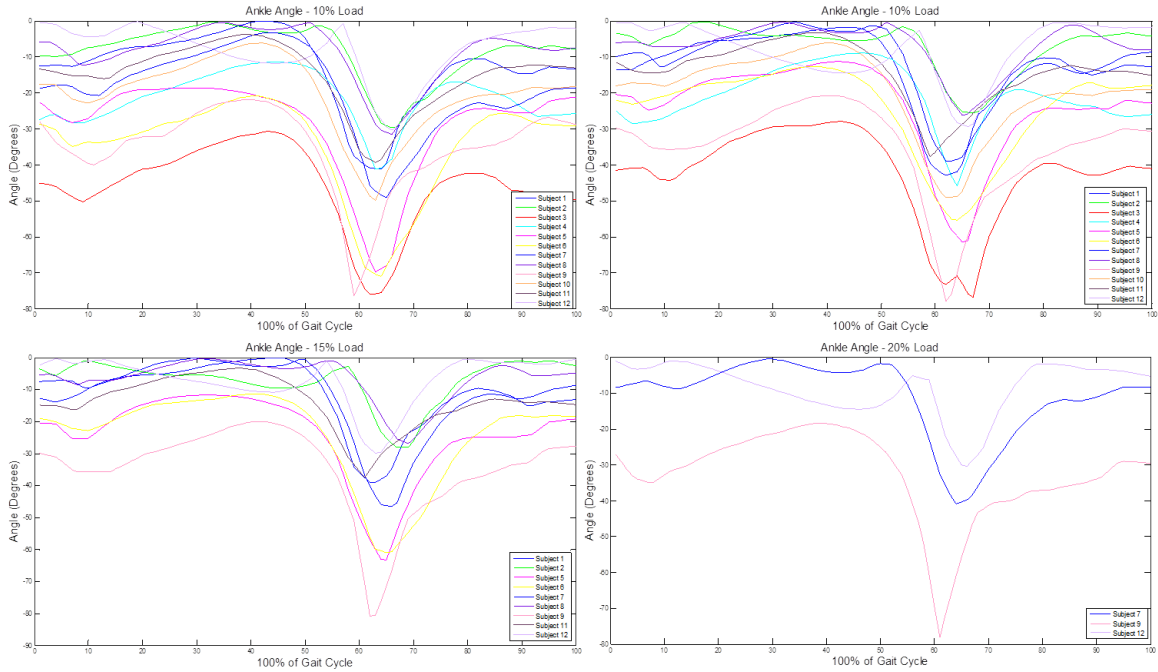
Figure 23. Ankle Angle for Entire Gait Cycle. Ankle joint angle plotted for each trial and for all 12 subjects: No Load top left, 10% Load top right, 15% bottom left, and 20% bottom right.

In order to get some insight on the behavior of the joint angles in gait motion, analysis was performed on one full gait cycle (100%) and the stance (60%), swing (40%) and transition phase (10%). Recall, that the gait cycle begins when the heel strikes the ground of one foot and ends when that same foot strikes the ground again. The stance phase begins with initial foot contact and accounts for the entire period of time while the foot is in contact with the ground. The swing phase begins with the toe off and accounts for the period of time when the foot is not in contact with the ground. The transition phase from stance to swing marks the shift of the body's weight on to the opposite leg. Hip, knee, and ankle joints were graphed and analyzed for each subject using the developed MATLAB GUI. The graphs are provided in Appendix D and they include the angles over the entire gait cycle, stance, and swing phase. Two forms of analysis were performed on the data obtained: angle variance and range of motion (ROM) for each joint angle due to carrying condition.

46

Gait Angle Variance.

One hundred points in the gait cycle were collected, and the MATLAB GUI produced the respective joint angles for those hundred points for each subject and each trial. Variance was graphed and calculated between the subjects gait while no load was carried vs. carrying 10%, 15%, or 20% additional load on the body. Figure 24, 25, and 26 show the gait variance plots while Table 5, 6, and 7 show the calculated gait variances for all subjects individually during the different phases of the gait cycle. Since no specific pattern could be detected by looking at each subject individually, average and standard deviations over all subjects were also calculated and the results are highlighted in their respective tables.

The calculated hip variance averages showed an increase of 0.54 degrees in hip angle during the stance phase with the addition of 10%, 0.80 degrees with 15%, and a decrease of 0.33 degrees with the addition of 20% load. With the hip swing phase, the results showed an increase of 0.71 degrees in angle with the addition of a 10% load and a smaller increase of 0.07 and 0.25 degrees in angle with the addition of 15% and 20% load, respectively. Lastly, for the hip's transition phase, the results showed an increase of 0.23 degrees in angle with the addition of 10% load and a decrease of 0.11 and 0.86 degrees in angle with the addition of 15% and 20% load. All the hip variance measured quantities are below one degree; therefore, no specific pattern is visible from increasing and decreasing load.

The calculated knee variance averages show an increase of 1.78, 2.38, and 0.95 degrees in angle during the stance phase with the addition of 10%, 15% and 20% additional load, respectively. The swing phase showed an increase of 1.57, 1.80, and 2.31 degrees in angle with the addition of 10%, 15%, and 20% load, respectively. Lastly, the transition phase of the knee angle showed an increase of 1.66 degrees with the addition of 10% an increase of 1.91 degrees with 15% load, and a decrease of

47

0.60 degrees in angle with the addition of 20% load. In contrast to the hip angle, the knee angle variances were higher than one degree, but all quantities were within three degrees.

The calculated ankle variance averages showed a constant increase in angle with both the stance and swing phase with the addition of extra load. During the stance phase, the average increase was 2.77 degrees for 10%, 3.54 degrees for 15% and 3.72 degrees for 20% additional load. Similarly for the swing phase, the average increase was 2.38 degrees for 10%, 2.68 degrees for 15% and 2.83 degrees for 20% additional load. The transition phase showed the greatest increase with 2.96 degrees for 10%, 4.69 degrees for 15% and 3.69 degrees for 20% additional load.
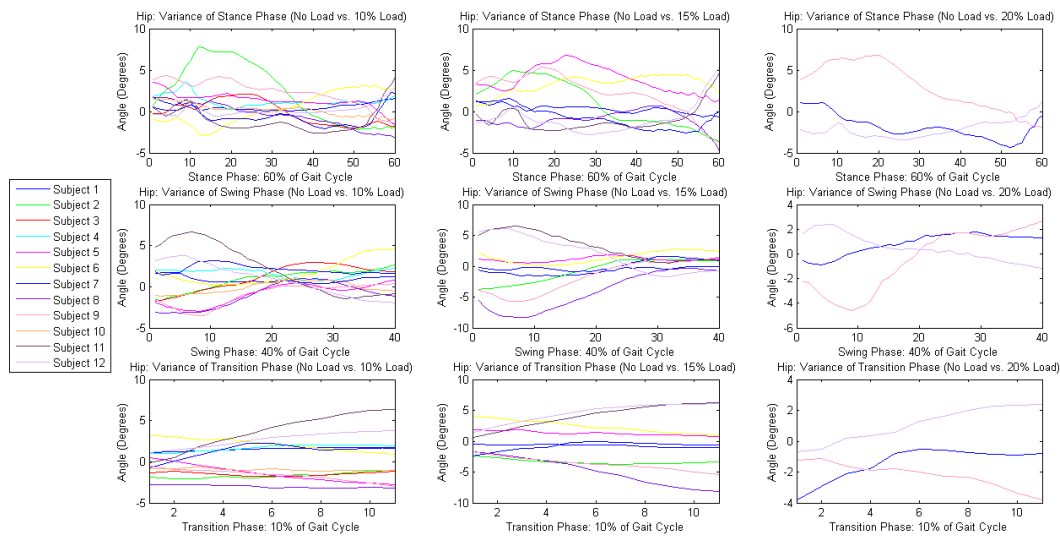
Figure 24. Hip Angle Variance. Variance was calculated and graphed for all twelve subjects. The figure shows the variance between load and no load influenced gait for the different phases.
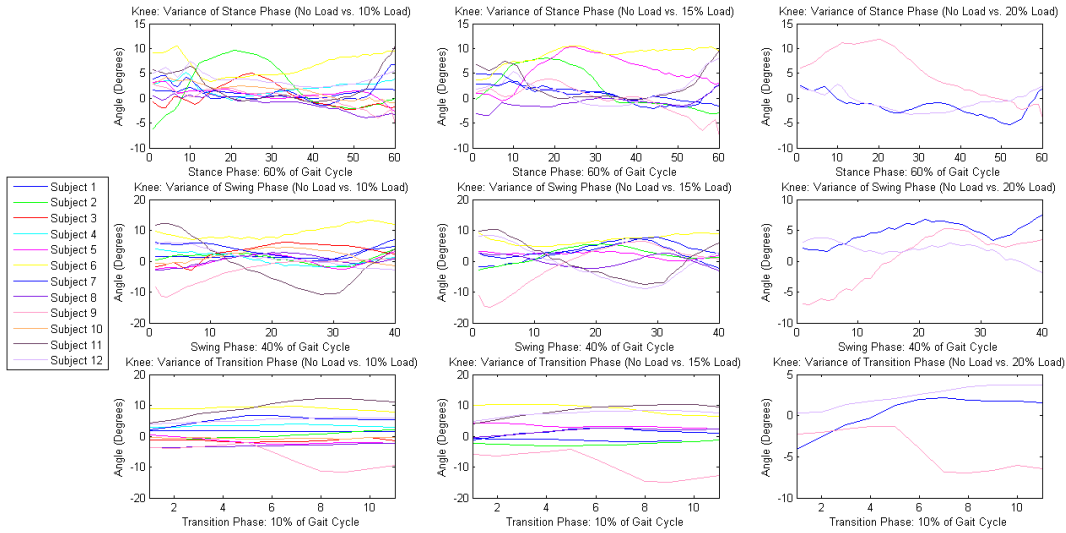
Figure 25. Knee Angle Variance. Variance was calculated and graphed for all twelve subjects. The figure shows the variance between load and no load influenced gait for the different phases.
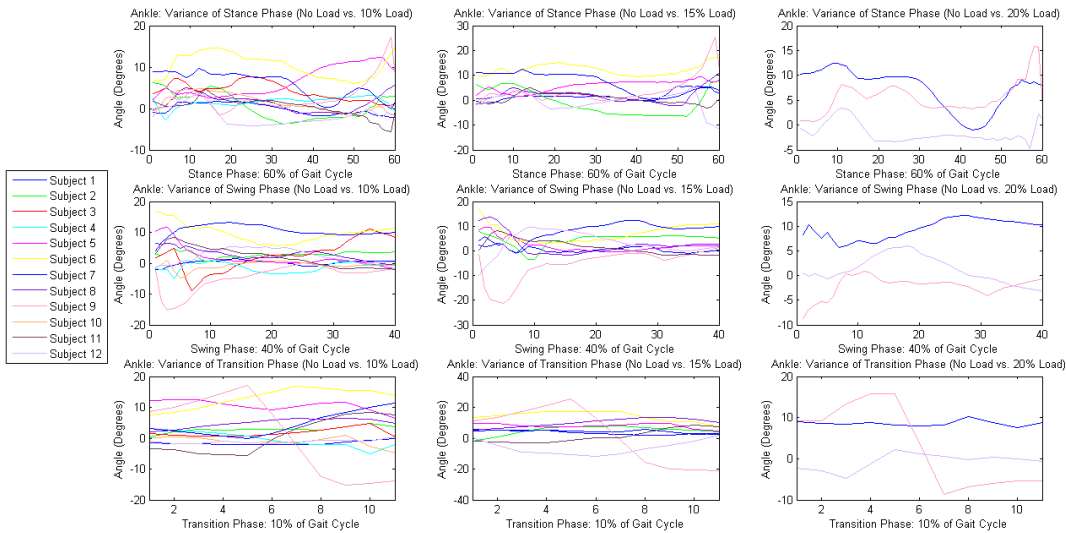
Figure 26. Ankle Angle Variance. Variance was calculated and graphed for all twelve subjects. The figure shows the variance between load and no load influenced gait for the different phases.

Table 5. Hip variance predicted for individual subjects' gait phases. Average and standard deviations were also calculated for all subjects combined.

Subject	Hip-Phase	No Load vs 10%	No Load vs 15%	No Load vs 20%
1	Stance	0.4750	0.2915	–
	Swing	0.8590	-0.8016	–
	Transition	1.5084	-0.7300	–
2	Stance	2.3681	1.0365	–
	Swing	0.9149	-0.6773	–
	Transition	-1.6730	-3.3034	–
3	Stance	-0.0914	–	–
	Swing	1.1471	–	–
	Transition	-1.4843	–	–
4	Stance	1.2801	–	–
	Swing	1.6408	–	–
	Transition	1.6755	–	–
5	Stance	1.3520	3.9031	–
	Swing	-0.8883	1.1019	–
	Transition	-1.4350	1.2862	–
6	Stance	0.3773	3.3267	–
	Swing	1.7330	1.4289	–
	Transition	2.1200	2.3824	–
7	Stance	-0.5105	-0.7572	-1.8827
	Swing	2.1219	0.1707	0.8241
	Transition	1.2949	-0.8031	-1.4286
8	Stance	-0.4511	-0.9806	–
	Swing	-1.0000	-4.0588	–
	Transition	-3.0138	-4.8879	–
9	Stance	2.3617	2.2529	2.9985
	Swing	-0.9474	-1.7167	-0.5252
	Transition	-1.6289	-3.6448	-2.2103
10	Stance	0.2429	–	–
	Swing	-0.1015	–	–
	Transition	-0.9357	–	–
11	Stance	-1.0430	-0.9923	–
	Swing	2.2081	3.2235	–
	Transition	3.7072	4.0691	–
12	Stance	0.1655	-0.8955	-2.1073
	Swing	0.8827	1.9788	0.4639
	Transition	2.6695	4.5792	1.0720
Average	Stance	0.5439 ± 1.4013	0.7983 ± 1.5360	-0.3305 ± 1.7957
	Swing	0.7142 ± 1.2813	0.0722 ± 1.6826	0.2542 ± 1.4678
	Transition	0.2337 ± 0.6940	-0.1169 ± 1.0924	-0.8556 ± 1.028

Table 6. Knee variance predicted for individual subjects' gait phases. Average and standard deviations were also calculated for all subjects combined.

Subject	Knee-Phase	No Load vs 10%	No Load vs 15%	No Load vs 20%
1	Stance	1.0054	1.2898	–
	Swing	1.7025	2.5309	–
	Transition	1.6877	-1.3205	–
2	Stance	2.3868	2.1919	–
	Swing	0.8812	2.1035	–
	Transition	-0.1608	-2.5698	–
3	Stance	0.3859	–	–
	Swing	3.1393	–	–
	Transition	-1.3594	–	–
4	Stance	2.1024	–	–
	Swing	0.6092	–	–
	Transition	3.3349	–	–
5	Stance	0.9344	5.5478	–
	Swing	-0.0904	2.0614	–
	Transition	-1.3247	3.4651	–
6	Stance	6.6678	8.7462	–
	Swing	9.4360	6.9958	–
	Transition	9.0618	9.1623	–
7	Stance	1.2583	0.6967	-1.5764
	Swing	3.4597	3.9535	4.6795
	Transition	4.7730	1.0761	-0.1646
8	Stance	-1.1132	-0.9344	–
	Swing	0.3853	0.0904	–
	Transition	-3.1869	1.3247	–
9	Stance	0.1843	-0.1720	5.1661
	Swing	-2.7297	-0.8709	0.4432
	Transition	-5.9955	-8.6126	-3.7136
10	Stance	1.6077	–	–
	Swing	1.8219	–	–
	Transition	-0.6250	–	–
11	Stance	2.1190	2.4329	–
	Swing	-1.0542	0.4295	–
	Transition	8.6636	7.6806	–
12	Stance	3.8601	1.6221	-0.7407
	Swing	1.2755	-1.1005	1.8175
	Transition	5.0709	7.0236	2.0706
Average	Stance	1.7832 ± 1.9350	2.3801 ± 2.4205	0.9496 ± 2.8970
	Swing	1.5697 ± 2.5910	1.7993 ± 3.3148	2.3134 ± 2.3729
	Transition	1.6616 ± 1.0953	1.9144 ± 1.4317	-0.6025 ± 1.9718

Table 7. Ankle variance predicted for individual subjects' gait phases. Average and standard deviations were also calculated for all subjects combined.

Subject	Ankle-Phase	No Load vs 10%	No Load vs 15%	No Load vs 20%
1	Stance	-0.1154	1.3756	–
	Swing	0.1840	0.5104	–
	Transition	-1.5959	3.4985	–
2	Stance	0.5827	-0.9175	–
	Swing	2.8402	4.5231	–
	Transition	2.8870	4.9944	–
3	Stance	4.2725	–	–
	Swing	2.5622	–	–
	Transition	1.7710	–	–
4	Stance	1.5571	–	–
	Swing	-1.2749	–	–
	Transition	-0.3263	–	–
5	Stance	6.4385	5.8168	–
	Swing	1.8313	2.1017	–
	Transition	10.5472	8.0057	–
6	Stance	10.3710	12.3147	–
	Swing	9.8111	7.0434	–
	Transition	13.0582	14.0313	–
7	Stance	5.7933	7.3575	7.2981
	Swing	10.5719	7.8714	9.4240
	Transition	4.4847	4.3772	8.6073
8	Stance	1.4259	1.9049	–
	Swing	2.8157	2.5481	–
	Transition	4.8727	9.9446	–
9	Stance	2.7150	3.7678	5.4824
	Swing	-4.5235	-5.4000	-2.1681
	Transition	1.1014	2.0878	3.1887
10	Stance	1.3976	–	–
	Swing	-0.7415	–	–
	Transition	-1.0272	–	–
11	Stance	0.4409	0.7042	–
	Swing	2.0816	1.6349	–
	Transition	0.7648	1.3867	–
12	Stance	-1.6255	-0.4460	-1.5915
	Swing	2.3885	3.3118	1.2243
	Transition	-1.0541	-6.0757	-0.7167
Average	Stance	2.7711 ± 2.4539	3.5420 ± 3.1210	3.7297 ± 3.0441
	Swing	2.3789 ± 2.4074	2.6828 ± 3.4625	2.8267 ± 2.2536
	Transition	2.9570 ± 3.1007	4.6945 ± 4.7129	3.6931 ± 4.1766

Gait Range of Motion.

Range of motion defines the angle's potential to move during the gait motion. ROM includes the maximum and minimum joint angles for a particular joint. The MATLAB GUI was capable of calculating the minimum and maximum angles of each trial for all the subjects collected. Each subject's gait performance was divided into the three phases (stance, swing, and transition) and minimum and maximum angles were determined for each trial, see Table 8. The purpose of this analysis was to determine the average ROM a person exhibits for a phase of the gait cycle with varying load conditions. Average and standard deviation over all subjects' ROM was also calculated and the results for the hip, knee, and ankle angle are shown in Tables 9, 10, and 11, respectively.

As seen in Table 9, that minimum and maximum ROM values for the hip's stance, swing and transition phase changed within a value of only two degrees with a standard deviation of at least two degrees. Consistent pattern was not seen for the ROM values in the hip angle.

As seen in Table 10, overall, the minimum and maximum knee angle values increased with increasing load during the stance and swing phase. For the transition phase, the minimum values increased with addition of 10% and 15% load and decreased with the addition of 20% load, while the maximum values overall increased with increasing load.

Table 11 showed the minimum and maximum values for the ankle joint and as seen from the values, this joint varied the most in comparison with hip and knee joint. Overall, minimum and maximum values increased for all phases of the gait cycle with the addition of load on the body. However, the standard deviation for the ankle angle was quite high to deduce any conclusions.

Table 8. Range of Motion predicted for individual subjects. Results show minimum and maximum angles (degrees) for each phase of the gait cycle for all trials.

Subject	Angle (Phase)	Min/Max	No Load	10% Load	15 %Load	20% Load
1	Hip(Stance)	Min	-17.2995	-16.5478	-17.6282	–
		Max	25.7982	26.3196	27.0818	–
	Hip(Swing)	Min	-5.9715	1.9695	-5.5077	–
		Max	26.9462	27.4711	26.7813	–
	Hip(Transition)	Min	-15.8341	-14.6771	-16.2444	–
		Max	1.0024	2.5889	-0.0916	–
	Knee(Stance)	Min	4.6568	6.2239	8.4624	–
		Max	51.9864	63.5970	52.7482	–
	Knee(Swing)	Min	3.7927	7.3793	3.6516	–
		Max	68.3772	69.7121	69.1686	–
	Knee(Transition)	Min	26.8380	28.7168	26.0643	–
		Max	62.7967	64.2567	61.5740	–
	Ankle(Stance)	Min	-40.8416	-43.0536	-39.6489	–
		Max	-0.0402	-1.7813	-0.0681	–
	Ankle(Swing)	Min	-41.3548	-41.6892	-39.6489	–
		Max	-10.4947	-10.2639	-9.5915	–
	Ankle(Transition)	Min	-19.7775	-21.2355	-15.1930	–
		Max	-41.2471	-42.8762	-39.1839	–
2	Hip(Stance)	Min	-12.2633	-14.3138	-14.7835	–
		Max	22.0515	26.0160	25.2590	–
	Hip(Swing)	Min	0.6316	-3.4467	-7.5802	–
		Max	21.6313	24.2568	22.6161	–
	Hip(Transition)	Min	-12.2456	-14.1516	-14.7042	–
		Max	-2.1912	-3.2454	-5.5472	–

Table 8 – continued from previous page

Subject	Angle (Phase)	Min/Max	No Load	10% Load	15% Load	20% Load
	Knee(Stance)	Min	12.4643	10.1761	11.5508	–
		Max	56.9092	52.9462	45.9290	–
	Knee(Swing)	Min	9.5787	9.7197	10.5322	–
		Max	67.0954	69.6713	71.4665	–
	Knee(Transition)	Min	24.8173	23.6377	22.3863	–
		Max	51.3524	53.2862	49.9940	–
	Ankle(Stance)	Min	-30.2089	-25.3766	-23.0858	–
		Max	-0.3349	-0.2155	-0.7941	–
	Ankle(Swing)	Min	-30.2089	-25.6786	-28.2604	–
		Max	-6.8212	-3.4290	-1.0170	–
	Ankle(Transition)	Min	-29.0919	-25.3887	-25.1557	–
		Max	-2.6894	-2.2047	-2.7421	–
3	Hip(Stance)	Min	-14.6838	-15.8497	–	–
		Max	18.7968	18.5418	–	–
	Hip(Swing)	Min	-10.5577	-12.2975	–	–
		Max	20.0347	22.9871	–	–
	Hip(Transition)	Min	-14.6320	-15.8299	–	–
		Max	-4.9628	-6.1054	–	–
	Knee(Stance)	Min	-2.1863	-2.9907	–	–
		Max	24.1200	22.5277	–	–
	Knee(Swing)	Min	-4.4461	-0.5500	–	–
		Max	51.3176	54.2216	–	–
	Knee(Transition)	Min	15.9604	14.7467	–	–
		Max	37.0828	35.6960	–	–
	Ankle(Stance)	Min	-76.0827	-73.8480	–	–

Table 8 – continued from previous page

Subject	Angle (Phase)	Min/Max	No Load	10% Load	15% Load	20% Load
		Max	-30.7274	-27.9773	–	–
	Ankle(Swing)	Min	-76.0827	-78.1123	–	–
		Max	-42.2865	-39.6603	–	–
	Ankle(Transition)	Min	-75.9828	-73.2637	–	–
		Max	-49.7651	-48.3377	–	–
4	Hip(Stance)	Min	-13.2381	-12.3172	–	–
		Max	21.2153	23.0138	–	–
	Hip(Swing)	Min	1.2902	4.8354	–	–
		Max	27.4532	28.2995	–	–
	Hip(Transition)	Min	-13.2321	-12.2741	–	–
		Max	-0.3739	1.5881	–	–
	Knee(Stance)	Min	4.1674	6.9538	–	–
		Max	50.0710	55.7669	–	–
	Knee(Swing)	Min	7.7716	8.8492	–	–
		Max	62.0598	64.7273	–	–
	Knee(Transition)	Min	16.7849	19.6202	–	–
		Max	46.8772	49.7403	–	–
	Ankle(Stance)	Min	-41.8164	-46.4788	–	–
		Max	-11.4122	-8.9701	–	–
	Ankle(Swing)	Min	-38.8875	-35.0986	–	–
		Max	-16.8923	-18.8870	–	–
	Ankle(Transition)	Min	-41.2071	-45.9098	–	–
		Max	-17.8414	-14.7067	–	–
5	Hip(Stance)	Min	-19.0354	-18.1229	-17.0067	–
		Max	23.3922	25.9714	26.0847	–
Continued on next page						

Table 8 – continued from previous page

Subject	Angle (Phase)	Min/Max	No Load	10% Load	15% Load	20% Load
	Hip(Swing)	Min	-6.2132	-2.1502	-0.9383	–
		Max	30.0050	30.3224	31.6429	–
	Hip(Transition)	Min	-18.2662	-17.8053	-16.4302	–
		Max	-0.9157	-3.7085	-0.1481	–
	Knee(Stance)	Min	9.0442	11.1479	10.0669	–
		Max	42.6154	50.3984	51.4244	–
	Knee(Swing)	Min	10.3960	9.8907	10.6624	–
		Max	66.1802	67.7226	68.6789	–
	Knee(Transition)	Min	20.3894	20.8386	24.7479	–
		Max	50.2330	48.0264	52.5622	–
	Ankle(Stance)	Min	-69.9391	-62.5810	-64.9964	–
		Max	-18.6132	-11.2323	-11.7588	–
	Ankle(Swing)	Min	-69.9391	-62.5810	-64.9964	–
		Max	-21.1720	-22.0458	-19.1688	–
	Ankle(Transition)	Min	-69.7345	-61.4347	-63.2957	–
		Max	-37.5344	-25.3183	-27.9878	–
6	Hip(Stance)	Min	-16.3973	-13.4351	-12.4007	–
		Max	23.1131	22.2168	23.8113	–
	Hip(Swing)	Min	-6.0899	-0.2879	-1.9406	–
		Max	24.7035	26.3552	26.6457	–
	Hip(Transition)	Min	-16.3343	-13.1526	-12.2683	–
		Max	-3.9486	-2.9937	-3.0496	–
	Knee(Stance)	Min	8.5660	15.6983	14.3911	–
		Max	41.5701	58.6789	54.2318	–
	Knee(Swing)	Min	4.6749	16.8822	13.7811	–

<div align="right">Continued on next page</div>

57

Table 8 – continued from previous page

Subject	Angle (Phase)	Min/Max	No Load	10% Load	15% Load	20% Load
		Max	63.6076	70.9618	68.7642	–
	Knee(Transition)	Min	18.1521	27.0934	28.2427	–
		Max	45.6689	53.5242	51.9882	–
	Ankle(Stance)	Min	-71.3679	-55.9706	-61.3930	–
		Max	-20.8069	-12.7076	-11.4079	–
	Ankle(Swing)	Min	-71.3679	-52.4172	-61.3930	–
		Max	-25.5993	-16.9661	-18.1867	–
	Ankle(Transition)	Min	-70.9715	-55.4020	-61.0081	–
		Max	-41.2320	-33.7403	-28.0433	–
7	Hip(Stance)	Min	-13.0931	-14.4729	-15.2938	-16.7517
		Max	26.0013	27.4021	27.1591	26.8838
	Hip(Swing)	Min	-0.9960	0.6887	1.5166	1.5894
		Max	26.6364	28.5208	27.6514	28.3601
	Hip(Transition)	Min	-13.0239	-13.6512	-15.2634	-16.7115
		Max	-0.8077	0.9292	-1.4477	-1.5773
	Knee(Stance)	Min	8.5173	10.4220	10.0073	8.6986
		Max	48.5474	53.8881	54.4523	55.5916
	Knee(Swing)	Min	6.5866	10.1208	10.0563	11.2739
		Max	61.1384	65.5133	63.7175	66.0823
	Knee(Transition)	Min	21.2707	23.2653	20.0705	17.1485
		Max	48.8128	54.1798	49.7282	50.4158
	Ankle(Stance)	Min	-49.3827	-39.3196	-46.5657	-40.9698
		Max	-3.2508	-0.3154	-0.1145	-0.4261
	Ankle(Swing)	Min	-49.3827	-38.0975	-46.5657	-39.3012
		Max	-18.6034	-8.6573	-8.7160	-8.2103
						Continued on next page

Table 8 – continued from previous page

Subject	Angle (Phase)	Min/Max	No Load	10% Load	15% Load	20% Load
	Ankle(Transition)	Min	-49.1126	-39.0603	-46.2800	-40.8864
		Max	-16.4101	-13.2322	-10.8969	-7.4319
8	Hip(Stance)	Min	-13.6616	-16.4387	-16.1591	–
		Max	15.3069	17.0056	14.2610	–
	Hip(Swing)	Min	2.4176	-2.2273	-4.6588	–
		Max	20.3490	21.3199	19.2844	–
	Hip(Transition)	Min	-13.6415	-16.4154	-16.1508	–
		Max	-4.0172	-7.2191	-12.2346	–
	Knee(Stance)	Min	2.2625	2.7966	3.7124	–
		Max	61.2358	57.7937	48.4076	–
	Knee(Swing)	Min	2.7519	3.4981	5.5568	–
		Max	67.6129	69.1577	63.6856	–
	Knee(Transition)	Min	23.6867	19.9155	13.4575	–
		Max	49.9862	47.5440	32.5750	–
	Ankle(Stance)	Min	-31.5238	-26.9048	-27.0661	–
		Max	-0.4844	-0.3607	-0.3380	–
	Ankle(Swing)	Min	-26.5085	-23.5466	-27.0661	–
		Max	-4.8262	-1.1463	-2.6052	–
	Ankle(Transition)	Min	-30.9945	-26.3303	-20.9561	–
		Max	-6.0250	-3.8740	-1.0443	–
9	Hip(Stance)	Min	-16.7216	-15.9938	-16.7694	-16.8265
		Max	22.1616	26.0342	25.6689	25.9539
	Hip(Swing)	Min	-3.0991	1.6553	-0.7438	-1.6457
		Max	28.8856	28.9954	29.2595	30.5761
	Hip(Transition)	Min	-14.8825	-15.3583	-16.6114	-16.1438

Table 8 – continued from previous page

Subject	Angle (Phase)	Min/Max	No Load	10% Load	15% Load	20% Load
		Max	3.5892	0.5813	-1.7900	-0.2078
	Knee(Stance)	Min	5.4128	6.8486	7.9227	9.7348
		Max	45.1894	49.7048	46.3638	47.7638
	Knee(Swing)	Min	9.5747	10.4620	10.1981	13.0293
		Max	66.1990	62.1163	63.4668	64.2318
	Knee(Transition)	Min	21.4021	17.7644	15.5631	19.1993
		Max	56.3448	47.0060	43.6486	49.9327
	Ankle(Stance)	Min	-76.9025	-79.8349	-83.7639	-78.0585
		Max	-21.8685	-20.7373	-20.1158	-18.3664
	Ankle(Swing)	Min	-64.3287	-61.4663	-69.2418	-58.9704
		Max	-26.6739	-30.0109	-27.6819	-28.9206
	Ankle(Transition)	Min	-76.3486	-78.0072	-80.8337	-78.0585
		Max	-45.9913	-37.4428	-34.6842	-36.7070
10	Hip(Stance)	Min	-13.4032	-14.0890	–	–
		Max	25.7648	27.2496	–	–
	Hip(Swing)	Min	-1.7048	0.8606	–	–
		Max	27.5436	28.1963	–	–
	Hip(Transition)	Min	-12.5355	-13.3306	–	–
		Max	2.5818	1.5730	–	–
	Knee(Stance)	Min	8.8905	11.8140	–	–
		Max	53.9122	58.7605	–	–
	Knee(Swing)	Min	7.1371	6.9942	–	–
		Max	66.1313	67.8080	–	–
	Knee(Transition)	Min	29.0551	28.5572	–	–

Table 8 – continued from previous page

Subject	Angle (Phase)	Min/Max	No Load	10% Load	15% Load	20% Load
		Max	60.0783	59.5662	–	–
	Ankle(Stance)	Min	-50.7048	-49.2025	–	–
		Max	-6.1130	-6.0212	–	–
	Ankle(Swing)	Min	-50.7048	-48.6439	–	–
		Max	-18.3330	-19.0921	–	–
	Ankle(Transition)	Min	-49.8414	-49.1299	–	–
		Max	-27.9003	-27.7789	–	–
11	Hip(Stance)	Min	-13.5881	-14.8585	-13.6685	–
		Max	26.5463	27.0210	26.1680	–
	Hip(Swing)	Min	-0.3716	-2.8053	1.3289	–
		Max	30.0481	29.4540	31.0141	–
	Hip(Transition)	Min	-13.5870	-13.7539	-13.0338	–
		Max	-3.4920	2.8935	2.7244	–
	Knee(Stance)	Min	12.2846	16.8747	17.3866	–
		Max	60.9412	55.2143	61.4150	–
	Knee(Swing)	Min	12.9427	14.9469	18.7347	–
		Max	74.7115	75.5159	75.7637	–
	Knee(Transition)	Min	24.3009	28.4991	28.1270	–
		Max	54.0053	65.1762	63.3870	–
	Ankle(Stance)	Min	-39.6724	-38.0905	-37.5912	–
		Max	-3.8007	-3.2909	-3.2751	–
	Ankle(Swing)	Min	-32.4989	-32.5226	-29.3551	–
		Max	-12.3399	-12.3538	-12.9236	–
	Ankle(Transition)	Min	-39.3070	-37.8397	-37.5912	–
					Continued on next page	

61

Table 8 – continued from previous page

Subject	Angle (Phase)	Min/Max	No Load	10% Load	15% Load	20% Load
		Max	-19.6925	-23.2169	-21.5616	–
12	Hip(Stance)	Min	-9.9467	-9.1338	-10.0824	-10.9585
		Max	23.2679	22.8833	21.8680	21.0365
	Hip(Swing)	Min	0.6799	6.0736	8.4029	2.8126
		Max	25.7253	25.7972	25.6714	25.7097
	Hip(Transition)	Min	-9.8137	-8.7145	-8.4006	-10.5280
		Max	-0.4174	3.3562	5.6912	1.9816
	Knee(Stance)	Min	6.5139	11.5251	8.2986	8.6303
		Max	53.7706	62.4038	62.9592	56.8917
	Knee(Swing)	Min	8.9826	6.1582	8.9577	7.0724
		Max	67.6337	69.9443	67.6862	68.7285
	Knee(Transition)	Min	25.1196	29.0825	29.8964	25.4350
		Max	51.6471	57.5784	59.0469	55.3475
	Ankle(Stance)	Min	-30.7804	-29.7189	-30.6440	-31.2822
		Max	-0.0654	-0.2979	-0.2443	-1.0050
	Ankle(Swing)	Min	-30.7804	-29.7189	-23.6670	-31.2822
		Max	-1.8757	-0.4149	-0.6024	-1.8590
	Ankle(Transition)	Min	-29.3829	-28.8629	-29.9119	-30.0026
		Max	-0.8425	-2.6825	-3.6371	-5.1590

Table 9. Hip: Range of Motion predicted during stance, swing, and transition phase of the gait cycle

Hip: Phase		No Load	10%	15%	20%
Min Stance	$\bar{x}$	-14.444	-14.631	-14.866	-14.846
	σ	2.504	2.335	2.452	3.367
Max Stance	$\bar{x}$	22.785	24.140	24.151	24.625
	σ	3.281	3.472	4.064	3.142
Min Swing	$\bar{x}$	-2.499	-0.594	-1.125	0.919
	σ	3.930	4.715	4.717	2.304
Max Swing	$\bar{x}$	25.830	26.831	26.730	28.215
	σ	3.498	2.765	3.925	2.436
Min Transition	$\bar{x}$	-14.002	-14.093	-14.345	-14.461
	σ	2.190	2.299	2.709	3.418
Max Transition	$\bar{x}$	-1.163	-0.813	-1.766	0.066
	σ	2.688	3.659	5.085	1.795

Table 10. Knee: Range of Motion predicted during stance, swing, and transition phase of the gait cycle

Knee: Phase		No Load	10%	15%	20%
Min Stance	$\bar{x}$	6.716	8.958	10.200	9.021
	σ	4.183	5.460	3.953	0.619
Max Stance	$\bar{x}$	49.239	53.473	53.103	53.416
	σ	10.184	10.643	6.033	4.938
Min Swing	$\bar{x}$	6.304	8.480	10.032	10.459
	σ	4.628	4.744	4.640	3.061
Max Swing	$\bar{x}$	65.172	67.256	68.044	66.348
	σ	5.562	5.317	4.066	2.260
Min Transition	$\bar{x}$	22.315	23.478	23.173	20.594
	σ	4.043	4.921	5.797	4.316
Max Transition	$\bar{x}$	51.240	52.965	51.612	51.899
	σ	6.772	8.209	9.528	2.997

Table 11. Ankle: Range of Motion predicted during stance, swing, and transition phase of the gait cycle

Ankle: Phase		No Load	10%	15%	20%
Min Stance	$\bar{x}$	-50.769	-47.532	-46.084	-50.103
	σ	18.121	17.704	20.170	24.690
Max Stance	$\bar{x}$	-9.793	-7.826	-5.346	-6.599
	σ	10.634	9.028	7.309	10.195
Min Swing	$\bar{x}$	-48.504	-44.131	-43.355	-43.185
	σ	17.917	16.829	17.905	14.247
Max Swing	$\bar{x}$	-17.160	-15.244	-11.166	-12.997
	σ	11.172	11.779	9.257	14.151
Min Transition	$\bar{x}$	-48.479	-45.155	-42.247	-49.649
	σ	20.226	18.899	22.224	25.198
Max Transition	$\bar{x}$	-25.598	-22.951	-18.865	-16.433
	σ	17.418	15.853	14.623	17.595

VI. Conclusions and Future Work

6.1 Chapter Overview

This chapter consists of two sections. The first section summarizes the results obtained from performing the two analysis in Chapter 5. The second section presents recommendations for future research on investigating gait patterns to obtain an understanding on the walking behavior of a suicide bomber.

6.2 Conclusions

The purpose and objective of this project was to contribute to the the gait cycle analysis study under the INSPIRE project and investigate the lower extremity kinematic behavior during the gait cycle to provide insight on the walking signatures of a potential suicide bomber. The goal was to distinguish between a person walking with and without load strapped on to the upper and mid-torso of the body. The data collection and analysis produced does show some variation between load and unloaded gait, however, more investigation is needed to make any rational conclusions. The next two sections give a detailed explanation of the conclusions derived from the analysis of the data.

Gait Variance.

Gait joint angle variance was calculated and reported for each subject and trial for the different phases of the gait cycle. Based on the average reported results over all subjects, all measurements were within 2.3 degrees, therefore no significant variation was seen in the hip or the knee angle. The greatest average variance was seen in the ankle angle, but, due to the high standard deviation calculated, no definitive conclusions can be made about the results.

While looking at individual subject's gait, subject 8 showed the greatest angle variance for the different gait phases of the hip joint, with a decrease of hip angle with the addition of 10% load. Subject 11 also showed more variation in the hip angle in comparison to the other subjects, but exhibited a decrease of hip angle in stance phase and an increase in swing and transition phase with additional load. An increase in hip angle shows the subject moving towards flexion, while a decrease in angle shows extension. Due to the inconsistency with the two subjects, no conclusion could be drawn for the hip angle variance seen in the different phases of the gait cycle with the additional load.

For the knee angle, subjects 5, 6, 9, and 12, all females, showed the greatest variance with the addition of load. Subject 5, 6, 9, and 12 all showed an increase in knee angle stance phase with the addition of 10% load with subjects 5 and 6 showing an increase of more than five degrees in the stance phase with the addition of 15% load. Subject 6 alone, showed an increase of more than six degrees for knee swing and transition phase with the addition of 10% and 15% load. An increase in knee angle shows the subject moving towards increased flexion and a decrease in angle shows decreased flexion. Recall the studies conducted by Wittman et al., Kinoshita, and Knapik et al. on load influenced gait patterns, [48, 31, 32]. The researchers concluded a proportional correlation between knee flexion and increased carrying load. Similar pattern was seen with subject 5 during all phases, subject 6 during stance and transition, subject 9 during swing, and subject 12 during transition phase of the gait cycle. Although all female subjects showed the greatest variance, no consistent increase or decrease in knee angles was seen for these subjects. In order to make any conclusions about the correlation between knee variance and increased load on female subjects, more data would have to be acquired that showed a variety of females with varying body mass. A more diverse subject pool will give insight on whether gait variance is

correlated with gender or subject's weight.

For the ankle angle, subjects 5, 6, 7, and 8 showed the greatest angle variance between the different loads. All four subjects increased in ankle angles with all phases of the gait cycle with the addition of load. Again, subject 6, female, exhibited the most change with up to thirteen and fourteen degrees of increased ankle angle with the addition of 10% and 15% load, respectively. An increase in ankle angle shows the subject moving towards dorsiflexion, while a decrease in ankle angle shows plantarflexion. Even though four out of twelve subject showed an increase in dorsiflexion with increased load more data needs to be captured to verify these results.

Range of Motion.

The standard clinical range of motion for the hip, knee, and ankle angles are displayed in Figure 27. The figure shows ROM values for the entire gait cycle: -10 to 30 degrees for the hip angle, 0 to 60 degrees for the knee angle, and -20 to 10 degrees for the ankle angle. Our analysis divided each subject's gait in three phases (stance, swing, and transition) and evaluated the ROM individually. The greatest average change in ROM was seen with the ankle angle, but due to the high standard deviation calculated, no rational conclusion could be drawn from the results. We believe that the high standard deviation could be due to the inverse kinematic model which was not validated 100% for the ankle angle. Recall from Chapter 3, the hip and the knee solutions were validated 100% for at least one solution while the ankle angle produced a minimum of 6% error. When comparing the predicted ankle ROM from our experiment, to actual ankle ROM values for an average human gait, one can see a marked variation in the overall angles. Specifically, the normal ROM values range from -20 to 10 degrees in the stance phase and 0 to -20 degrees in the swing phase of the gait cycle; however, values predicted in this experiment with no additional load

range from -9 to -50 degrees for the stance phase and -17 to -48 degrees for the swing phase of the gait cycle. The immense difference in the measured and predicted angles could be due to the unvalidated portions of the gait model. Further investigation will discover the source of the error introduced during validation which will give us a better understanding of the skewed values observed during the ankle angle's ROM.

In conclusion, with the small sample of subjects captured, no proportional conclusions can be drawn for variances between load carriage or angle's exhibited ROM values. Female subjects showing an increase in knee flexion during heavy load carriage suggest further investigation with a bigger sample size may lead to a positive logical conclusion. The inverse kinematic model not being fully validated for the ankle angle may have skewed the values produced in the data analysis. Further inspection of the inverse kinematics and a reduction of the Groebner basis equations could help determine the source of error.
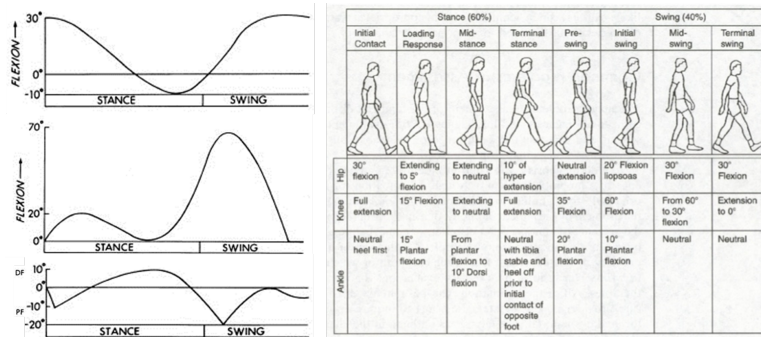
Figure 27. Standard Range of Motion. The figure shows the standard ROM exhibited for an average human during their gait cycle. Top left figure represents the hip angle, middle left figure is the knee angle, and bottom left figure is the ankle angle [39]. PF and DF stand for plantarflexion and dorsiflexion, respectively. Figure on the right shows the angles measured for an average human being during different phases of the gait cycle [15].

6.3   Future Work

A few possible courses for future work will briefly be outlined in this section. The first course deals with the inverse kinematic derived equations and the applications

of Groebner basis theory. The second course considers data collection techniques and recommendations for their improvement.

As seen previously, the inverse kinematic model derived in Chapter 3 was not validated 100% for the ankle motion during the gait cycle. The error from the validation could have introduced skewed values into the data analysis. Therefore, validation of the solutions to the model is highly recommended for future analysis. Also, recall the solutions derived from the system of equations produced only partial solutions with certain variables acting as denominators of the rational terms in equations (7) - (12). A future recommendation would be to find all the solutions to the inverse kinematic problem by reanalyzing the system of equations and solving them for cases where those listed variables equal zero.

Recommendations on data collection include collecting a larger sample size. This research investigated joint angle motion for twelve subjects. Not only a bigger sample size is recommended, but also recruiting a good number of both females and males would develop a strong database. An exploration of lower joint kinematics under greater load should be incorporated into the experiment. Due to the weight restrictions for this experiment, the subjects were not allowed to exceed carrying 26 pounds. With that restriction, not all subjects were able to walk with 15% and 20% additional load causing a weaker database. Studies have shown that suicide bombs on average weight 15 to 40 pounds, depending on their construction and the amount of explosives included [25] . Experimenting in the higher range could give us more insight on the walking behavior of a suicide bomber. The next recommendation is to use a tight fit VICON body suit for subjects with a thinner body profile. People with thinner body profiles had more difficulty keeping the markers at the same location through out the data capture. Due to the loose clothing, the markers could have moved causing the data to alter. Research on accurate marker placement on clothing versus skin should

be investigated and incorporated into the experiment. The participants could walk in tighter fit clothing or shorts to ensure marker placement on the bony prominence.

Appendix A. MAGMA code for Calculating the Groebner Basis

(1) SetVerbose(Groebner,1);

(2) Q:= RationalField();

(3) F<L1,L2,L3,x4,y4,y2>:= FunctionField (Q,6);

(4) P<c3,s3,c2,s2,c1,s1>:= PolynomialRing(F,6,"lex");

(5) f1:= L1*c1 + L2*c1*c2 + L3*c1*c2*c3 - L2*s1*s2 - L3*c3*s1*s2 - L3*c2*s1*s3 - L3*c1*s2*s3-x4;

(6) f2:= L1*s1 + L2*c2*s1 + L3*c2*c3*s1 + L2*c1*s2 + L3*c1*c3*s2 + L3*c1*c2*s3 - L3*s1*s2*s3-z4;

(7) f3:= $c1^2 + s1^2$ - 1;

(8) f4:= $c2^2 + s2^2$ - 1;

(9) f5:= $c1^3 + s1^3$ - 1;

(10) f6:= (z2/L1) - s1;

(11) I:=ideal<P|f1,f2,f3,f4,f5,f6>;

(12) G:=GroebnerBasis(I);

(13) G;

Line (1): Sets the verbosity level for the Groebner basis algorithm.

Line (2): Creates a Rational Field which is used as the coefficient ring for a polynomial ring. A rational field is created when rational numbers together with certain operation of addition and multiplication form a field.

Line (3): A fucntion field allows the listed variables to act as coefficient

Line (4): Forms a polynomial ring from the set of polynomials in one or more variables with coefficients in another ring.

Line (5) - Line (10): Defines the system of equations.

Line (11): Defining I as an ideal containing the system of equations. An ideal is a subset of a ring that was defined above.

Line (12): Defining G as a Groebner basis which is a particular subset of an ideal I in a polynomial ring

Line (13): Calculates a Groebner basis for the given equations

Appendix B. Code of Calculating Root Mean Square Error (RMSE) using MATLAB

(1) measured = VICON's PIG model angle;

(2) predicted = Inverse Kinematic model angle ;

(3) difference = single(measured) - single(predicted);

(4) squaredError = difference .^2;

(5) meanSquaredError = sum(squaredError(:)) / numel(measured);

(6) rmsError = sqrt(meanSquaredError)

Appendix C. Expanded Groebner Basis

Variables $a, b, c, ..., x$ are defined below.

These variables correlate with Equations (7) - (12)

$\mathbf{a} = L1^4 * x4 - L1^2 * x4^3 - L1^2 * x4 * y4^2$

$\mathbf{b} = L1^4 * L3 - L1^2 * L3 * x4^2 - 2 * L1^2 * L3 * y4 * y2 + L3 * x4^2 * y2^2 + L3 * y4^2 * y2^2$

$\mathbf{c} = -L1^5 + L1^3 * x4^2 - L1^3 * y4^2 + 3 * L1^3 * y4 * y2 + L1 * x4^2 * y4 * y2 - 2 * L1 * x4^2 * y2^2 + L1 * y4^3 * y2 - 2 * L1 * y4^2 * y2^2$

$\mathbf{d} = L1^4 * L3 - L1^2 * L3 * x4^2 - 2 * L1^2 * L3 * y4 * y2 + L3 * x4^2 * y2^2 + L3 * y4^2 * y2^2$

$\mathbf{e} = 0.5 * L1^5 * y4 + 0.5 * L1^3 * L2^2 * y4 - 0.5 * L1^3 * L3^2 * y4 - 0.5 * L1^3 * x4^2 * y4 + 0.5 * L1^3 * x4^2 * y2 + 0.5 * L1^3 * y4^3 - 1.5 * L1^3 * y4^2 * y2 - 0.5 * L1 * L2^2 * x4^2 * y2 - 0.5 * L1 * L2^2 * y4^2 * y2 + 0.5 * L1 * L3^2 * x4^2 * y2 + 0.5 * L1 * L3^2 * y4^2 * y2 - 0.5 * L1 * x4^4 * y2 - L1 * x4^2 * y4^2 * y2 + L1 * x4^2 * y4 * y2^2 - 0.5 * L1 * y4^4 * y2 + L1 * y4^3 * y2^2$

$\mathbf{f} = L1^4 * L2 * L3 - L1^2 * L2 * L3 * x4^2 - 2 * L1^2 * L2 * L3 * y4 * y2 + L2 * L3 * x4^2 * y2^2 + L2 * L3 * y4^2 * y2^2$

$\mathbf{g} = -0.5 * L1^4 * x4 * y4 - 0.5 * L1^4 * x4 * y2 + 0.5 * L1^2 * L2^2 * x4 * y4 - 0.5 * L1^2 * L2^2 * x4 * y2 - 0.5 * L1^2 * L3^2 * x4 * y4 + 0.5 * L1^2 * L3^2 * x4 * y2 + 0.5 * L1^2 * x4^3 * y4 + 0.5 * L1^2 * x4^3 * y2 + 0.5 * L1^2 * x4 * y4^3 - 0.5 * L1^2 * x4 * y4^2 * y2 + 2 * L1^2 * x4 * y4 * y2^2 - x4^3 * y2^3 - x4 * y4^2 * y2^3$

$\mathbf{h} = L1^4 * L2 * L3 - L1^2 * L2 * L3 * x4^2 - 2 * L1^2 * L2 * L3 * y4 * y2 + L2 * L3 * x4^2 * y2^2 + L2 * L3 * y4^2 * y2^2$

$$\mathbf{i} = -L1^3 * y4 + L1 * x4^2 * y2 + L1 * y4^2 * y2$$

$$\mathbf{j} = L1^4 - L1^2 * x4^2 - 2 * L1^2 * y4 * y2 + x4^2 * y2^2 + y4^2 * y2^2$$

$$\mathbf{k} = -L1^2 * x4 * y4 + L1^2 * x4 * y2$$

$$\mathbf{l} = L1^4 - L1^2 * x4^2 - 2 * L1^2 * y4 * y2 + x4^2 * y2^2 + y4^2 * y2^2$$

$$\mathbf{m} = -0.5 * L1^4 * x4 + 0.5 * L1^2 * L2^2 * x4 - 0.5 * L1^2 * L3^2 * x4 + 0.5 * L1^2 * x4^3 + 0.5 * L1^2 * x4 * y4^2$$

$$\mathbf{n} = L1^4 * L2 - L1^2 * L2 * x4^2 - 2 * L1^2 * L2 * y4 * y2 + L2 * x4^2 * y2^2 + L2 * y4^2 * y2^2$$

$$\mathbf{o} = 0.5 * L1^5 + 0.5 * L1^3 * L2^2 - 0.5 * L1^3 * L3^2 - 0.5 * L1^3 * x4^2 + 0.5 * L1^3 * y4^2 - 1.5 * L1^3 * y4 * y2 - 0.5 * L1 * L2^2 * y4 * y2 + 0.5 * L1 * L3^2 * y4 * y2 - 0.5 * L1 * x4^2 * y4 * y2 + L1 * x4^2 * y2^2 - 0.5 * L1 * y4^3 * y2 + L1 * y4^2 * y2^2$$

$$\mathbf{p} = L1^4 * L2 - L1^2 * L2 * x4^2 - 2 * L1^2 * L2 * y4 * y2 + L2 * x4^2 * y2^2 + L2 * y4^2 * y2^2$$

$$\mathbf{q} = -L1^4 * y4 - L1^2 * L2^2 * y4 + L1^2 * L3^2 * y4 + 2 * L1^2 * x4^2 * y4 - 2 * L1^2 * y4^3 + 4 * L1^2 * y4^2 * y2 - L2^2 * x4^2 * y4 + 2 * L2^2 * x4^2 * y2 - L2^2 * y4^3 + 2 * L2^2 * y4^2 * y2 + L3^2 * x4^2 * y4 - 2 * L3^2 * x4^2 * y2 + L3^2 * y4^3 - 2 * L3^2 * y4^2 * y2 - x4^4 * y4 - 2 * x4^2 * y4^3 + 4 * x4^2 * y4^2 * y2 - 4 * x4^2 * y4 * y2^2 - y4^5 + 4 * y4^4 * y2 - 4 * y4^3 * y2^2$$

$$\mathbf{r} = L1^4 * L2 - 2 * L1^2 * L2 * x4^2 + 2 * L1^2 * L2 * y4^2 - 4 * L1^2 * L2 * y4 * y2 + L2 * x4^4 + 2 * L2 *$$

$$x4^2*y4^2 - 4*L2*x4^2*y4*y2 + 4*L2*x4^2*y2^2 + L2*y4^4 - 4*L2*y4^3*y2 + 4*L2*y4^2*y2^2$$

$$\mathbf{s} = L1^4*x4*y2 - 2*L1^2*L2^2*x4*y4 + L1^2*L2^2*x4*y2 + 2*L1^2*L3^2*x4*y4 -$$
$$L1^2*L3^2*x4*y2 - 2*L1^2*x4^3*y2 + 2*L1^2*x4*y4^2*y2 - 4*L1^2*x4*y4*y2^2 +$$
$$L2^2*x4^3*y2 + L2^2*x4*y4^2*y2 - L3^2*x4^3*y2 - L3^2*x4*y4^2*y2 + x4^5*y2 + 2*x4^3*$$
$$y4^2*y2 - 4*x4^3*y4*y2^2 + 4*x4^3*y2^3 + x4*y4^4*y2 - 4*x4*y4^3*y2^2 + 4*x4*y4^2*y2^3$$

$$\mathbf{t} = L1^5*L2 - 2*L1^3*L2*x4^2 + 2*L1^3*L2*y4^2 - 4*L1^3*L2*y4*y2 + L1*$$
$$L2*x4^4 + 2*L1*L2*x4^2*y4^2 - 4*L1*L2*x4^2*y4*y2 + 4*L1*L2*x4^2*y2^2 +$$
$$L1*L2*y4^4 - 4*L1*L2*y4^3*y2 + 4*L1*L2*y4^2*y2^2$$

$$\mathbf{u} = -0.5*L1^6*x4 + L1^4*x4^3 - L1^4*x4*y4^2 + 2*L1^4*x4*y4*y2 + 0.5*L1^2*$$
$$L2^4*x4 - L1^2*L2^2*L3^2*x4 + 2*L1^2*L2^2*x4*y4^2 - 2*L1^2*L2^2*x4*y4*$$
$$y2 + 0.5*L1^2*L3^4*x4 - 0.5*L1^2*x4^5 - L1^2*x4^3*y4^2 + 2*L1^2*x4^3*y4*y2 -$$
$$2*L1^2*x4^3*y2^2 - 0.5*L1^2*x4*y4^4 + 2*L1^2*x4*y4^3*y2 - 2*L1^2*x4*y4^2*$$
$$y2^2 - 2*L2^2*x4^3*y4*y2 + 2*L2^2*x4^3*y2^2 - 2*L2^2*x4*y4^3*y2 + 2*L2^2*x4*y4^2*y2^2$$

$$\mathbf{v} = L1^5*L2^2 - 2*L1^3*L2^2*x4^2 + 2*L1^3*L2^2*y4^2 - 4*L1^3*L2^2*y4*y2 + L1*$$
$$L2^2*x4^4 + 2*L1*L2^2*x4^2*y4^2 - 4*L1*L2^2*x4^2*y4*y2 + 4*L1*L2^2*x4^2*$$
$$y2^2 + L1*L2^2*y4^4 - 4*L1*L2^2*y4^3*y2 + 4*L1*L2^2*y4^2*y2^2$$

$$\mathbf{w} = 0.25*L1^8 - 0.5*L1^6*L2^2 - 0.5*L1^6*L3^2 - 0.25*L1^6*x4^2 + 0.75*L1^6*y4^2 - 1.5*L1^6*$$
$$y4*y2 + 0.25*L1^4*L2^4 - 0.5*L1^4*L2^2*L3^2 + L1^4*L2^2*x4^2 + 2*L1^4*L2^2*y4*y2 + 0.25*$$
$$L1^4*L3^4 + L1^4*L3^2*x4^2 - L1^4*L3^2*y4^2 + 2*L1^4*L3^2*y4*y2 - 0.25*L1^4*x4^4 + 0.5*L1^4*$$
$$x4^2*y4^2 - L1^4*x4^2*y4*y2 + L1^4*x4^2*y2^2 + 0.75*L1^4*y4^4 - 3*L1^4*y4^3*y2 + 3*L1^4*$$
$$y4^2*y2^2 + 0.25*L1^2*L2^4*x4^2 + 0.25*L1^2*L2^4*y4^2 - 0.5*L1^2*L2^4*y4*y2 - 0.5*L1^2*$$

$L2^2*L3^2*x4^2-0.5*L1^2*L2^2*L3^2*y4^2+L1^2*L2^2*L3^2*y4*y2-0.5*L1^2*L2^2*x4^4-2*L1^2*L2^2*x4^2*y4*y2-L1^2*L2^2*x4^2*y2^2+0.5*L1^2*L2^2*y4^4-3*L1^2*L2^2*y4^2*y2^2+0.25*L1^2*L3^4*x4^2+0.25*L1^2*L3^4*y4^2-0.5*L1^2*L3^4*y4*y2-0.5*L1^2*L3^2*x4^4-L1^2*L3^2*x4^2*y4^2+2*L1^2*L3^2*x4^2*y4*y2-2*L1^2*L3^2*x4^2*y2^2-0.5*L1^2*L3^2*y4^4+2*L1^2*L3^2*y4^3*y2-2*L1^2*L3^2*y4^2*y2^2+0.25*L1^2*x4^6+0.75*L1^2*x4^4*y4^2-1.5*L1^2*x4^4*y4*y2+L1^2*x4^4*y2^2+0.75*L1^2*x4^2*y4^4-3*L1^2*x4^2*y4^3*y2+4*L1^2*x4^2*y4^2*y2^2-2*L1^2*x4^2*y4*y2^3+0.25*L1^2*y4^6-1.5*L1^2*y4^5*y2+3*L1^2*y4^4*y2^2-2*L1^2*y4^3*y2^3+L2^2*x4^4*y2^2+2*L2^2*x4^2*y4*y2^3-L2^2*y4^4*y2^2+2*L2^2*y4^3*y2^3$

$\mathbf{x} = L1^6*L2^2 - 2*L1^4*L2^2*x4^2 + 2*L1^4*L2^2*y4^2 - 4*L1^4*L2^2*y4*y2 + L1^2*L2^2*x4^4 + 2*L1^2*L2^2*x4^2*y4^2 - 4*L1^2*L2^2*x4^2*y4*y2 + 4*L1^2*L2^2*x4^2*y2^2 + L1^2*L2^2*y4^4 - 4*L1^2*L2^2*y4^3*y2 + 4*L1^2*L2^2*y4^2*y2^2$

Appendix D. Gait Angles Plotted for Individual Subjects

The graphical representations below show the gait angle motion graphs produced by the MATLAB GUI. The data was plotted for each subject's gait performance for each trial of the gait cycle, excluding trial 1 static capture. The graphs show subject's entire gait cycle, stance and swing phase.
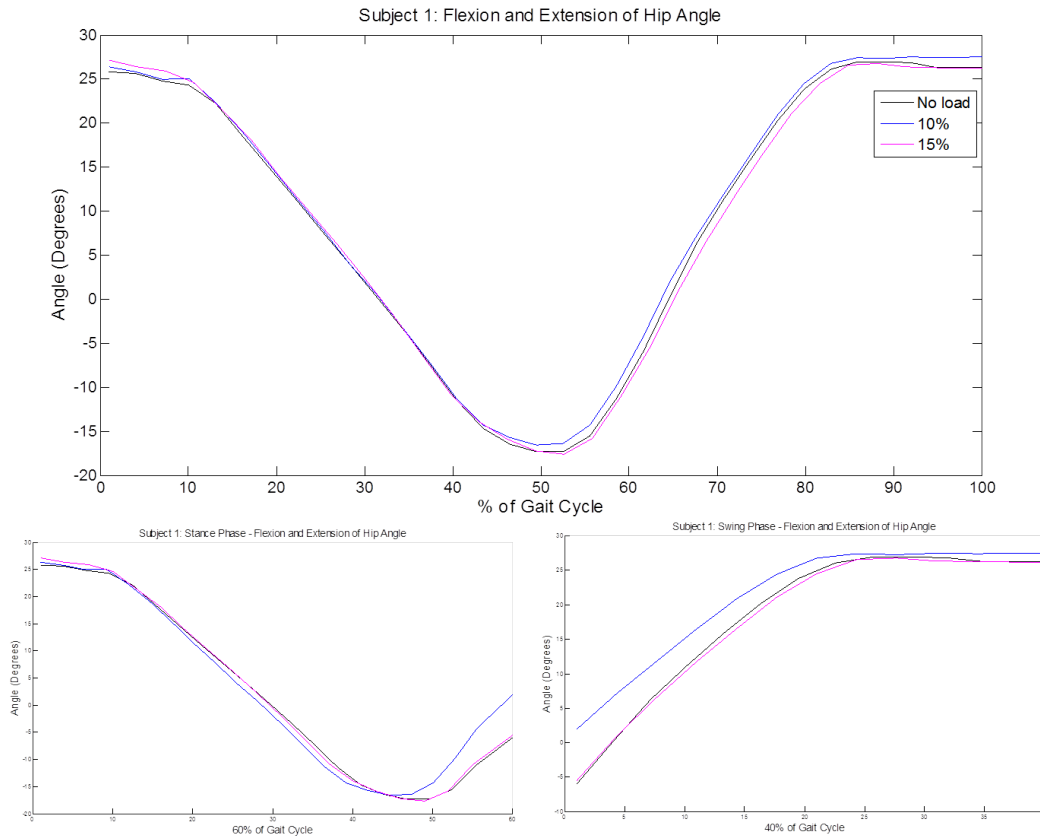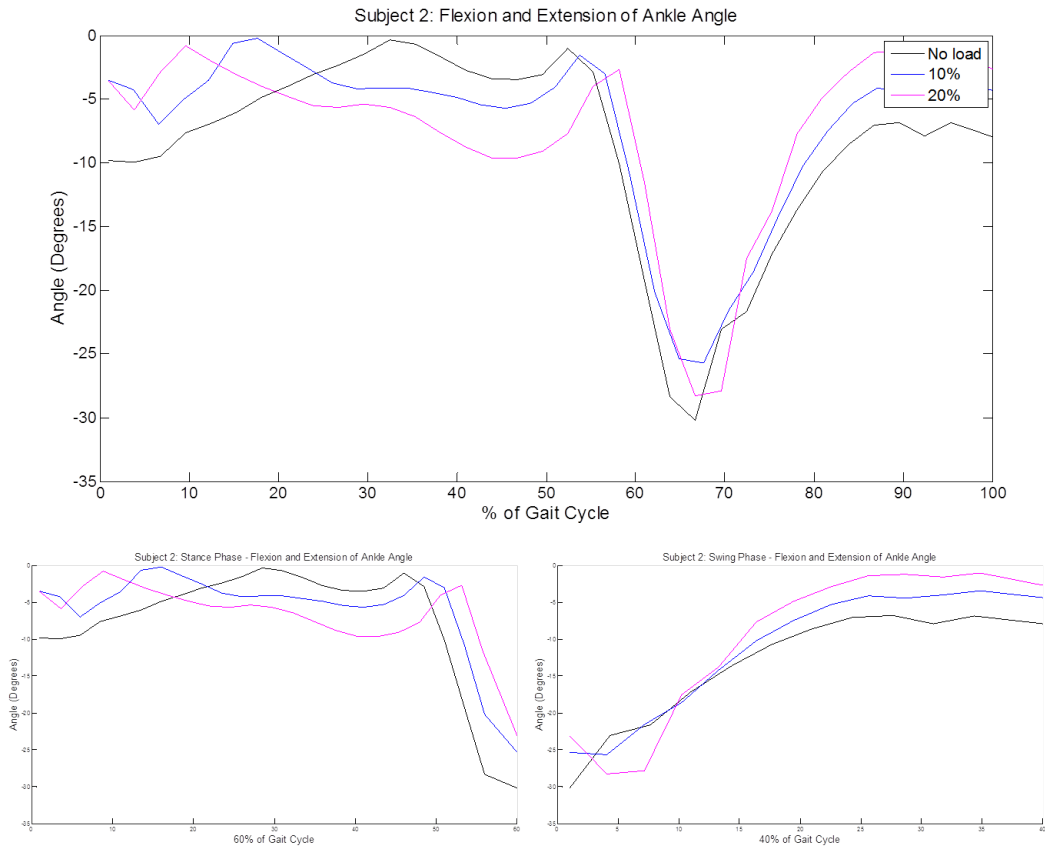

Figure 28. Subject 1: Hip Angle. Hip joint movement plotted for each trial: 100% of gait cycle (top), Stance Phase (bottom left), Swing Phase (bottom right).
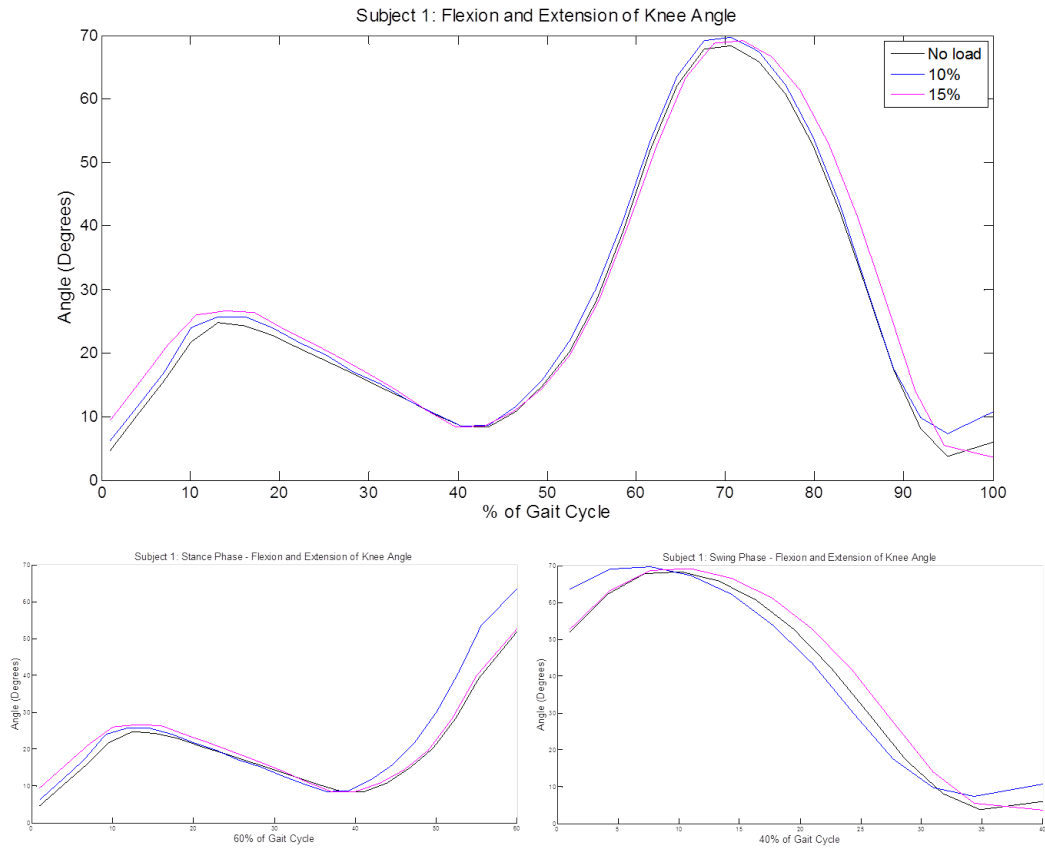
Figure 29. Subject 1: Knee Angle. Knee joint movement plotted for each trial: 100% of gait cycle (top), Stance Phase (bottom left), Swing Phase (bottom right).
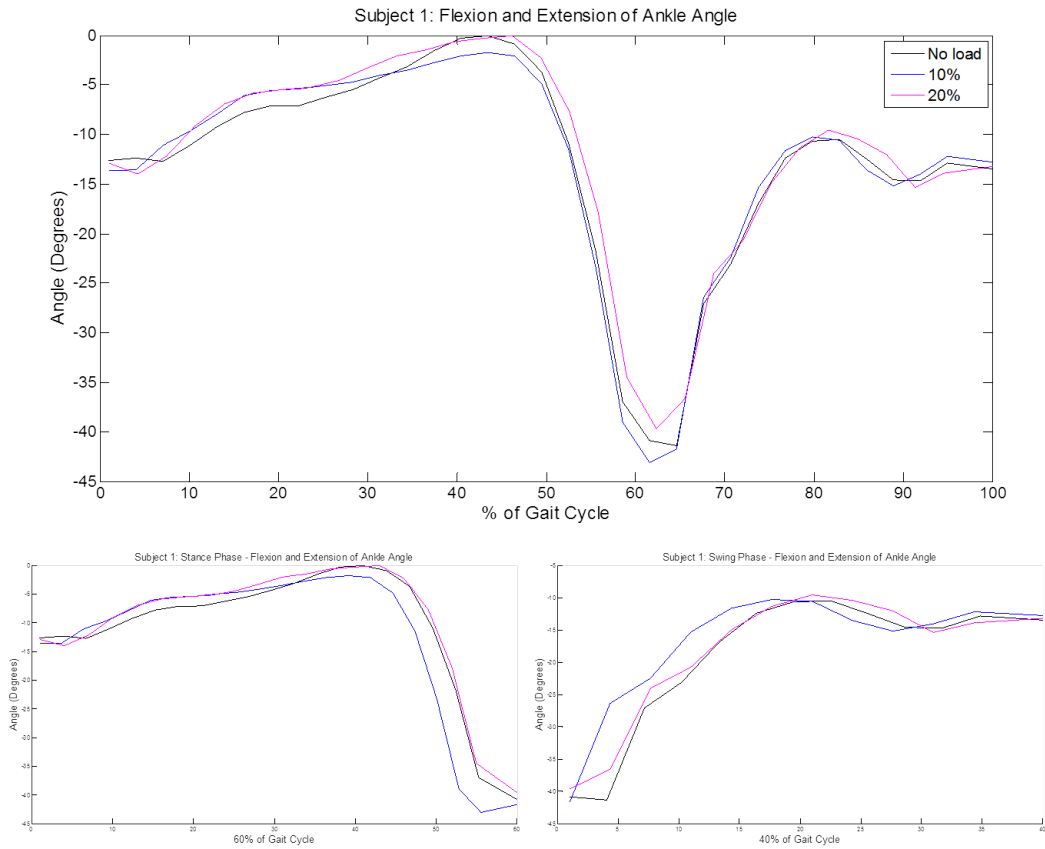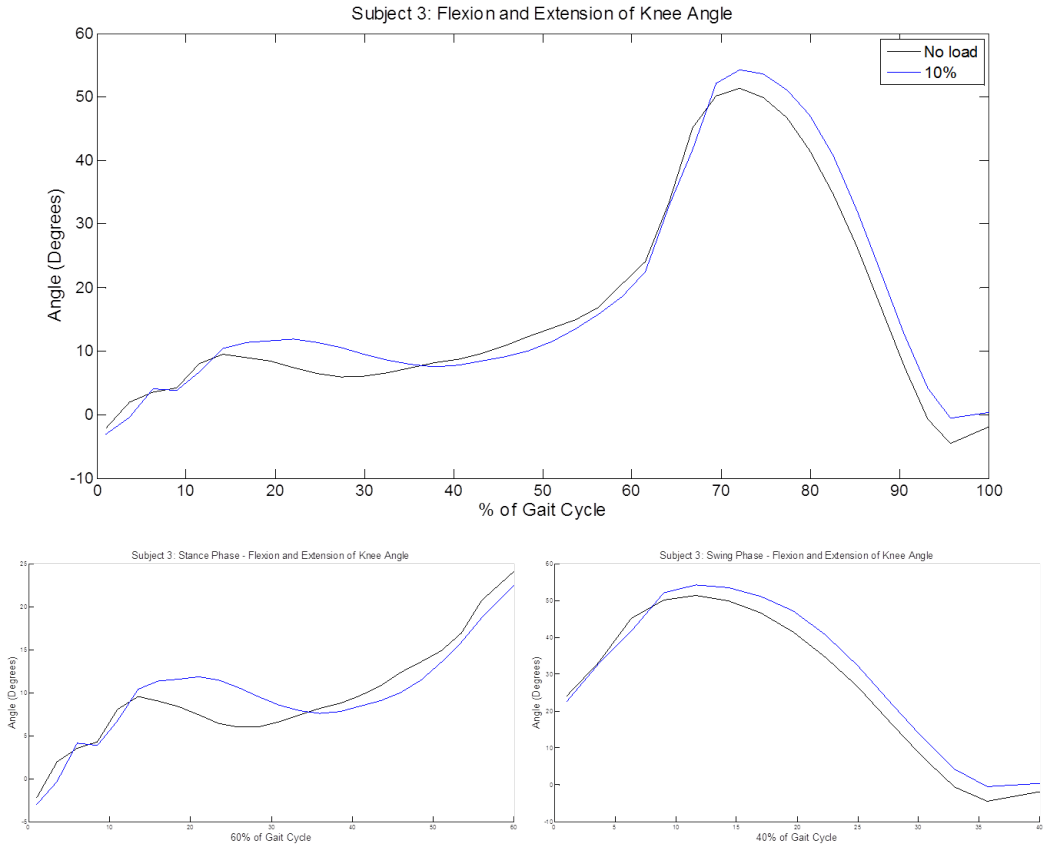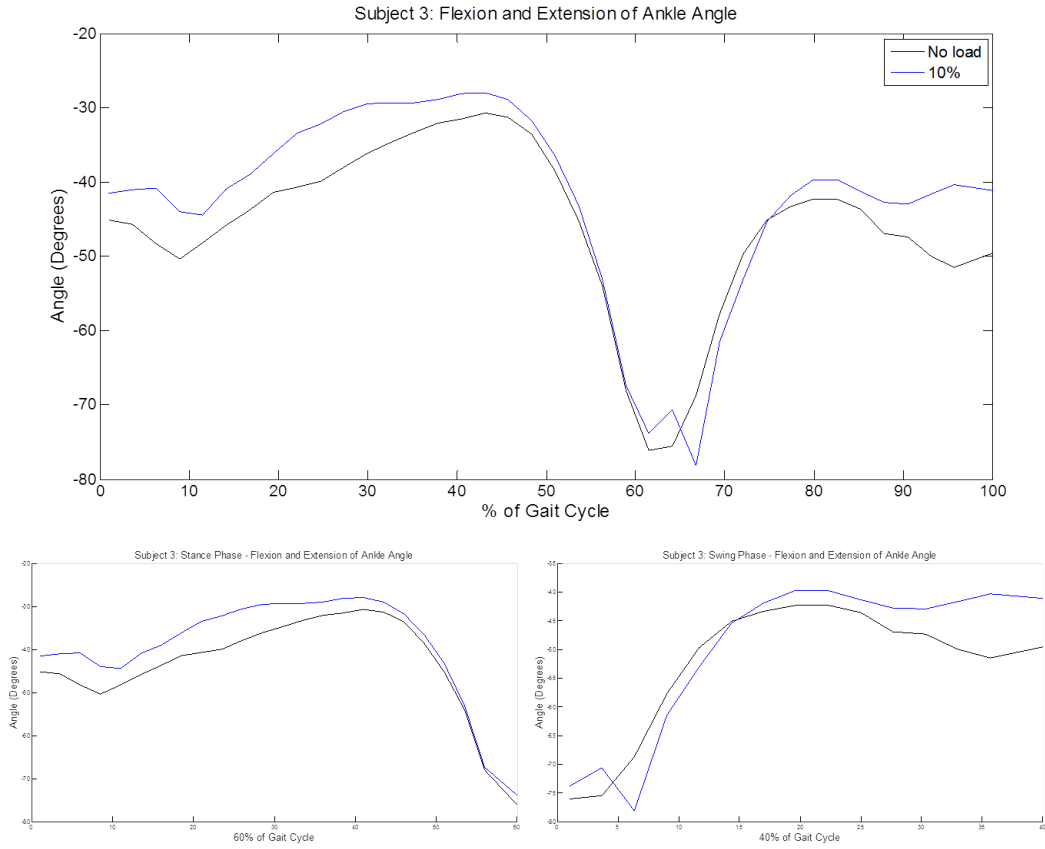
Figure 30. Subject 1: Ankle Angle. Ankle joint movement plotted for each trial: 100% of gait cycle (top), Stance Phase (bottom left), Swing Phase (bottom right).
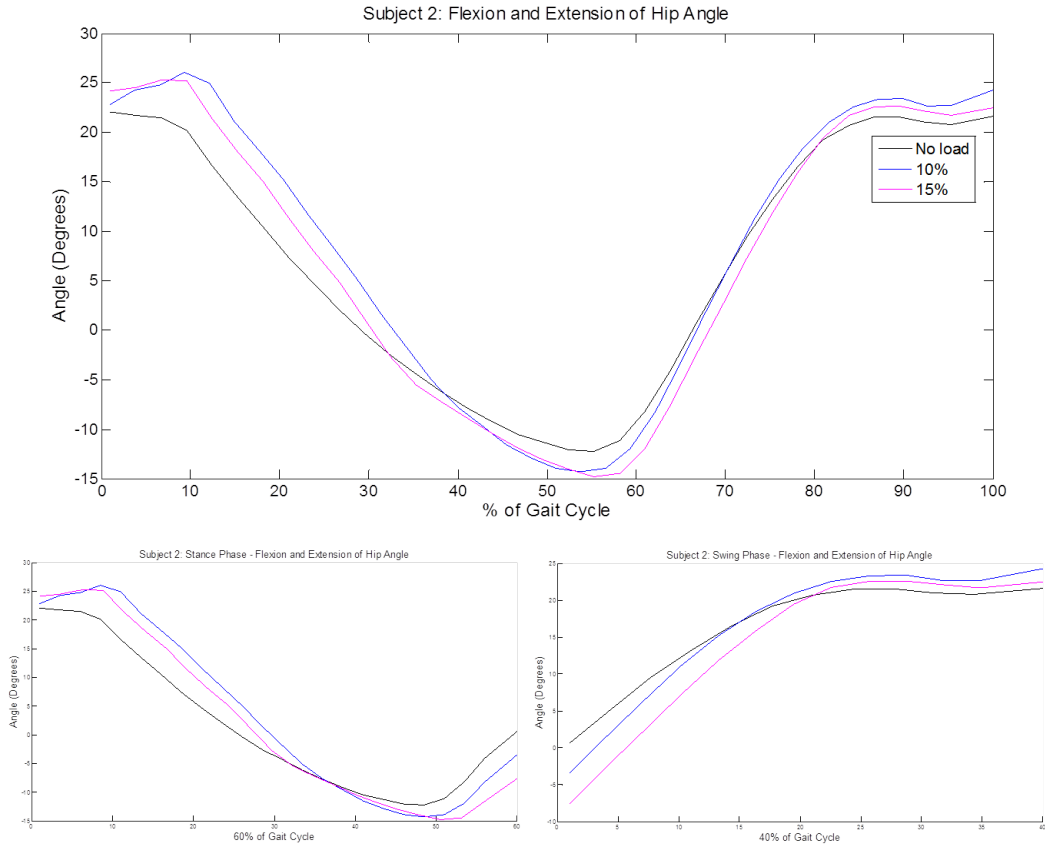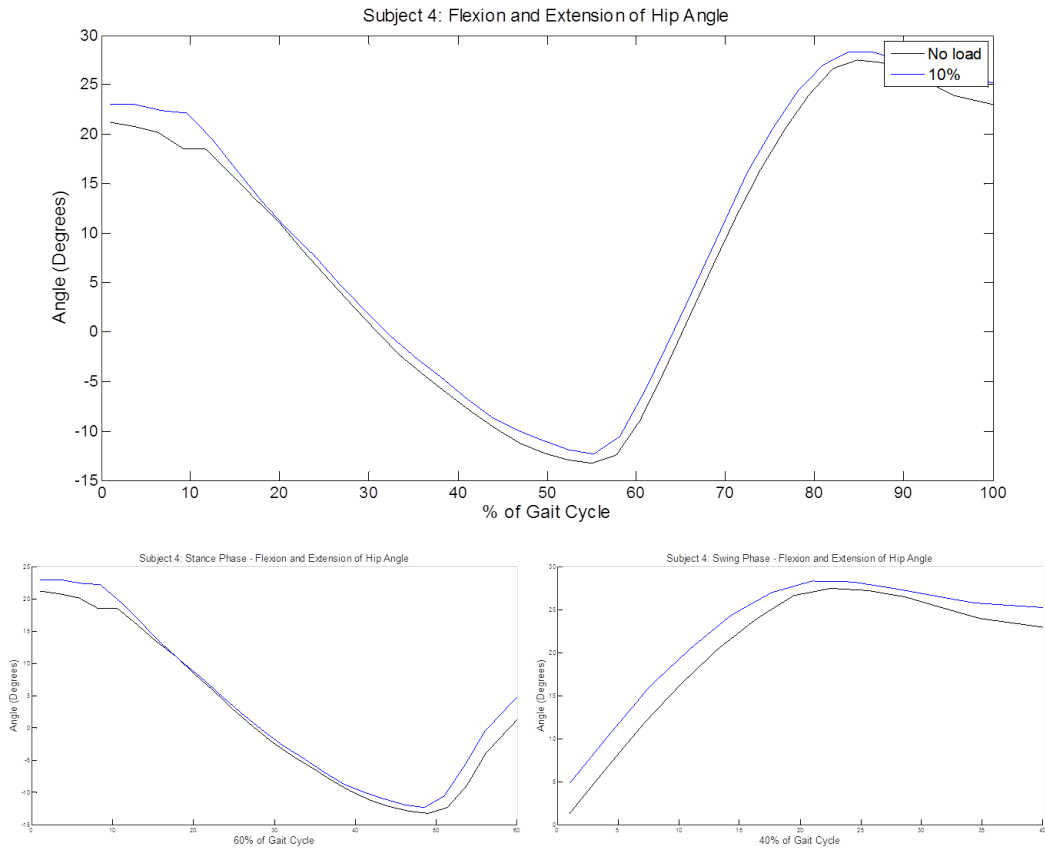
Figure 31. Subject 2: Hip Angle. Hip joint movement plotted for each trial: 100% of gait cycle (top), Stance Phase (bottom left), Swing Phase (bottom right).
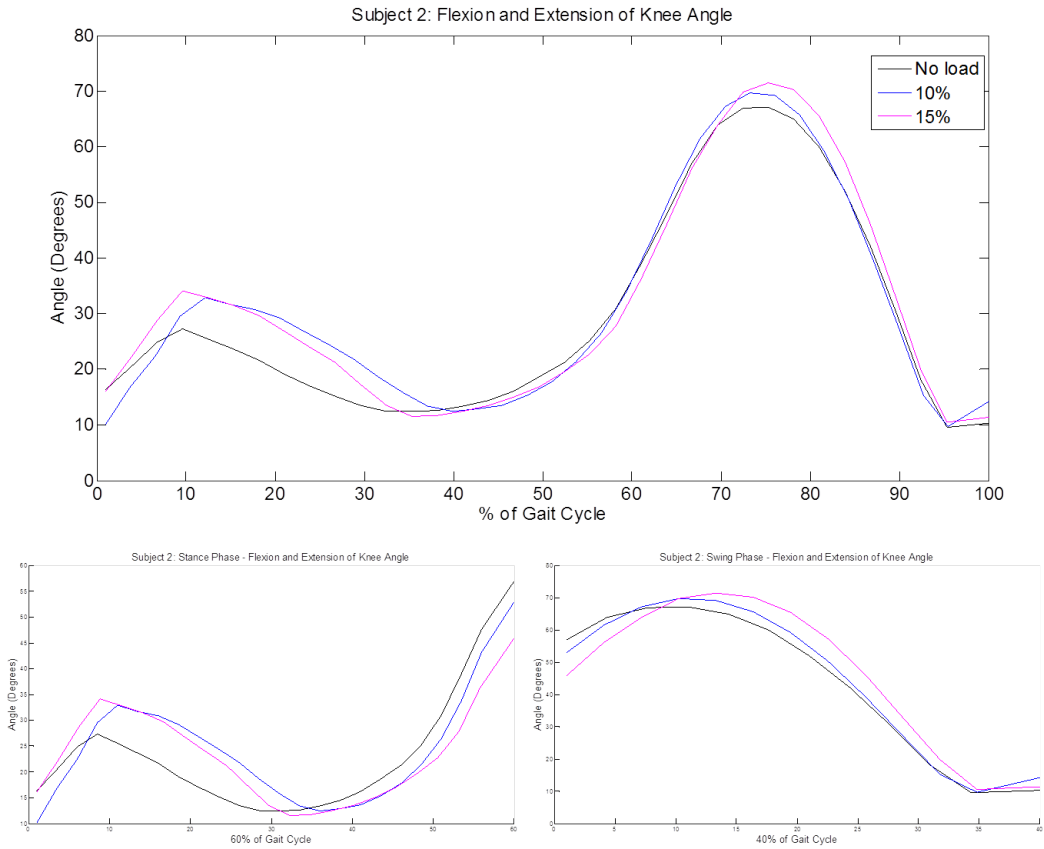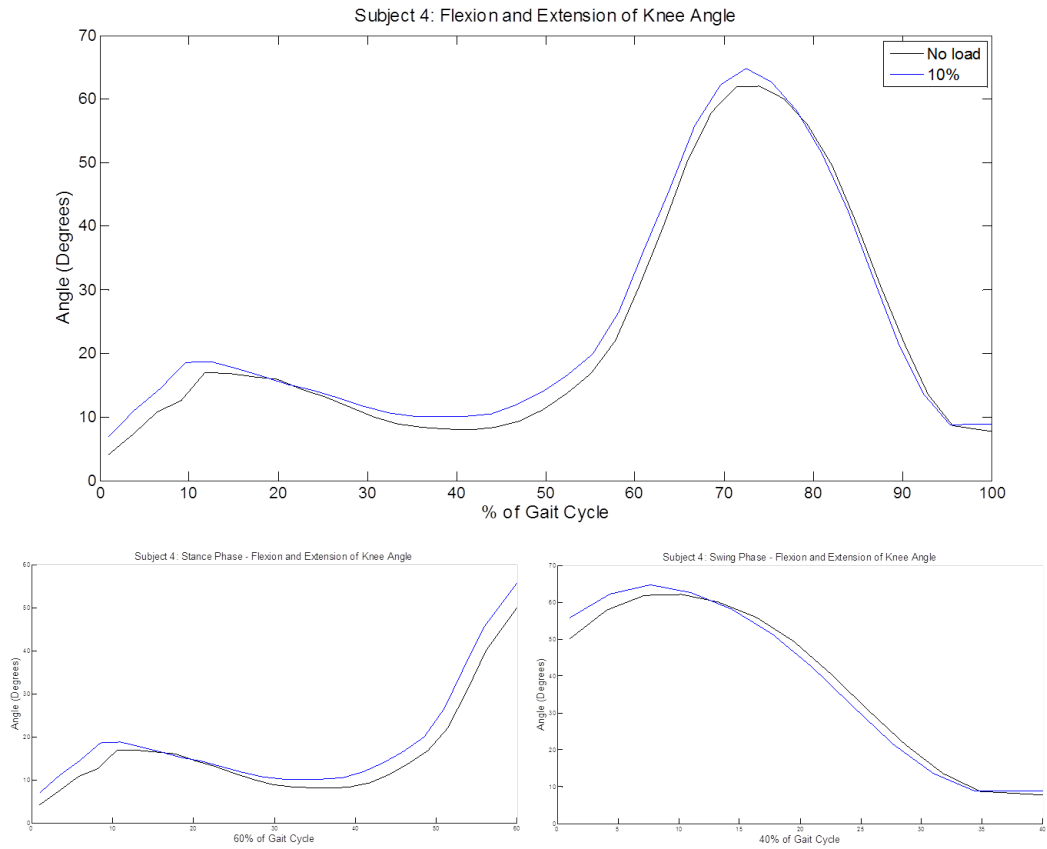
Figure 32. Subject 2: Knee Angle. Knee joint movement plotted for each trial: 100% of gait cycle (top), Stance Phase (bottom left), Swing Phase (bottom right).

Figure 33. Subject 2: Ankle Angle. Ankle joint movement plotted for each trial: 100% of gait cycle (top), Stance Phase (bottom left), Swing Phase (bottom right).
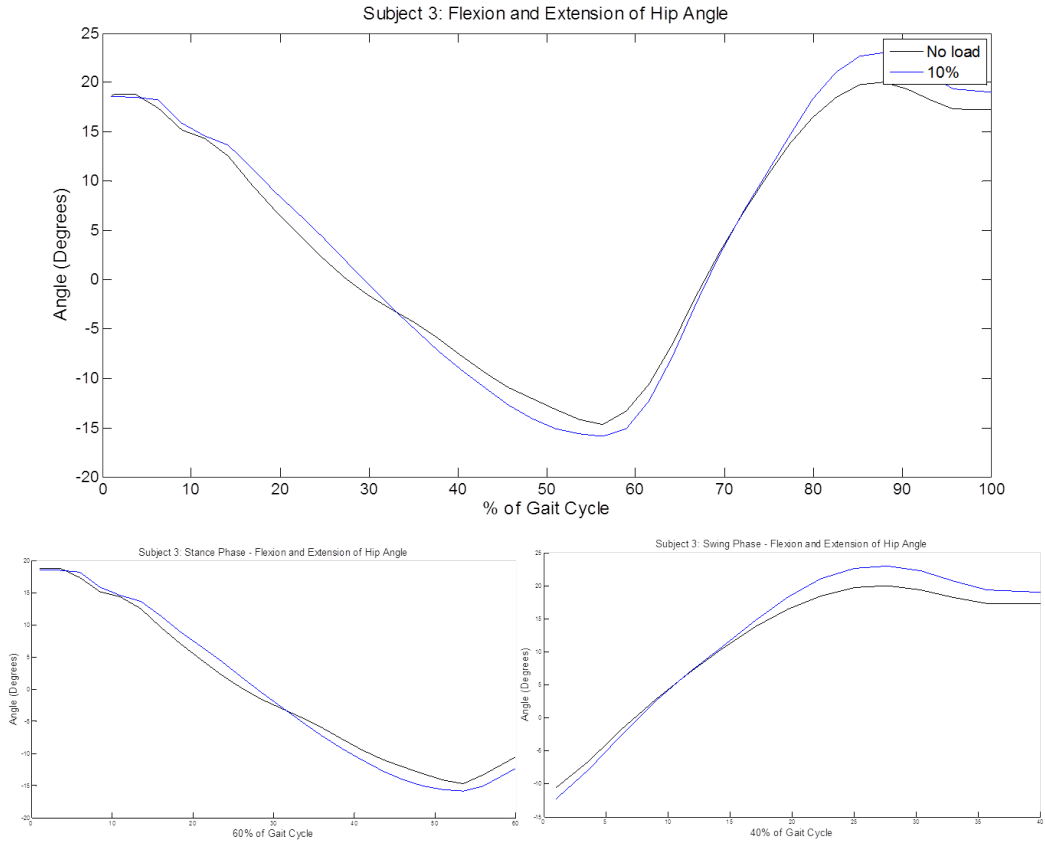
Figure 34. Subject 3: Hip Angle. Hip joint movement plotted for each trial: 100% of gait cycle (top), Stance Phase (bottom left), Swing Phase (bottom right).

Figure 35. Subject 3: Knee Angle. Knee joint movement plotted for each trial: 100% of gait cycle (top), Stance Phase (bottom left), Swing Phase (bottom right)
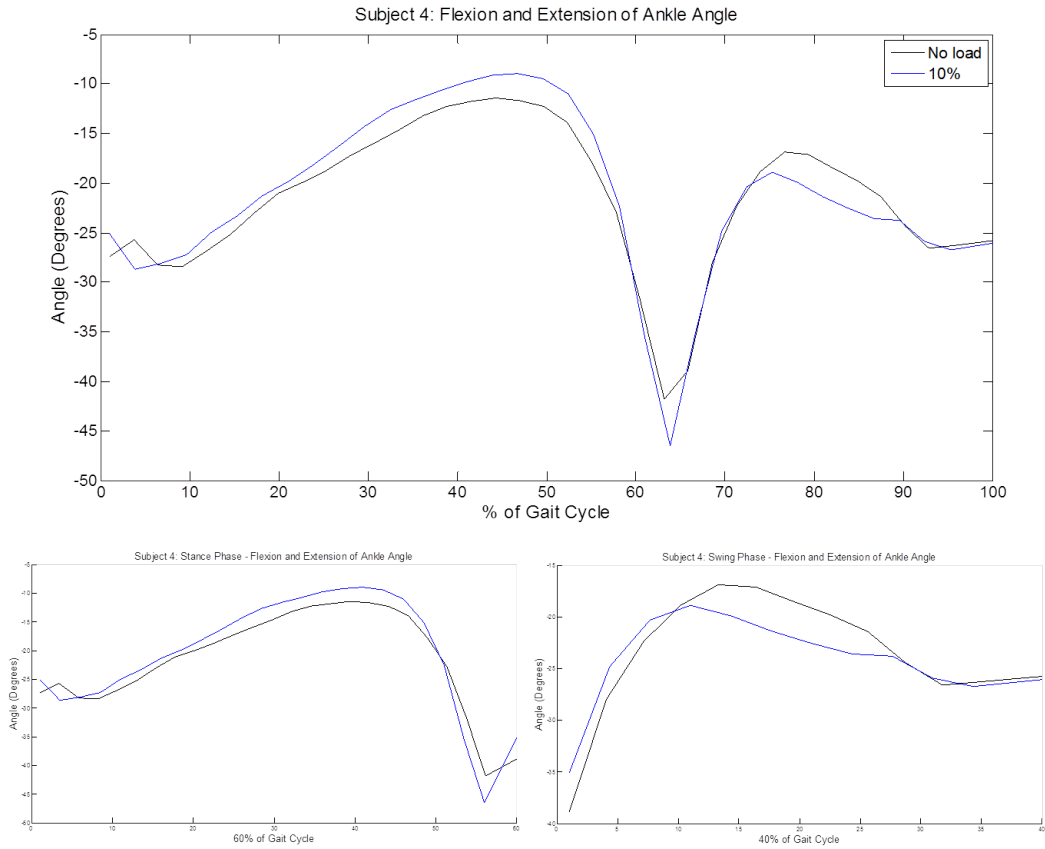
Figure 36. Subject 3: Ankle Angle. Ankle joint movement plotted for each trial: 100% of gait cycle (top), Stance Phase (bottom left), Swing Phase (bottom right).
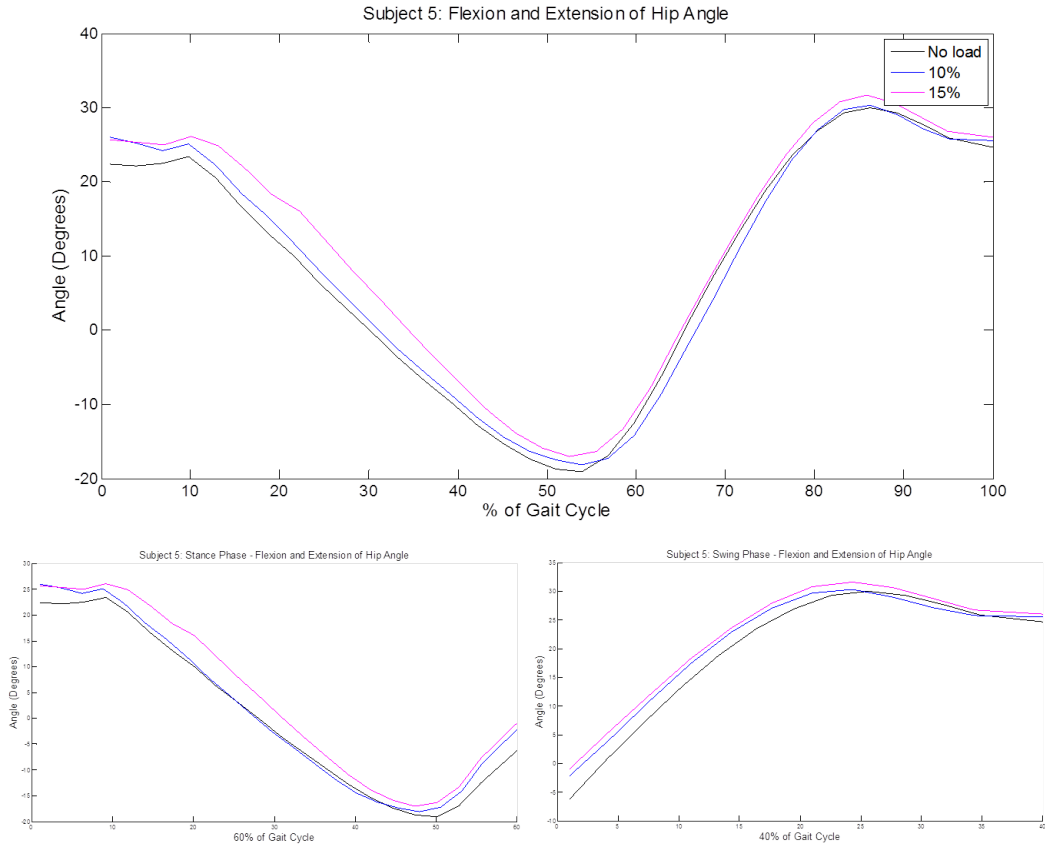
Figure 37. Subject 4: Hip Angle. Hip joint movement plotted for each trial: 100% of gait cycle (top), Stance Phase (bottom left), Swing Phase (bottom right).

Figure 38. Subject 4: Knee Angle. Knee joint movement plotted for each trial: 100% of gait cycle (top), Stance Phase (bottom left), Swing Phase (bottom right).
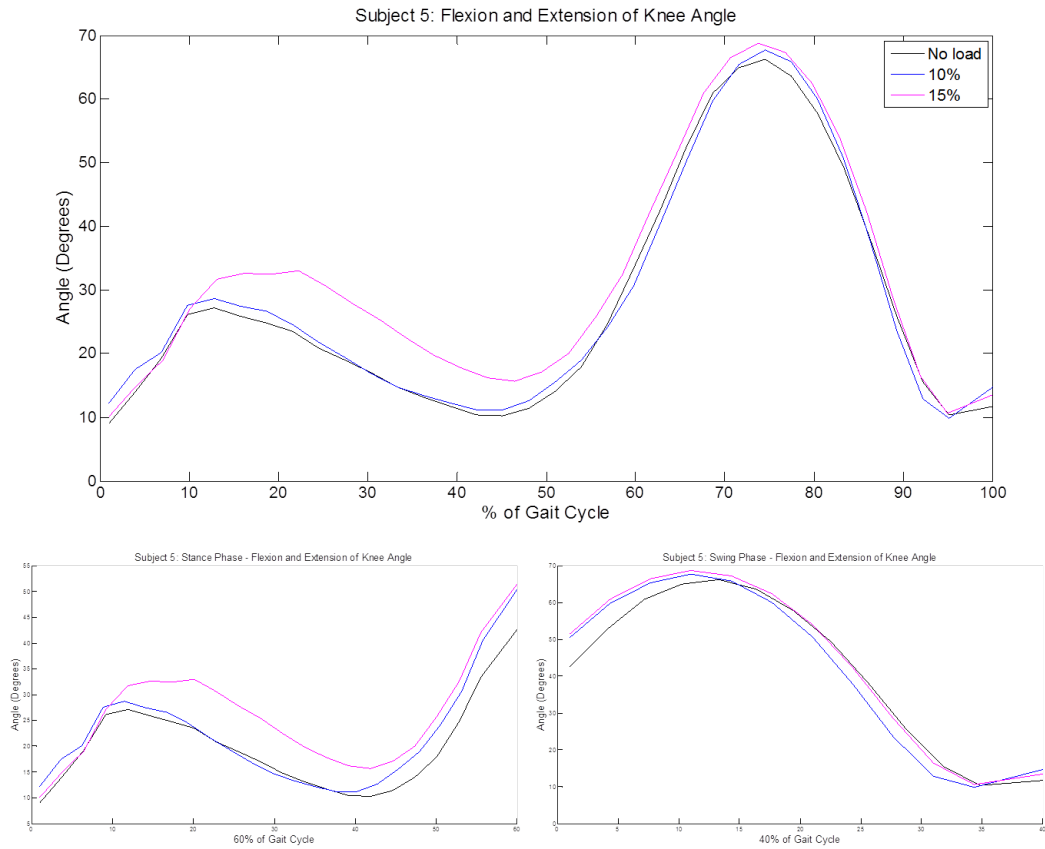
Figure 39. Subject 4: Ankle Angle. Ankle joint movement plotted for each trial: 100% of gait cycle (top), Stance Phase (bottom left), Swing Phase (bottom right).

Figure 40. Subject 5: Hip Angle. Hip joint movement plotted for each trial: 100% of gait cycle (top), Stance Phase (bottom left), Swing Phase (bottom right).

Figure 41. Subject 5: Knee Angle. Knee joint movement plotted for each trial: 100% of gait cycle (top), Stance Phase (bottom left), Swing Phase (bottom right).

Figure 42. Subject 5: Ankle Angle. Ankle joint movement plotted for each trial: 100% of gait cycle (top), Stance Phase (bottom left), Swing Phase (bottom right).
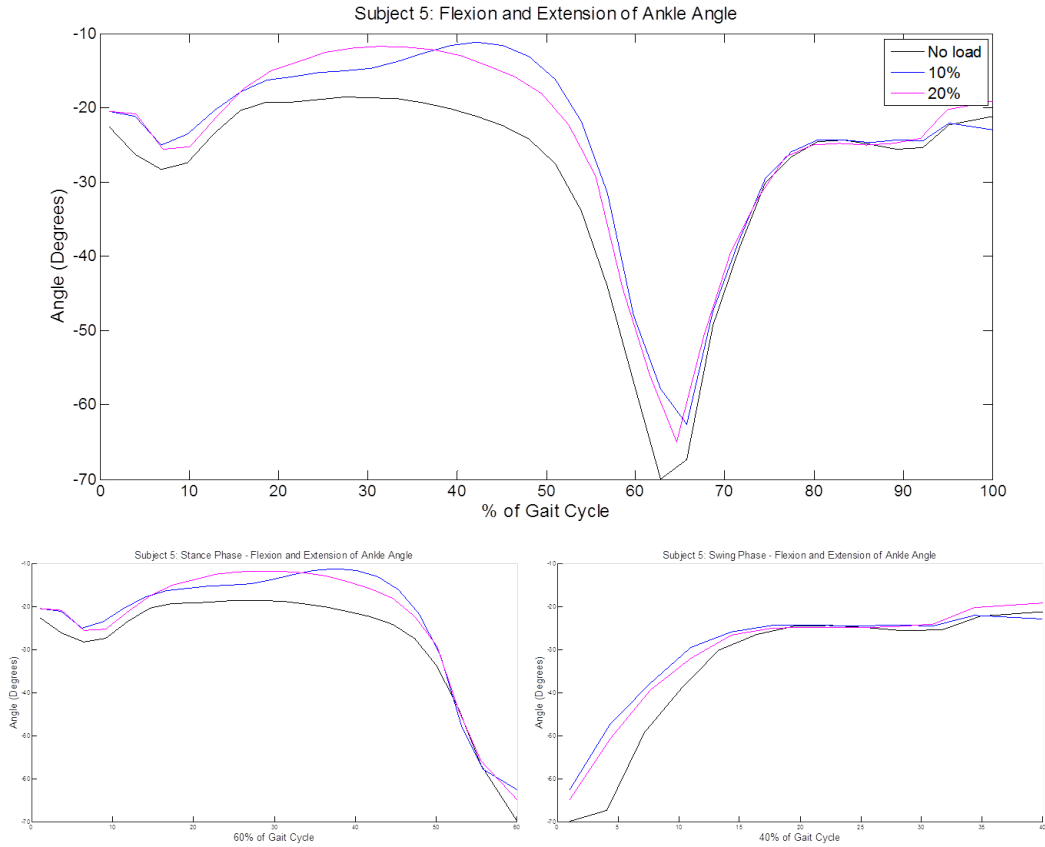
Figure 43. Subject 6: Hip Angle. Hip joint movement plotted for each trial: 100% of gait cycle (top), Stance Phase (bottom left), Swing Phase (bottom right).
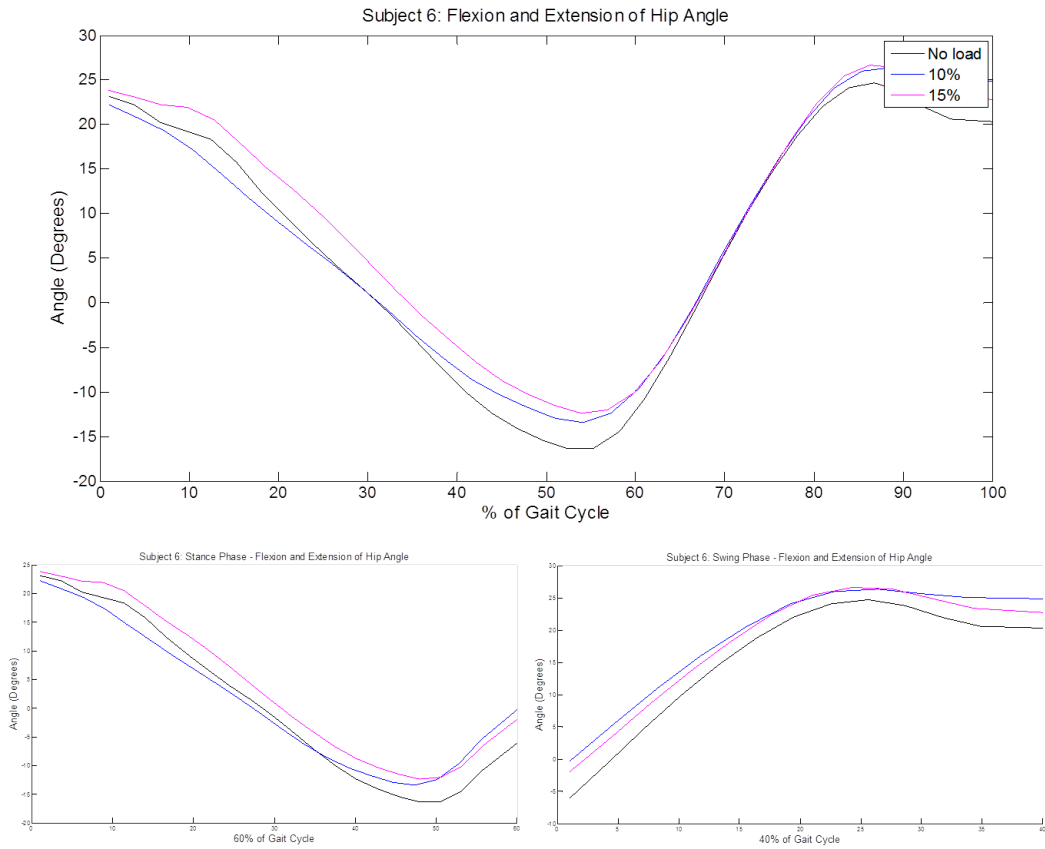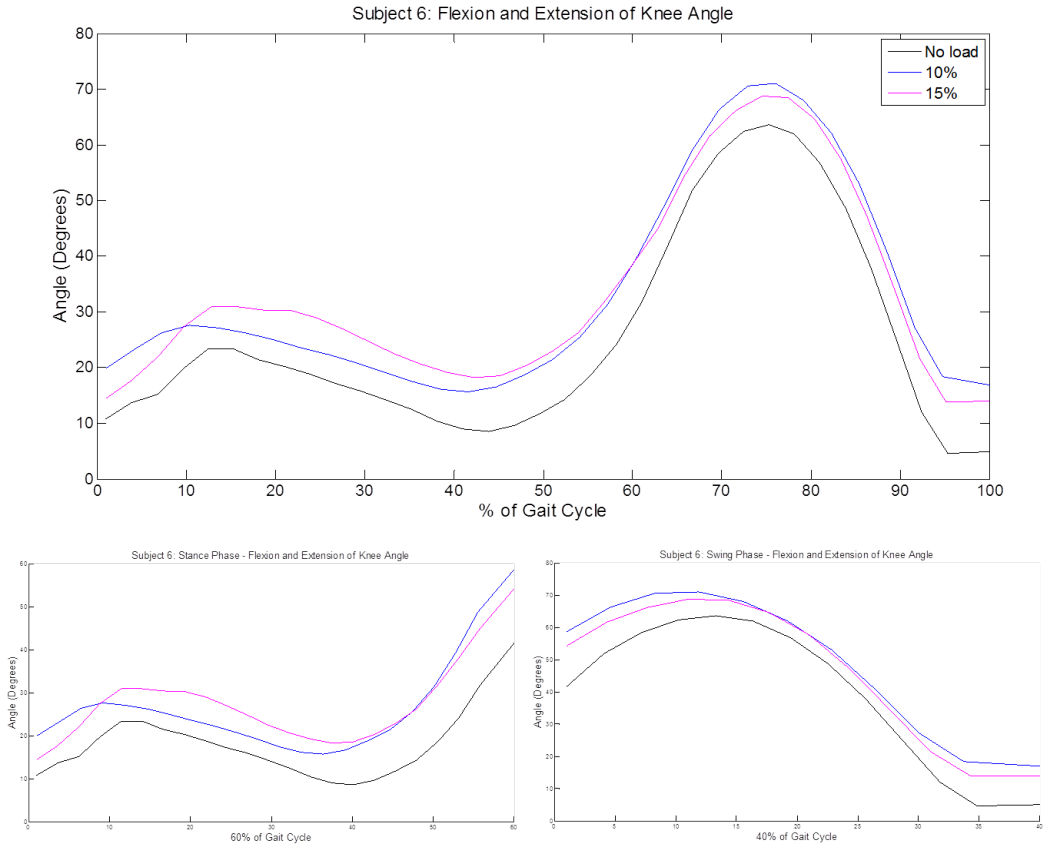
Figure 44. Subject 6: Knee Angle. Knee joint movement plotted for each trial: 100% of gait cycle (top), Stance Phase (bottom left), Swing Phase (bottom right).

Figure 45. Subject 6: Ankle Angle. Ankle joint movement plotted for each trial: 100% of gait cycle (top), Stance Phase (bottom left), Swing Phase (bottom right).

Figure 46. Subject 7: Hip Angle. Hip joint movement plotted for each trial: 100% of gait cycle (top), Stance Phase (bottom left), Swing Phase (bottom right).

Figure 47. Subject 7: Knee Angle. Knee joint movement plotted for each trial: 100% of gait cycle (top), Stance Phase (bottom left), Swing Phase (bottom right).
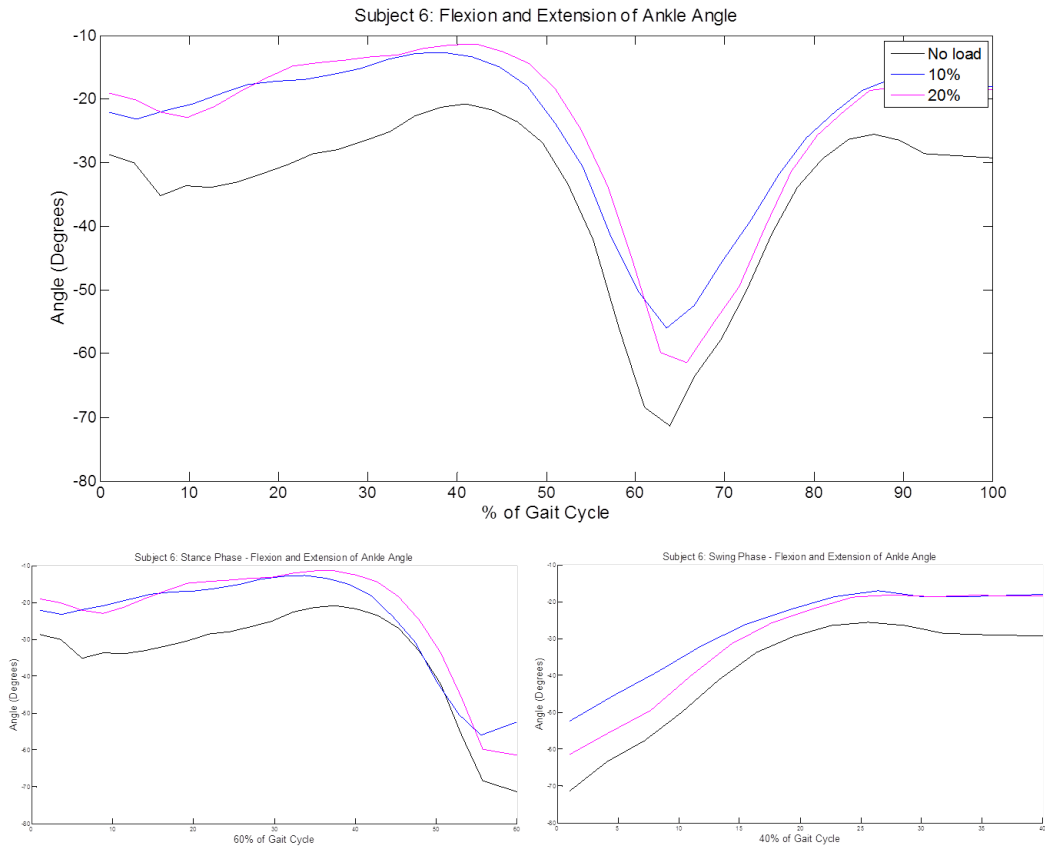
Figure 48. Subject 7: Ankle Angle. Ankle joint movement plotted for each trial: 100% of gait cycle (top), Stance Phase (bottom left), Swing Phase (bottom right).
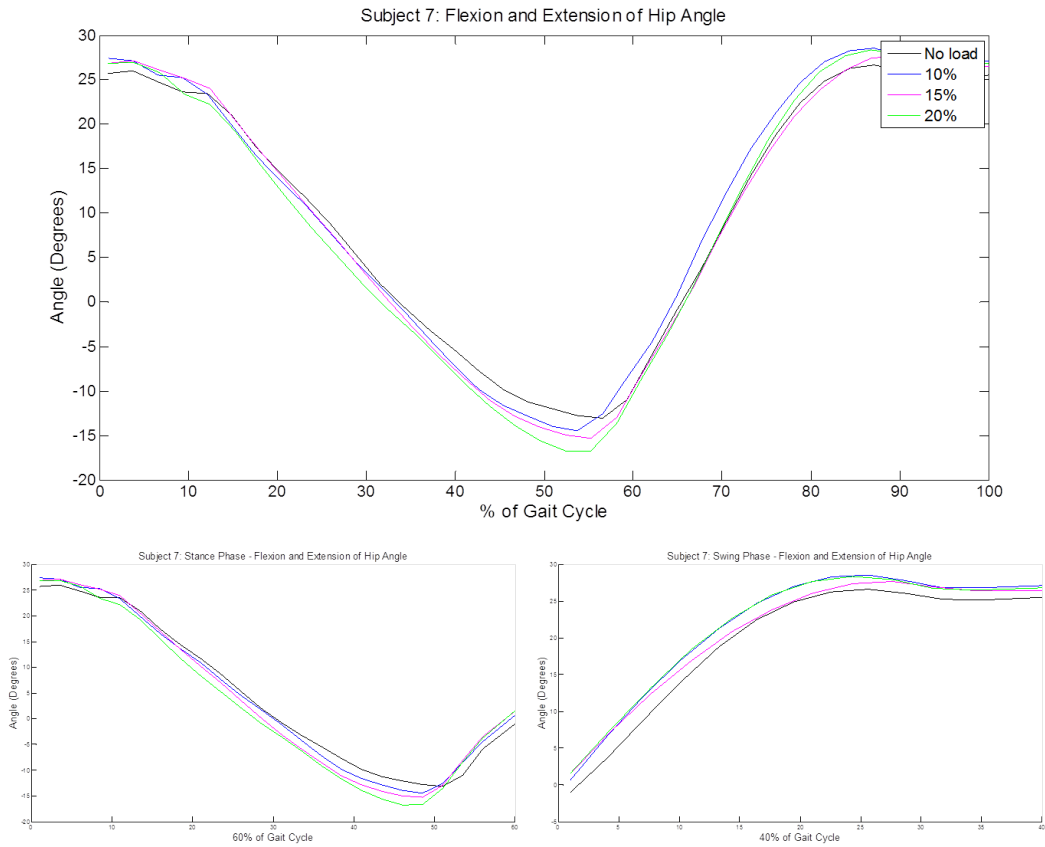
Figure 49. Subject 8: Hip Angle. Hip joint movement plotted for each trial: 100% of gait cycle (top), Stance Phase (bottom left), Swing Phase (bottom right).
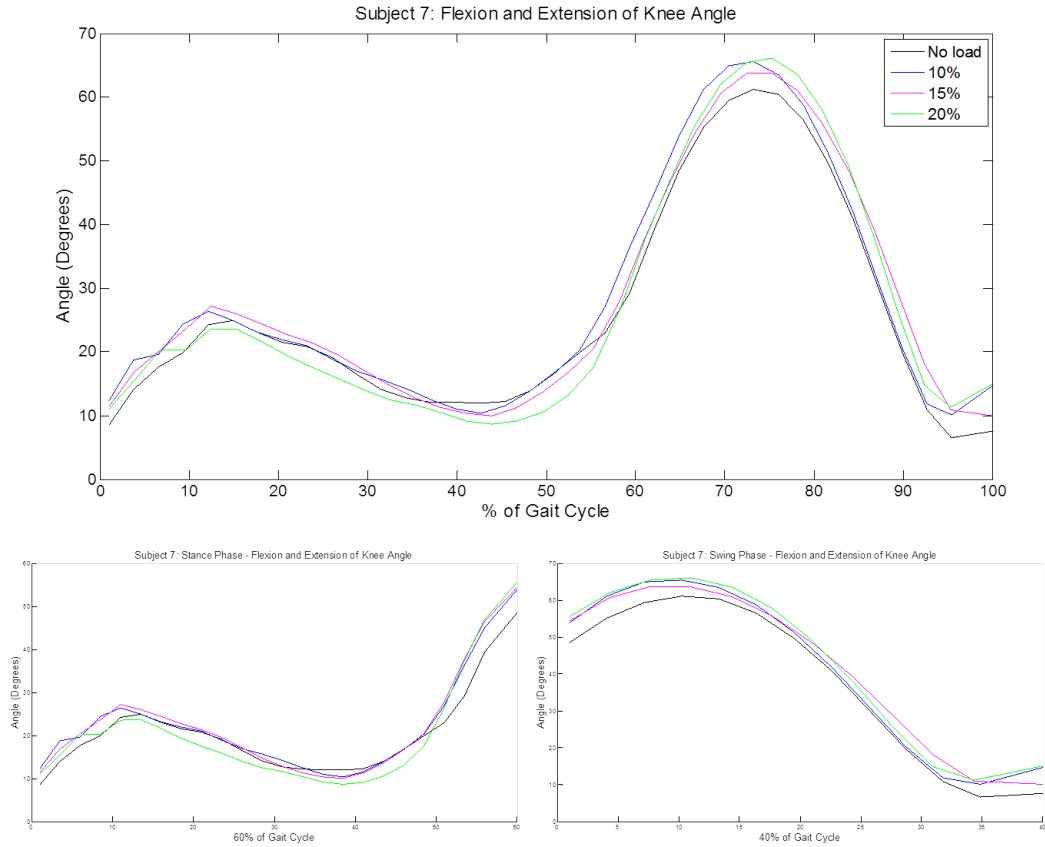
Figure 50. Subject 8: Knee Angle. Knee joint movement plotted for each trial: 100% of gait cycle (top), Stance Phase (bottom left), Swing Phase (bottom right).

Figure 51. Subject 8: Ankle Angle. Ankle joint movement plotted for each trial: 100% of gait cycle (top), Stance Phase (bottom left), Swing Phase (bottom right).

Figure 52. Subject 9: Hip Angle. Hip joint movement plotted for each trial: 100% of gait cycle (top), Stance Phase (bottom left), Swing Phase (bottom right).

Figure 53. Subject 9: Knee Angle. Knee joint movement plotted for each trial: 100% of gait cycle (top), Stance Phase (bottom left), Swing Phase (bottom right).
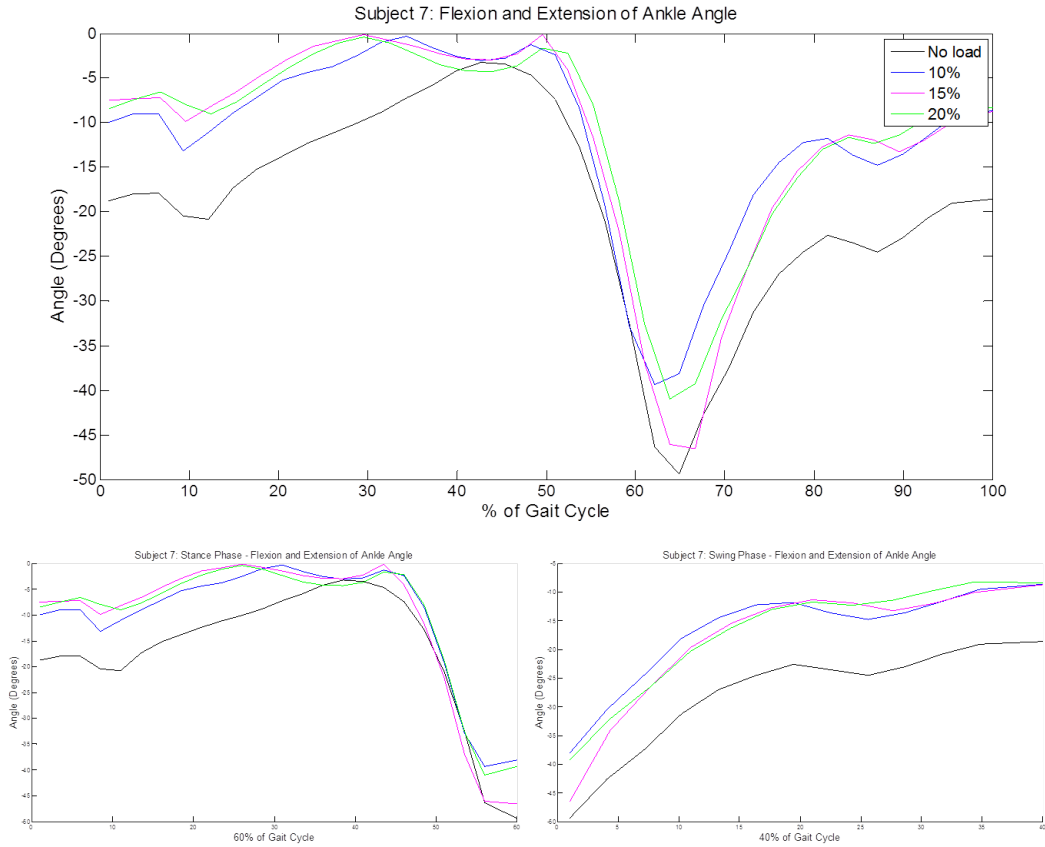
Figure 54. Subject 9: Ankle Angle. Ankle joint movement plotted for each trial: 100% of gait cycle (top), Stance Phase (bottom left), Swing Phase (bottom right).
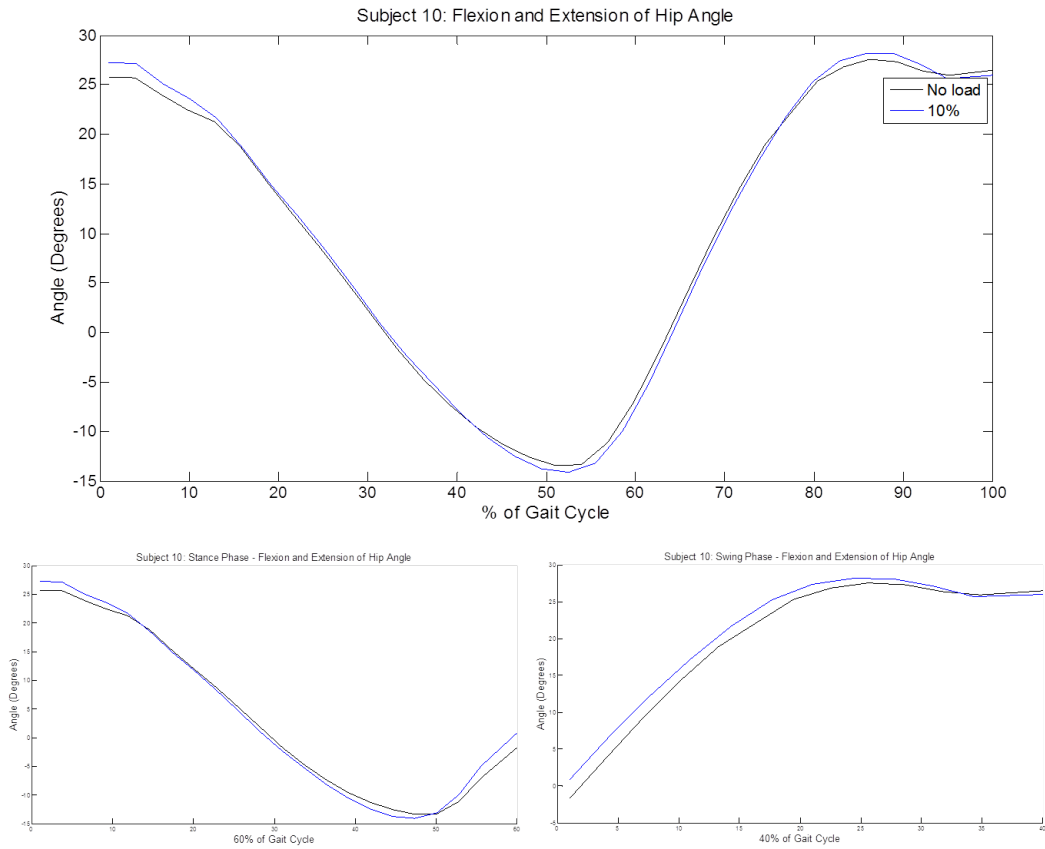
Figure 55. Subject 10: Hip Angle. Hip joint movement plotted for each trial: 100% of gait cycle (top), Stance Phase (bottom left), Swing Phase (bottom right).
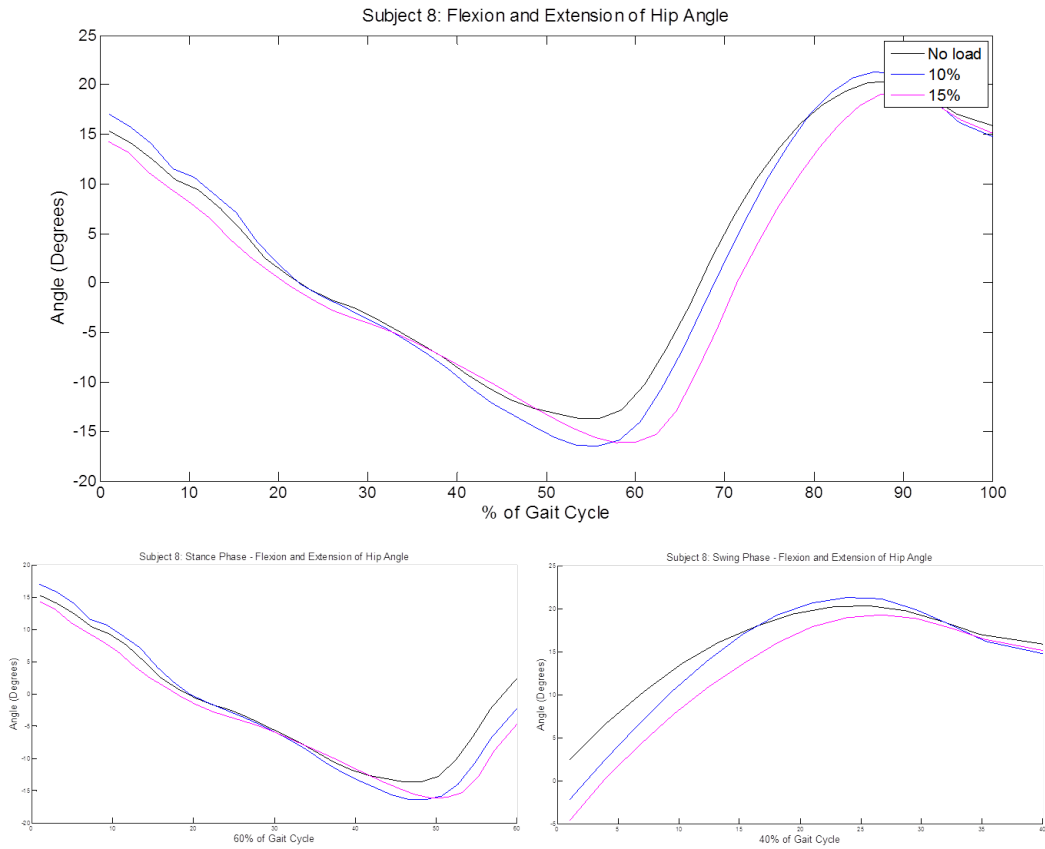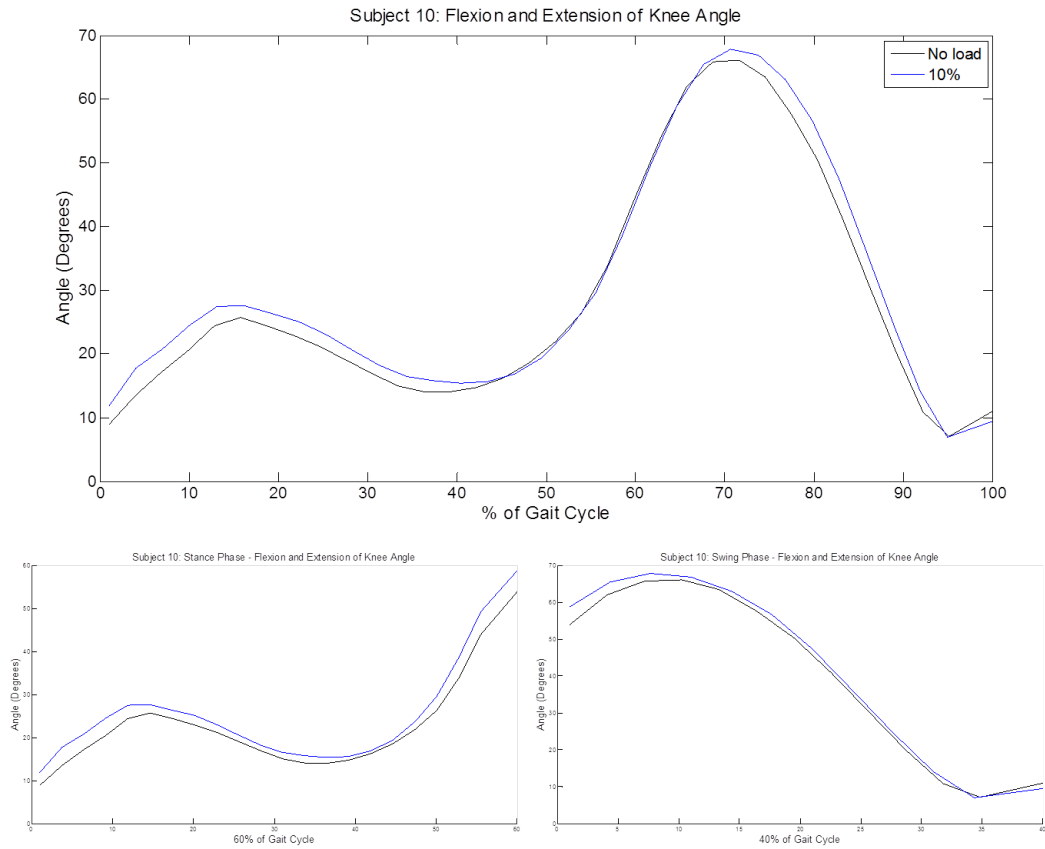
Figure 56. Subject 10: Knee Angle. Knee joint movement plotted for each trial: 100% of gait cycle (top), Stance Phase (bottom left), Swing Phase (bottom right).
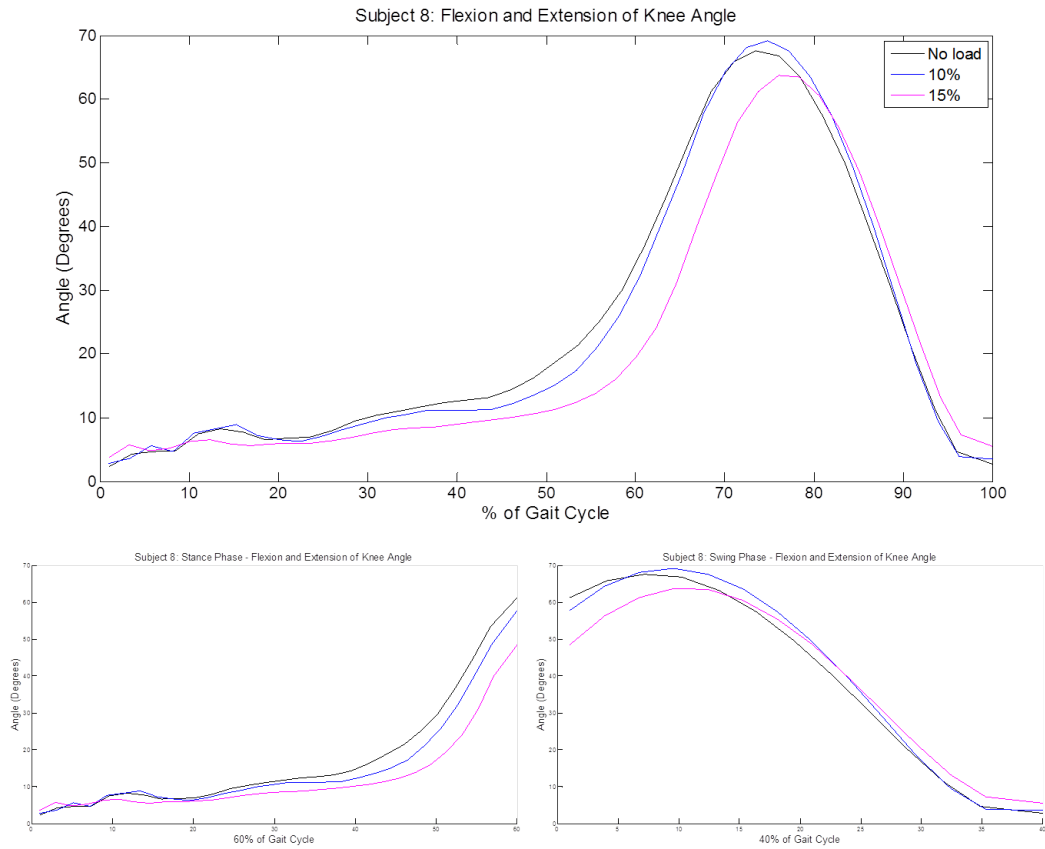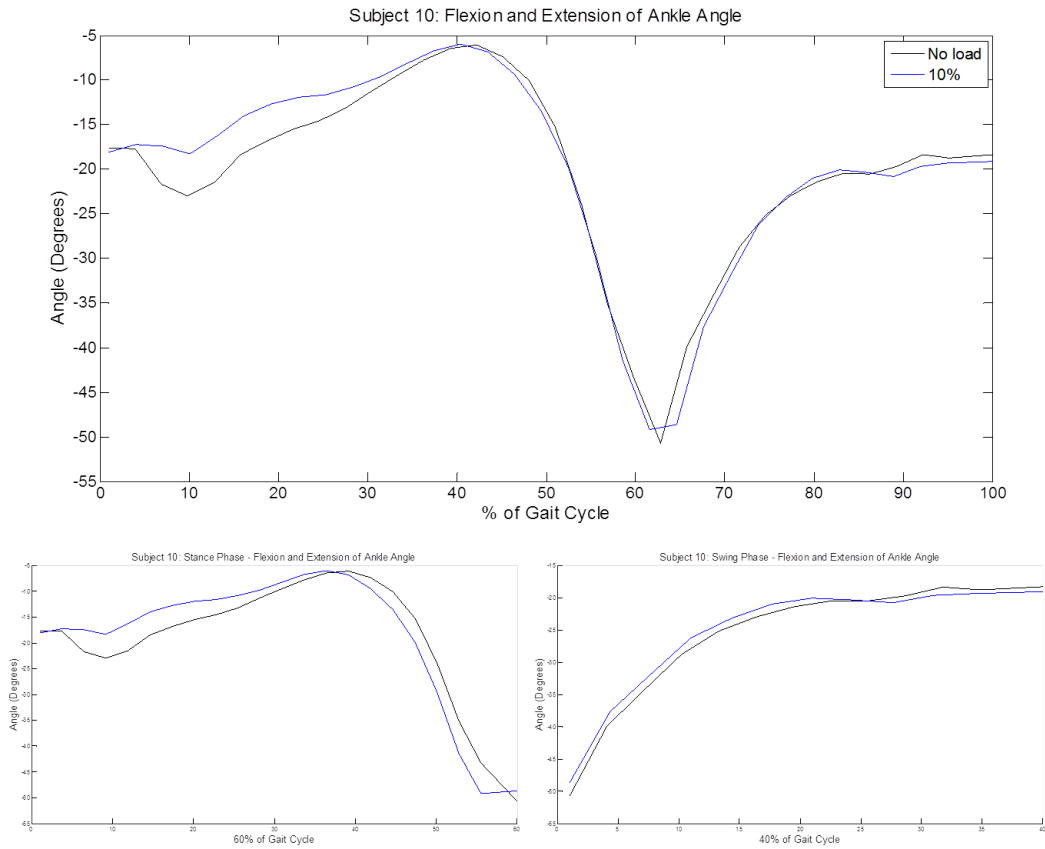
Figure 57. Subject 10: Ankle Angle. Ankle joint movement plotted for each trial: 100% of gait cycle (top), Stance Phase (bottom left), Swing Phase (bottom right).
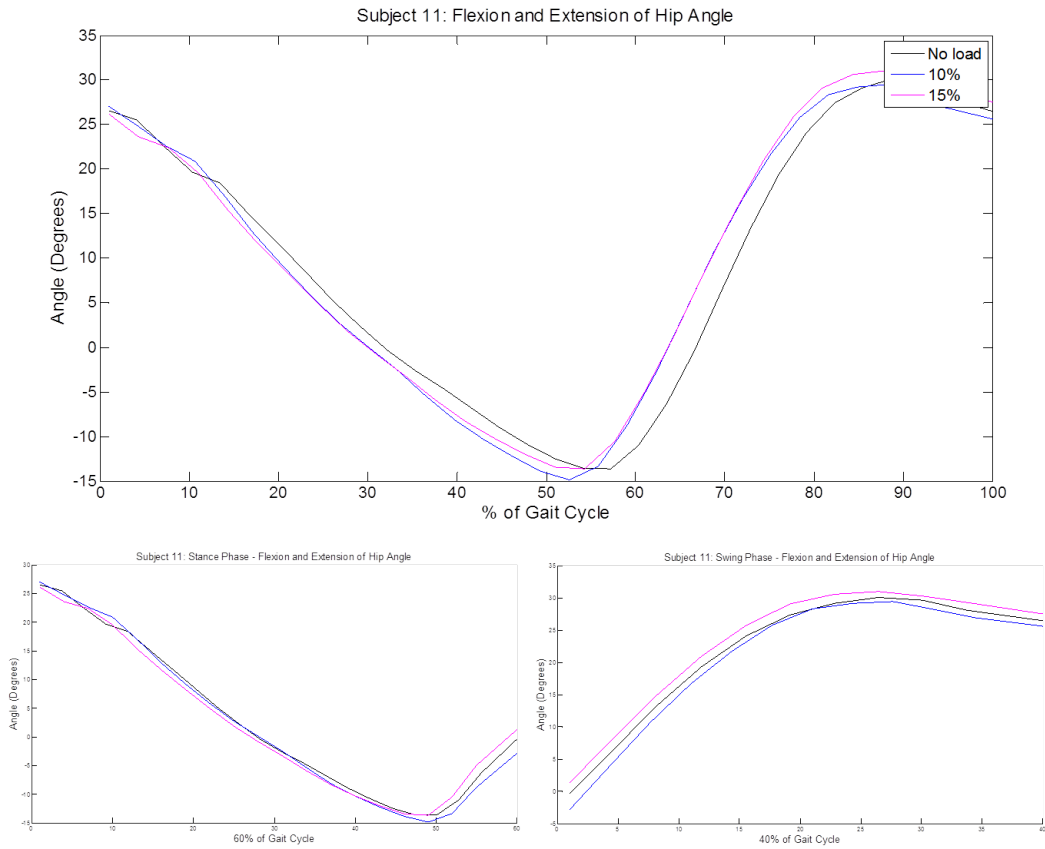
Figure 58. Subject 11: Hip Angle. Hip joint movement plotted for each trial: 100% of gait cycle (top), Stance Phase (bottom left), Swing Phase (bottom right).
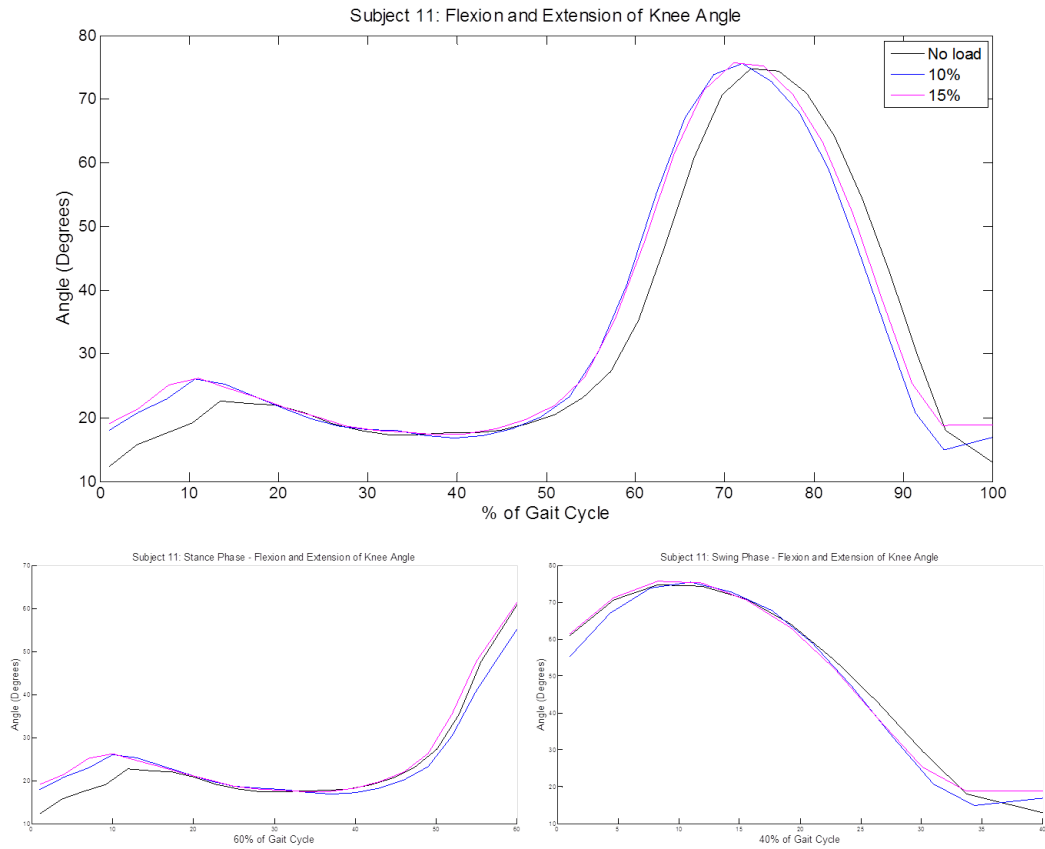
Figure 59. Subject 11: Knee Angle. Knee joint movement plotted for each trial: 100% of gait cycle (top), Stance Phase (bottom left), Swing Phase (bottom right).
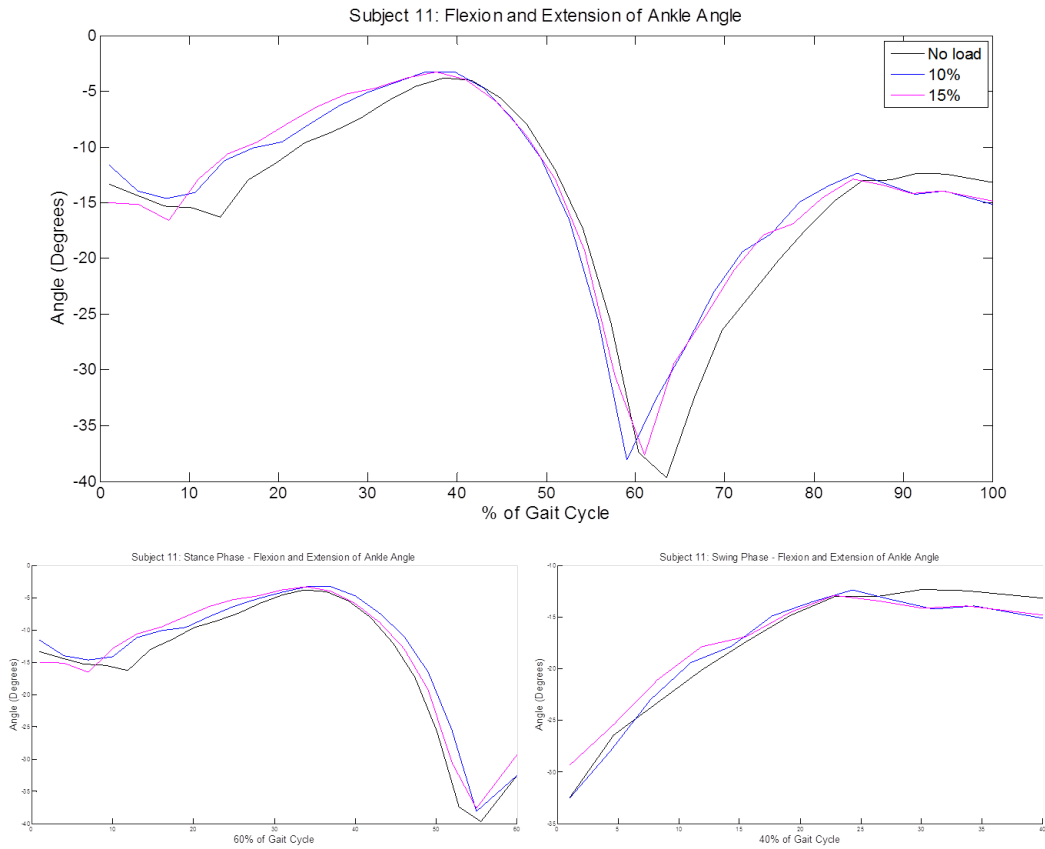
Figure 60. Subject 11: Ankle Angle. Ankle joint movement plotted for each trial: 100% of gait cycle (top), Stance Phase (bottom left), Swing Phase (bottom right).
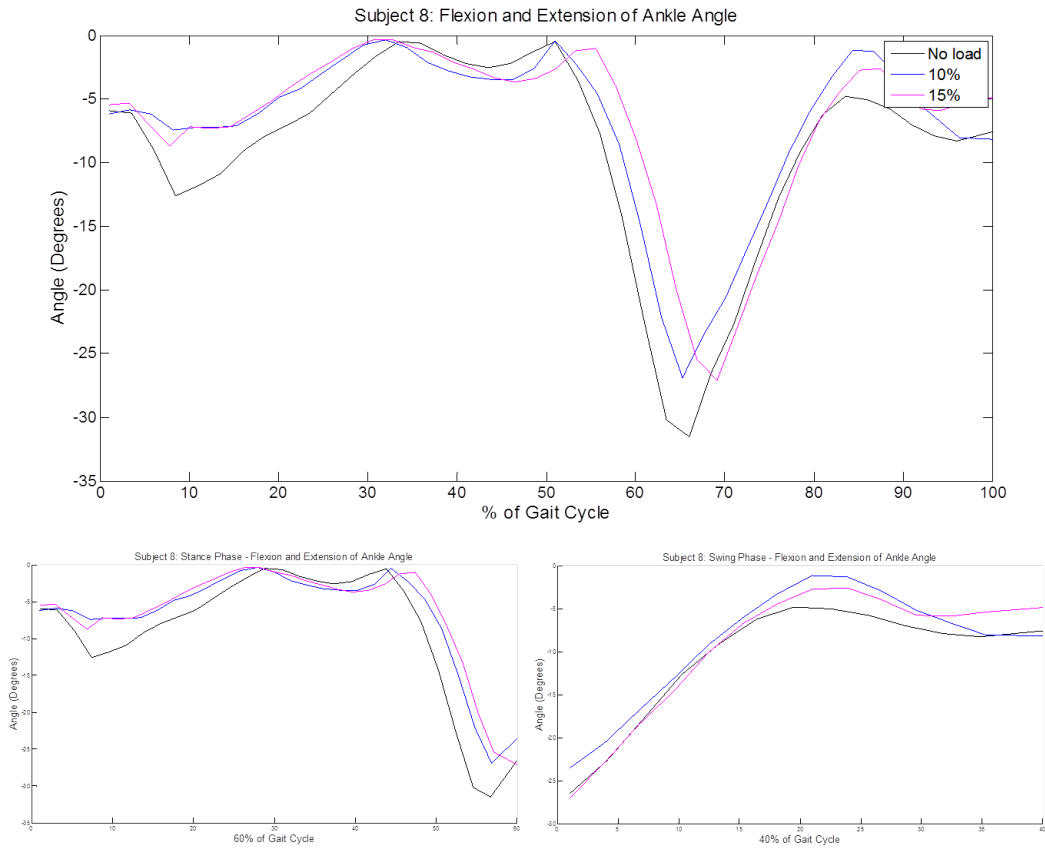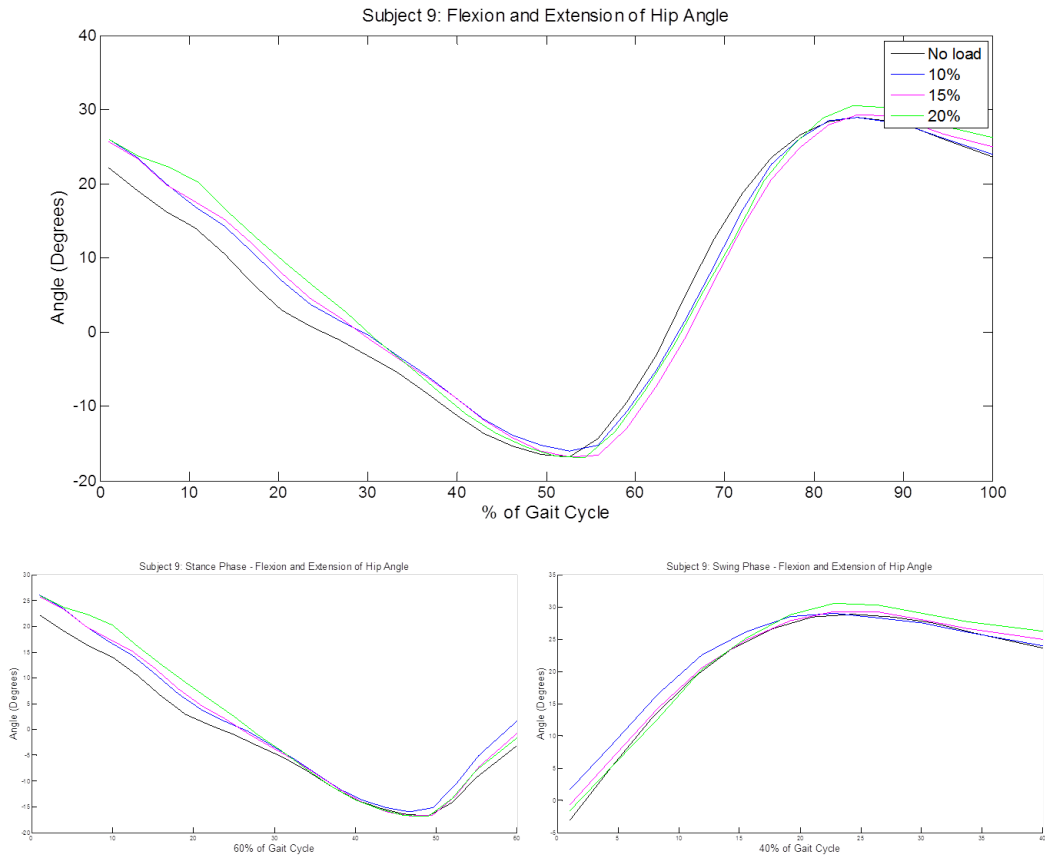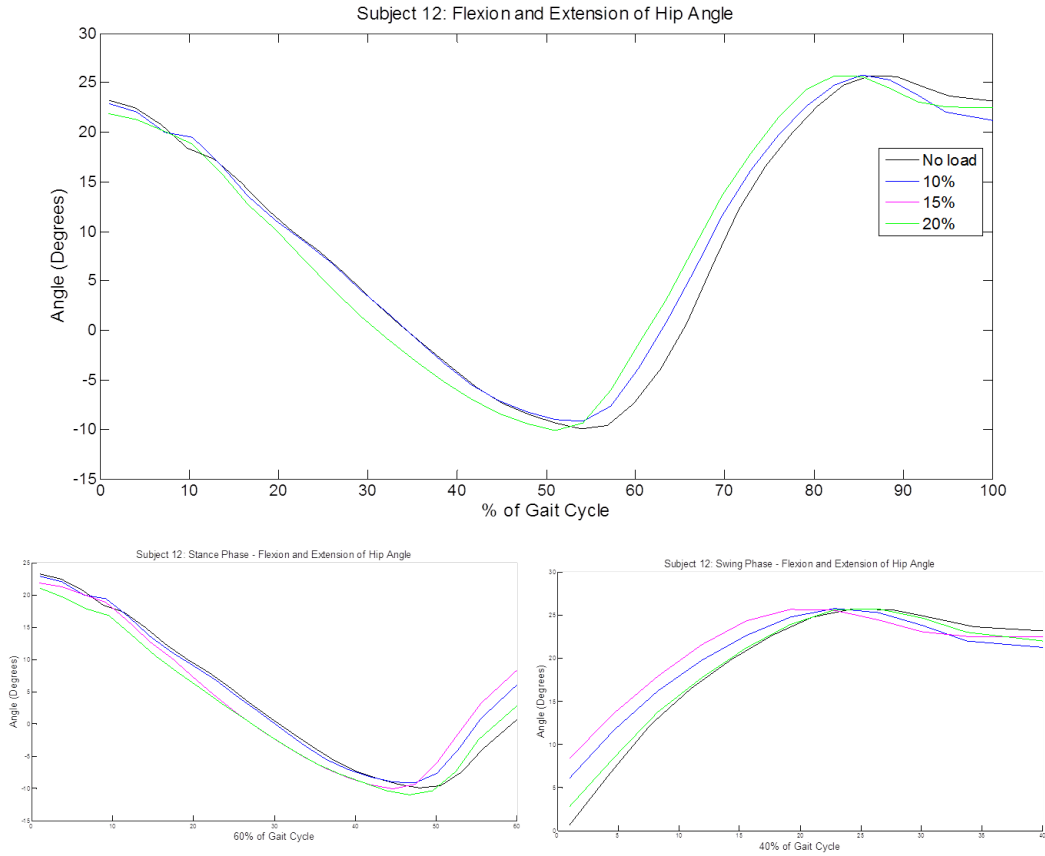
Figure 61. Subject 12: Hip Angle. Hip joint movement plotted for each trial: 100% of gait cycle (top), Stance Phase (bottom left), Swing Phase (bottom right)
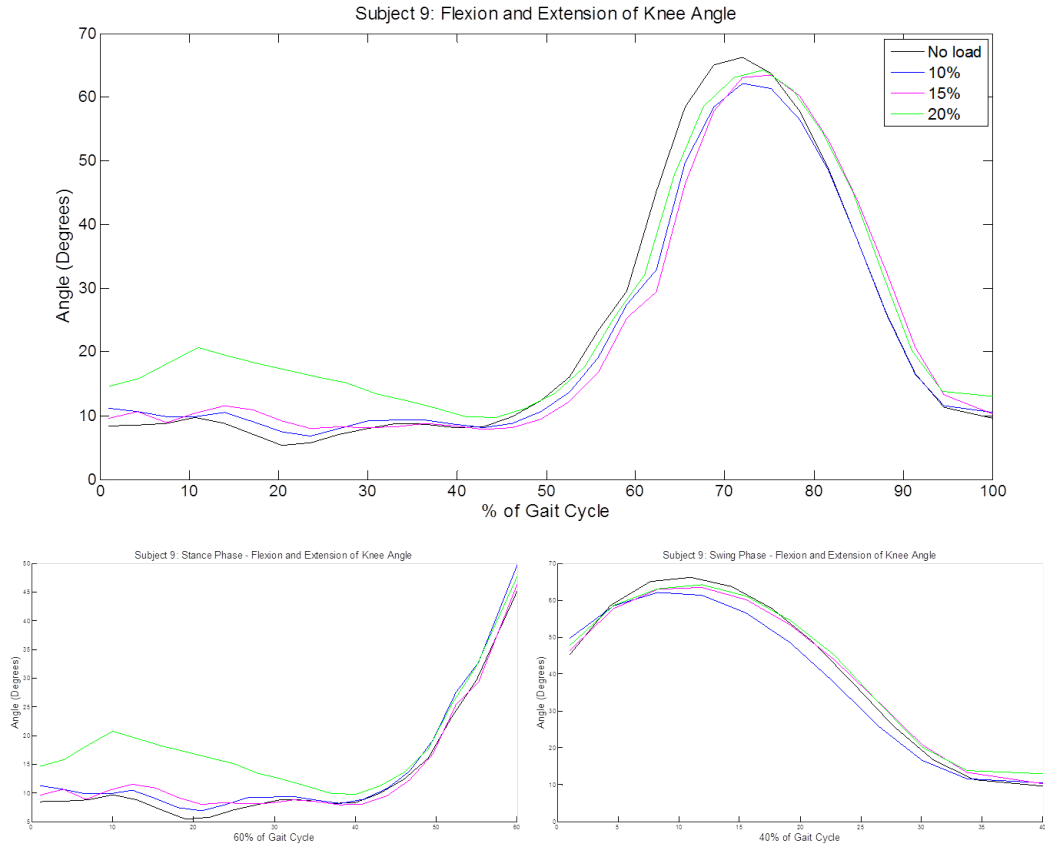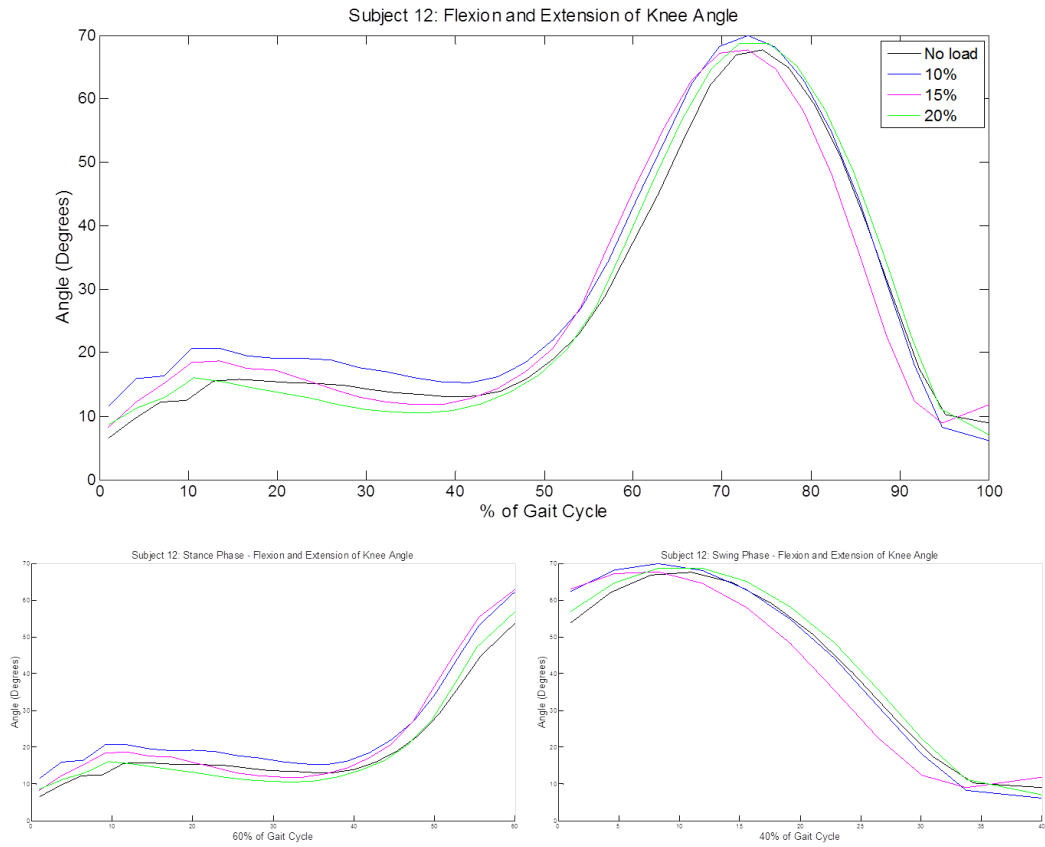
Figure 62. Subject 12: Knee Angle. Knee joint movement plotted for each trial: 100% of gait cycle (top), Stance Phase (bottom left), Swing Phase (bottom right).
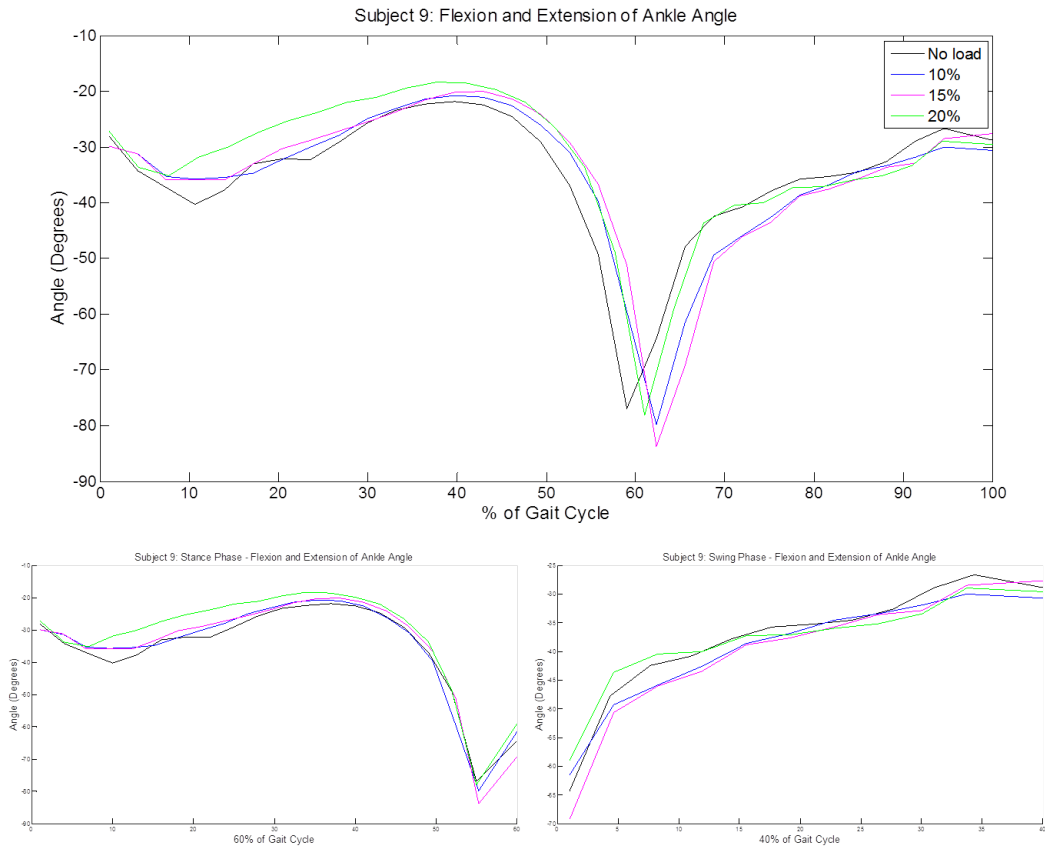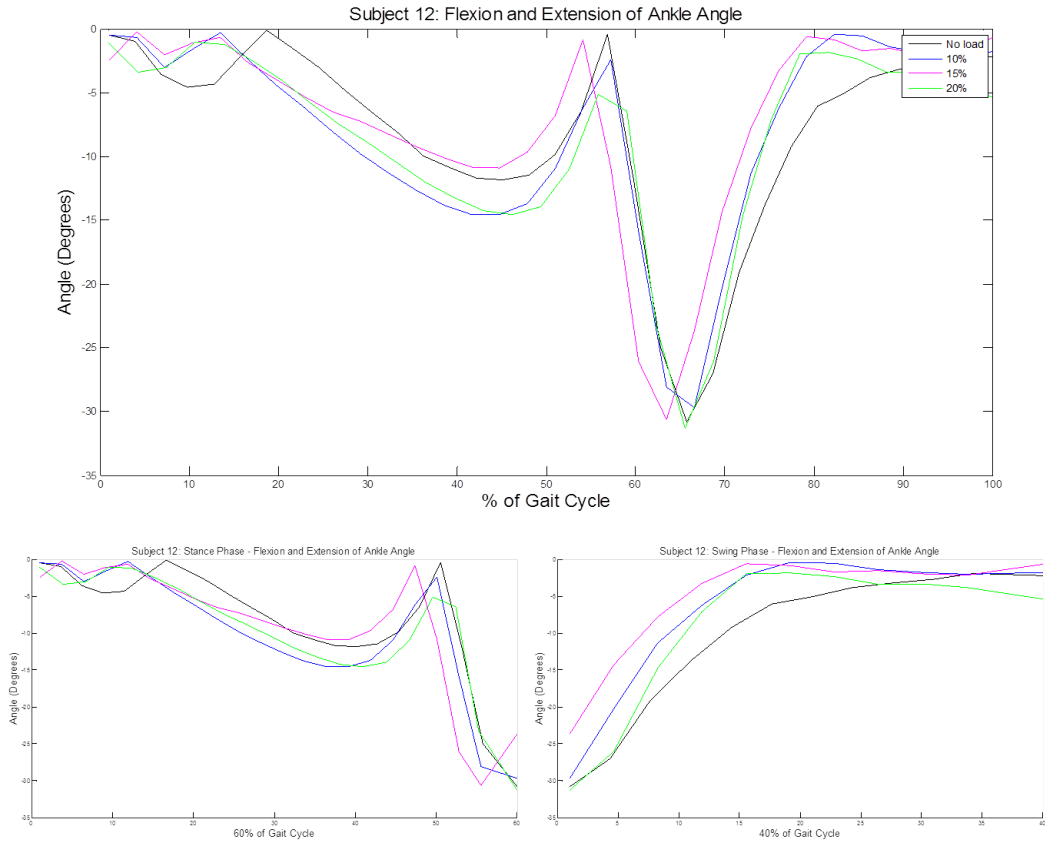
Figure 63. Subject 12: Ankle Angle. Ankle joint movement plotted for each trial: 100% of gait cycle (top), Stance Phase (bottom left), Swing Phase (bottom right).

Appendix E. MATLAB Graphical User Interface Code

The following code was used to develop the MATLAB graphical interface (GUI).

```matlab
function R= allstats(A,varargin)
%R= ALLSTATS(A) returns a structure R with several statistics of ...
    vector A.
%   Groups within the data can be defined in optional vector G ...
    using a
%   numeric value for each group: R= ALLSTATS(A,G), see examples ...
    below.
%   In case a groups vector is provided all the statistics will be
%   calculated independently for each group. Each statistics is ...
    returned
%   as a field of structure R. Requires Statistics toolbox.
%
% The stats calculated are:
% R.min= minimum
% R.max= maximum
% R.mean= mean
% R.std= standard deviation
% R.mode= mode (of freq. distribution produced by HIST)
% R.q2p5= 2.5 percentile
% R.q5=   5 percentile
% R.q25=    25 percentile
% R.q50=    50 percentile (median)
% R.q75=    75 percentile
% R.q95= 95 percentile
% R.q97p5= 97.5 percentile
% R.kurt= Kurtosis
% R.skew= Skewness
%
```

```matlab
25  % Example without groups
26  %   x= rand(10,1);
27  %   R= allstats(x)
28  %
29  % Example with 2 groups (coded as 1 and 2 in vector G)
30  %   G= [1;1;1;1;1;2;2;2;2;2];
31  %   R= allstats(x,G)
32
33  A= shiftdim(A);
34
35  % Some error checking
36  if ¬isnumeric(A) error('First argument must be numeric'); end
37  if ¬isempty(varargin)
38      factors= shiftdim(varargin{1});
39      if ¬isnumeric(factors) error('Second argument must be ...
            numeric'); end
40      if length(A) ≠ length(factors)
41          error('Length of first and second arguments must be the ...
              same');
42      end
43  end
44
45  % We have groups
46  if ¬isempty(varargin)
47
48      % Extract unique values for groups
49      fval= unique(factors);
50      s= length(fval);
51
52      % Create the structure
53      R= struct('min',zeros(s,1),'max',zeros(s,1),'mean',zeros(s,1),...
54          'std',zeros(s,1),'q2p5',zeros(s,1),'q5',zeros(s,1),'q25',...
```

115

```matlab
55          zeros(s,1),'q50',zeros(s,1),'q75',zeros(s,1),'q95',zeros(s,1),...
56          'q97p5',zeros(s,1),'kurt',zeros(s,1),'skew',zeros(s,1));

57

58      % Do calculations for each value of the groups
59      for k= 1:s
60          rows= find(factors == fval(k)); % Elements of group 'k'
61          R(k).min=    nanmin(A(rows,:));
62          R(k).max=    nanmax(A(rows,:));
63          R(k).mean=  nanmean(A(rows,:));
64          R(k).std=    nanstd(A(rows,:));
65          [f,n]= hist(A(rows,:),30);
66          R(k).mode=  n(find(f==max(f)));
67          R(k).q2p5=  prctile(A(rows,:),2.5);
68          R(k).q5=         prctile(A(rows,:),5);
69          R(k).q25=   prctile(A(rows,:),25);
70          R(k).q50=   prctile(A(rows,:),50);
71          R(k).q75=   prctile(A(rows,:),75);
72          R(k).q95=   prctile(A(rows,:),95);
73          R(k).q97p5= prctile(A(rows,:),97.5);
74          R(k).kurt=  kurtosis(A(rows,:));
75          R(k).skew=  skewness(A(rows,:));
76      end
77  else % No groups
78      R.min=   nanmin(A);
79      R.max=   nanmax(A);
80      R.mean=  nanmean(A);
81      R.std=   nanstd(A);
82      [f,n]= hist(A,30);
83      R.mode=   n(find(f==max(f)));
84      R.q2p5= prctile(A,2.5);
85      R.q5=         prctile(A,5);
86      R.q25=   prctile(A,25);
```

```matlab
87     R.q50=  prctile(A,50);

88     R.q75=  prctile(A,75);

89     R.q95=  prctile(A,95);

90     R.q97p5=    prctile(A,97.5);

91     R.kurt= kurtosis(A);

92     R.skew= skewness(A);

93 end
```

```matlab
1  clc

2  clear all

3  close all

4

5  trial1 = xlsread('Predicted Angles1');trial2 =xlsread('Predicted ...
       Angles2');

6  trial3 = xlsread('Predicted Angles3');

7

8  %load plug in gait data into matlab

9  data = xlsread('Walking0.xlsx',1);

10

11 %load all the angles

12 hip_d = data(:,1);knee_d = data(:,2);ankle_d = data(:,3);

13 theta1_1 = trial1(:,1);theta2_1 = trial1(:,2);theta3_1 = trial1(:,3);

14 theta1_2 = trial2(:,1);theta2_2 = trial2(:,2);theta3_2 = trial2(:,3);

15 theta1_3 = trial3(:,1);theta2_3 = trial3(:,2);theta3_3 = trial3(:,3);

16 xa = 1:33;xb = 1:33;xc = 1:31;xd = 1:124;

17

18 x1 = xa./33.*100;x2 = xb./33.*100;x3 = xc./31.*100;x4 = xd./124.*100;

19

20 plot(xa,theta1_1,'b');hold on ...
       ;plot(xb,theta1_2,'k');plot(xc,theta1_3,'r')
```

```matlab
21  plot(xd,hip_d,'m');hold off;title('Hip Angle');xlabel('% of Gait ...
        Cycle')
22  ylabel('Angle (Degrees)');hleg1 = legend('No ...
        Vest','10%','15%','vicon')
23  figure
24  plot(-theta2_1,'b');hold on ;plot(-theta2_2,'k');plot(-theta2_3,'r');
25  plot(knee_d,'m');hold off;title('Knee Angle');xlabel('% of Gait ...
        Cycle')
26  ylabel('Angle (Degrees)');hleg2 = legend('No ...
        Vest','10%','15%','vicon')
27  figure
28  plot(theta3_1,'b');hold on ...
        ;plot(theta3_2,'k');plot(theta3_3,'r');hold off
29  title('Ankle Angle');xlabel('% of Gait Cycle');ylabel('Angle ...
        (Degrees)')
30  hleg3 = legend('No Vest','10%','15%')
```

```matlab
1   function varargout = compare_predicted_angles_plots(varargin)
2   % COMPARE_PREDICTED_ANGLES_PLOTS MATLAB code for
3   %       compare_predicted_angles_plots.fig
4   %       COMPARE_PREDICTED_ANGLES_PLOTS, by itself, creates a new
5   %       COMPARE_PREDICTED_ANGLES_PLOTS or raises the existing
6   %       singleton*.
7   %
8   %       H = COMPARE_PREDICTED_ANGLES_PLOTS returns the handle to a new
9   %       COMPARE_PREDICTED_ANGLES_PLOTS or the handle to
10  %       the existing singleton*.
11  %
12  %       COMPARE_PREDICTED_ANGLES_PLOTS
13  %       ('CALLBACK',hObject,eventData,handles,...) calls the local
```

```matlab
14  %        function named CALLBACK in COMPARE_PREDICTED_ANGLES_PLOTS.M
15  %        with the given input arguments.
16  %
17  %        COMPARE_PREDICTED_ANGLES_PLOTS('Property','Value',...)
18  %         creates a new COMPARE_PREDICTED_ANGLES_PLOTS or raises the
19  %        existing singleton*.  Starting from the left, property ...
       value pairs
20  %        applied to the GUI before ...
       compare_predicted_angles_plots_OpeningFcn
21  %        gets called.  An unrecognized property name or invalid ...
       value makes
22  %        property application stop. All inputs are passed to
23  %        compare_predicted_angles_plots_OpeningFcn via varargin.
24  %
25  %        *See GUI Options on GUIDE's Tools menu.  Choose "GUI ...
       allows only one
26  %        inSwing to run (singleton)".
27  %
28  % See also: GUIDE, GUIDATA, GUIHANDLES
29
30  % Edit the above text to modify the response to help
31  %compare_predicted_angles_plots
32
33  % Last Modified by GUIDE v2.5 06-Mar-2013 22:51:33
34
35  % Begin initialization code - DO NOT EDIT
36  gui_Singleton = 1;
37  gui_State = struct('gui_Name',        mfilename, ...
38              'gui_Singleton',  gui_Singleton, ...
39              'gui_OpeningFcn', ...
                    @compare_predicted_angles_plots_OpeningFcn, ...
```

```matlab
40          'gui_OutputFcn',  ...
                @compare_predicted_angles_plots_OutputFcn, ...
41          'gui_LayoutFcn',  [] , ...
42          'gui_Callback',   []);
43 if nargin & ischar(varargin{1})
44     gui_State.gui_Callback = str2func(varargin{1});
45 end
46
47 if nargout
48     [varargout{1:nargout}] = gui_mainfcn(gui_State, varargin{:});
49 else
50     gui_mainfcn(gui_State, varargin{:});
51 end
52 % End initialization code — DO NOT EDIT
53 % ——— Executes just before compare_predicted_angles_plots is made ...
       visible.
54 function compare_predicted_angles_plots_OpeningFcn(hObject, ...
       eventdata,...
55      handles, varargin)
56 % This function has no output args, see OutputFcn.
57 % hObject    handle to figure
58 % eventdata  reserved — to be defined in a future version of MATLAB
59 % handles    structure with handles and user data (see GUIDATA)
60 % varargin   command line arguments to compare_predicted_angles_plots
61 %(see VARARGIN)
62
63 % Choose default command line output for ...
        compare_predicted_angles_plots
64 handles.output = hObject;
65
66 % Update handles structure
67 guidata(hObject, handles);
```

```matlab
68
69 % UIWAIT makes compare_predicted_angles_plots wait for user response
70 %(see UIRESUME)
71 % uiwait(handles.figure1);
72 % --- Outputs from this function are returned to the command line.
73 function varargout = ...
       compare_predicted_angles_plots_OutputFcn(hObject, ...
       eventdata, handles)
75 % varargout  cell array for returning output args (see VARARGOUT);
76 % hObject    handle to figure
77 % eventdata  reserved - to be defined in a future version of MATLAB
78 % handles    structure with handles and user data (see GUIDATA)
79
80 % Get default command line output from handles structure
81 varargout{1} = handles.output;
82 % --- Executes on button press in browse_for_image.
83 function browse_for_image_Callback(hObject, eventdata, handles)
84 global org_dir pathname rr
85 addpath('C:\Anum_Thesis')
86 org_dir = pwd;
87 pathname = uigetdir;
88 cd(pathname)
89 rr = dir('*Predicted*.xls');
90 set(handles.textbox_for_browsed_image,'string',pathname);
91 set(handles.numer_of_predicted_xls,'string',size(rr,1));
92
93 function textbox_for_browsed_image_Callback(hObject, eventdata, ...
       handles)
94 % hObject    handle to textbox_for_browsed_image (see GCBO)
95 % eventdata  reserved - to be defined in a future version of MATLAB
96 % handles    structure with handles and user data (see GUIDATA)
97
```

121

```matlab
98  % Hints: get(hObject,'String') returns contents of
99  %textbox_for_browsed_image as text
100 %          str2double(get(hObject,'String'))
101 %returns contents of textbox_for_browsed_image as a double
102 % ---- Executes during object creation, after setting all properties.
103 function textbox_for_browsed_image_CreateFcn(hObject, eventdata, ...
        handles)
104 % hObject    handle to textbox_for_browsed_image (see GCBO)
105 % eventdata  reserved - to be defined in a future version of MATLAB
106 % handles    empty - handles not created until after all ...
        CreateFcns called
107
108 % Hint: edit controls usually have a white background on Windows.
109 %        See ISPC and COMPUTER.
110 if ispc & isequal(get(hObject,'BackgroundColor'), ...
111         get(0,'defaultUicontrolBackgroundColor'))
112     set(hObject,'BackgroundColor','white');
113 end
114 % ---- Executes on button press in clear_all_button.
115 function clear_all_button_Callback(hObject, eventdata, handles)
116 closeGUI = handles.figure1; %handles.figure1 is the GUI figure
117
118 guiName = get(handles.figure1,'Name'); %get the name of the GUI
119 close(closeGUI); %close the old GUI
120
121 eval(guiName) %call the GUI again
122 % maxfig(gcf,1)
123 clear all;
124 clc;
125 evalin('base','clear all');
126
127 function numer_of_predicted_xls_Callback(hObject, eventdata, handles)
```

```matlab
128 % hObject    handle to numer_of_predicted_xls (see GCBO)
129 % eventdata  reserved — to be defined in a future version of MATLAB
130 % handles    structure with handles and user data (see GUIDATA)
131
132 % Hints: get(hObject,'String') returns contents of ...
       numer_of_predicted_xls
133 %as text
134 %str2double(get(hObject,'String')) returns contents of
135 %numer_of_predicted_xls as a double
136 % ——— Executes during object creation, after setting all properties.
137 function numer_of_predicted_xls_CreateFcn(hObject, eventdata, ...
       handles)
138 % hObject    handle to numer_of_predicted_xls (see GCBO)
139 % eventdata  reserved — to be defined in a future version of MATLAB
140 % handles    empty — handles not created until after all ...
       CreateFcns called
141
142 % Hint: edit controls usually have a white background on Windows.
143 %       See ISPC and COMPUTER.
144 if ispc & isequal(get(hObject,'BackgroundColor'),...
145         get(0,'defaultUicontrolBackgroundColor'))
146    set(hObject,'BackgroundColor','white');
147 end
148 % ——— Executes on button press in checkbox1_x.
149 function checkbox1_x_Callback(hObject, eventdata, handles)
150 % hObject    handle to checkbox1_x (see GCBO)
151 % eventdata  reserved — to be defined in a future version of MATLAB
152 % handles    structure with handles and user data (see GUIDATA)
153
154 % Hint: get(hObject,'Value') returns toggle state of checkbox1_x
155 global x_col_val
156 x_col_val = get(hObject,'Value');
```

123

```matlab
157
158 % ——— Executes on button press in checkbox2_y.
159 function checkbox2_y_Callback(hObject, eventdata, handles)
160 % hObject    handle to checkbox2_y (see GCBO)
161 % eventdata  reserved − to be defined in a future version of MATLAB
162 % handles    structure with handles and user data (see GUIDATA)
163
164 % Hint: get(hObject,'Value') returns toggle state of checkbox2_y
165 global y_col_val
166 y_col_val = get(hObject,'Value');
167
168 % ——— Executes on button press in checkbox3_z.
169 function checkbox3_z_Callback(hObject, eventdata, handles)
170 % hObject    handle to checkbox3_z (see GCBO)
171 % eventdata  reserved − to be defined in a future version of MATLAB
172 % handles    structure with handles and user data (see GUIDATA)
173
174 % Hint: get(hObject,'Value') returns toggle state of checkbox3_z
175 global z_col_val
176 z_col_val = get(hObject,'Value');
177
178 function edit_x_Callback(hObject, eventdata, handles)
179 % hObject    handle to edit_x (see GCBO)
180 % eventdata  reserved − to be defined in a future version of MATLAB
181 % handles    structure with handles and user data (see GUIDATA)
182
183 % Hints: get(hObject,'String') returns contents of edit_x as text
184 % str2double(get(hObject,'String')) returns contents of edit_x as ...
      a double
185
186
187 % ——— Executes during object creation, after setting all properties.
```

```matlab
188  function edit_x_CreateFcn(hObject, eventdata, handles)
189  % hObject    handle to edit_x (see GCBO)
190  % eventdata  reserved - to be defined in a future version of MATLAB
191  % handles    empty - handles not created until after all ...
         CreateFcns called
192
193  % Hint: edit controls usually have a white background on Windows.
194  %       See ISPC and COMPUTER.
195  if ispc & isequal(get(hObject,'BackgroundColor'), ...
196          get(0,'defaultUicontrolBackgroundColor'))
197      set(hObject,'BackgroundColor','white');
198  end
199
200  function edit_y_Callback(hObject, eventdata, handles)
201  % hObject    handle to edit_y (see GCBO)
202  % eventdata  reserved - to be defined in a future version of MATLAB
203  % handles    structure with handles and user data (see GUIDATA)
204
205  % Hints: get(hObject,'String') returns contents of edit_y as text
206  % str2double(get(hObject,'String')) returns contents of edit_y as ...
         a double
207
208  % --- Executes during object creation, after setting all properties.
209  function edit_y_CreateFcn(hObject, eventdata, handles)
210  % hObject    handle to edit_y (see GCBO)
211  % eventdata  reserved - to be defined in a future version of MATLAB
212  % handles    empty - handles not created until after all ...
         CreateFcns called
213
214  % Hint: edit controls usually have a white background on Windows.
215  %       See ISPC and COMPUTER.
216  if ispc & isequal(get(hObject,'BackgroundColor'),...
```

125

```matlab
217            get(0,'defaultUicontrolBackgroundColor'))
218        set(hObject,'BackgroundColor','white');
219 end
220
221 function edit_z_Callback(hObject, eventdata, handles)
222 % hObject    handle to edit_z (see GCBO)
223 % eventdata  reserved - to be defined in a future version of MATLAB
224 % handles    structure with handles and user data (see GUIDATA)
225
226 % Hints: get(hObject,'String') returns contents of edit_z as text
227 %        str2double(get(hObject,'String')) returns contents of
228 %edit_z as a double
229
230 % --- Executes during object creation, after setting all properties.
231 function edit_z_CreateFcn(hObject, eventdata, handles)
232 % hObject    handle to edit_z (see GCBO)
233 % eventdata  reserved - to be defined in a future version of MATLAB
234 % handles    empty - handles not created until after all ...
        CreateFcns called
235
236 % Hint: edit controls usually have a white background on Windows.
237 %       See ISPC and COMPUTER.
238 if ispc & isequal(get(hObject,'BackgroundColor'),...
239            get(0,'defaultUicontrolBackgroundColor'))
240        set(hObject,'BackgroundColor','white');
241 end
242
243 % --- Executes on button press in generate_plot_and_vals.
244 function generate_plot_and_vals_Callback(hObject, eventdata, handles)
245 global x_col_val y_col_val z_col_val rr pathname
246 global vals_x vals_y vals_z x_list Rx Ry Rz
247 global allstats_listx allstats_listy allstats_listz
```

126

```matlab
248  allstats_listx = [];
249  allstats_listy = [];
250  allstats_listz = [];
251  subject_number1 = find(pathname == '\');
252  subject_number = pathname(subject_number1(end)+1:end);
253      percent_val = (get(handles.percent_values,'String'));
254      percent_val = str2num(percent_val);
255      if percent_val <=40
256          phase = 'Swing Phase';
257      elseif percent_val >=60
258          phase = 'Stance Phase';
259      end
260  if x_col_val == 1
261      vals_x = (get(handles.edit_x,'String'));
262      vals_x = str2num(vals_x);
263  end
264  if y_col_val == 1
265      vals_y = (get(handles.edit_y,'String'));
266      vals_y = str2num(vals_y);
267  end
268  if z_col_val == 1
269      vals_z = (get(handles.edit_z,'String'));
270      vals_z = str2num(vals_z);
271  end
272  % clf
273  for i = 1:size(rr,1)
274     xlsname = rr(i,1).name;
275     spreadsheet = xlsread(xlsname);
276     if x_col_val == 1
277         x_list = spreadsheet(vals_x((i*2)-1):vals_x(i*2),1);
278         Rx= allstats(x_list);
279         allstats_listx(1,i) = Rx.min;
```

```matlab
280         allstats_listx(2,i) = Rx.max;
281         allstats_listx(3,i) = Rx.mean;
282         allstats_listx(4,i) = Rx.std;
283 %           allstats_listx(5,i) = num2str(Rx.mode);
284         allstats_listx(6,i) = Rx.q2p5;
285         allstats_listx(7,i) = Rx.q5;
286         allstats_listx(8,i) = Rx.q25;
287         allstats_listx(9,i) = Rx.q50;
288         allstats_listx(10,i) = Rx.q75;
289         allstats_listx(11,i) = Rx.q95;
290         allstats_listx(12,i) = Rx.q97p5;
291         allstats_listx(13,i) = Rx.kurt;
292         allstats_listx(14,i) = Rx.skew;
293 %          filename =strcat('x',num2str(i),'.txt');
294 %          save ( filename,'Rx')
295     else
296         x_col_val = 0;
297     end
298     if y_col_val == 1
299         y_list = spreadsheet(vals_y((i*2)-1):vals_y(i*2),2);
300         Ry= allstats(y_list);
301         allstats_listy(1,i) = Ry.min;
302         allstats_listy(2,i) = Ry.max;
303         allstats_listy(3,i) = Ry.mean;
304         allstats_listy(4,i) = Ry.std;
305 %           allstats_listy(5,i) = num2str(Ry.mode);
306         allstats_listy(6,i) = Ry.q2p5;
307         allstats_listy(7,i) = Ry.q5;
308         allstats_listy(8,i) = Ry.q25;
309         allstats_listy(9,i) = Ry.q50;
310         allstats_listy(10,i) = Ry.q75;
311         allstats_listy(11,i) = Ry.q95;
```

```matlab
312         allstats_listy(12,i) = Ry.q97p5;
313         allstats_listy(13,i) = Ry.kurt;
314         allstats_listy(14,i) = Ry.skew;
315 %           filename =strcat('y',num2str(i),'.txt');
316 %           save ( filename,'Ry')
317     else
318         y_col_val = 0;
319     end
320     if z_col_val == 1
321         z_list = spreadsheet(vals_z((i*2)-1):vals_z(i*2),3);
322         Rz= allstats(z_list);
323         allstats_listz(1,i) = Rz.min;
324         allstats_listz(2,i) = Rz.max;
325         allstats_listz(3,i) = Rz.mean;
326         allstats_listz(4,i) = Rz.std;
327 %           allstats_listz(5,i) = num2str(Rz.mode);
328         allstats_listz(6,i) = Rz.q2p5;
329         allstats_listz(7,i) = Rz.q5;
330         allstats_listz(8,i) = Rz.q25;
331         allstats_listz(9,i) = Rz.q50;
332         allstats_listz(10,i) = Rz.q75;
333         allstats_listz(11,i) = Rz.q95;
334         allstats_listz(12,i) = Rz.q97p5;
335         allstats_listz(13,i) = Rz.kurt;
336         allstats_listz(14,i) = Rz.skew;
337 %           filename =strcat('z',num2str(i),'.txt');
338 %           save ( filename,'Rz')
339     else
340         z_col_val = 0;
341     end
342 if x_col_val == 1 & y_col_val == 1 & z_col_val == 1
343      p = 3;
```

```matlab
elseif (x_col_val == 1 & y_col_val == 1 & z_col_val == 0) ...
        | (x_col_val == 0 & y_col_val == 1 & z_col_val == 1)...
        | (x_col_val == 1 & y_col_val == 0 & z_col_val == 1)
    p = 2;
elseif (x_col_val == 1 & y_col_val == 0 & z_col_val == 0)...
        | (x_col_val == 0 & y_col_val == 1 & z_col_val == 0)....
        | (x_col_val == 0 & y_col_val == 0 & z_col_val == 1)
    p = 1;
end
if i == 1;
    plot_color = 'black';
elseif i == 2;
    plot_color = 'blue';
elseif i == 3;
    plot_color = 'magenta';
elseif i == 4;
    plot_color = 'green';
end
if i == 1
    figure(1)
    close(figure(1))
    figure(1)
end
hold on
if p == 3
%     figure(1);
    subplot(2,2,1); plot(x_list,'Color',plot_color);...
        title('Subject: Swing Phase Hip Angle','FontSize',16);...
        xlabel('Swing Phase - 40% of Gait Cycle','FontSize',16);...
        ylabel('Angle (Degrees)','FontSize',16);...
        legend('No load','10%','15%','20%');...
        set(gca, 'XTickLabelMode', 'Manual');set(gca, 'XTick', []);
```

130

```matlab
376     subplot(2,2,2); plot(y_list,'Color',plot_color); ...
377         title('Subject: Swing Phase Knee Angle','FontSize',16);...
378         xlabel('Swing Phase - 40% of Gait Cycle','FontSize',16);...
379         ylabel('Angle (Degrees)','FontSize',16);...
380         legend('No load','10%','15%','20%');...
381         set(gca, 'XTickLabelMode', 'Manual');set(gca, 'XTick', []);
382     subplot(2,2,3); plot(z_list,'Color',plot_color);...
383         title('Subject: Swing Phase Ankle Angle','FontSize',16);...
384         xlabel('Swing Phase - 40% of Gait Cycle','FontSize',16);...
385         ylabel('Angle (Degrees)','FontSize',16);...
386         legend('No load','10%','15%','20%');...
387         set(gca, 'XTickLabelMode', 'Manual');set(gca, 'XTick', []);
388 elseif p == 2
389     if (x_col_val == 1 & y_col_val == 1 & z_col_val == 0)
390 %       figure(1);
391     subplot(1,2,1); plot(x_list,'Color',plot_color); ...
392         title('Subject: Swing Phase Hip Angle','FontSize',16);...
393         xlabel('Swing Phase - 40% of Gait Cycle','FontSize',16);...
394         ylabel('Angle (Degrees)','FontSize',16);...
395         legend('No load','10%','15%','20%');...
396         set(gca, 'XTickLabelMode', 'Manual');...
397         set(gca, 'XTick', []);
398     subplot(1,2,2); plot(y_list,'Color',plot_color);...
399         title('Subject: Swing Phase Knee Angle','FontSize',16);...
400         xlabel('Swing Phase - 40% of Gait Cycle','FontSize',16);...
401         ylabel('Angle (Degrees)','FontSize',16);...
402         legend('No load','10%','15%','20%');...
403         set(gca, 'XTickLabelMode', 'Manual');...
404         set(gca, 'XTick', []);
405     elseif(x_col_val == 0 & y_col_val == 1 & z_col_val == 1)
406     figure(1);
407     subplot(1,2,1); plot(y_list,'Color',plot_color);...
```

131

```matlab
            title('Subject: Swing Phase Knee Angle','FontSize',16);...
            xlabel('Swing Phase - 40% of Gait Cycle','FontSize',16);...
            ylabel('Angle (Degrees)','FontSize',16);...
            legend('No load','10%','15%','20%');...
            set(gca, 'XTickLabelMode', 'Manual');set(gca, 'XTick', []);
        subplot(1,2,2); plot(z_list,'Color',plot_color);...
            title('Subject: Swing Phase Ankle Angle','FontSize',16)...
            ;xlabel('Swing Phase - 40% of Gait Cycle','FontSize',16);...
            ylabel('Angle (Degrees)','FontSize',16);...
            legend('No load','10%','15%','20%');...
            set(gca, 'XTickLabelMode', 'Manual');...
            set(gca, 'XTick', [])  ;
        elseif(x_col_val == 1 & y_col_val == 0 & z_col_val == 1)
%      figure(1);
        subplot(1,2,1); plot(x_list,'Color',plot_color); ...
            title('Subject: Swing Phase Hip Angle','FontSize',16);...
            xlabel('Swing Phase - 40% of Gait Cycle','FontSize',16);...
            ylabel('Angle (Degrees)','FontSize',16);...
            legend('No load','10%','15%','20%');...
            set(gca, 'XTickLabelMode', 'Manual');set(gca, 'XTick', []);
        subplot(1,2,2); plot(z_list,'Color',plot_color);...
            title('Subject: Swing Phase  Ankle Angle','FontSize',16);...
            xlabel('Swing Phase - 40% of Gait Cycle','FontSize',16);...
            ylabel('Angle (Degrees)','FontSize',16);...
            legend('No load','10%','15%','20%');...
            set(gca, 'XTickLabelMode', 'Manual');set(gca, 'XTick', ...
                [])  ;
    end
elseif p == 1
    if (x_col_val == 1 & y_col_val == 0 & z_col_val == 0)
%      figure(1);
percentaxis = 1:percent_val/size(x_list,1):percent_val;
```

```matlab
439 percentaxis(size(x_list,1)) = percent_val;
440     plot(percentaxis, x_list,'Color',plot_color);...
441         title([subject_number ':' ' ' phase ' - Flexion/Extension ...
                of Hip'],...
442         'FontSize',16);xlabel([num2str(percent_val) '% of Gait ...
                Cycle'],...
443         'FontSize',16);ylabel('Angle (Degrees)','FontSize',16);...
444         set(gca, 'XTickLabelMode', 'Manual');%set(gca, 'XTick', []);
445     elseif (x_col_val == 0 & y_col_val == 1 & z_col_val == 0)
446 %     figure(1);
447 percentaxis = 1:percent_val/size(y_list,1):percent_val;
448 percentaxis(size(y_list,1)) = percent_val;
449     plot(percentaxis, y_list,'Color',plot_color); ...
450         title([subject_number ':' ' ' phase ' - Flexion/Extension ...
                of Knee'],...
451         'FontSize',16);xlabel([num2str(percent_val) '% of Gait ...
                Cycle'],...
452         'FontSize',16);ylabel('Angle (Degrees)','FontSize',16);...
453         set(gca, 'XTickLabelMode', 'Manual');%set(gca, 'XTick', ...
                [])     ;
454     elseif(x_col_val == 0 & y_col_val == 0 & z_col_val == 1)
455 %     figure(1);
456 percentaxis = 1:percent_val/size(z_list,1):percent_val;
457 percentaxis(size(z_list,1)) = percent_val;
458     plot(percentaxis, z_list,'Color',plot_color); ...
459 title([subject_number ':' ' ' phase ' - ...Flexion/Extension of ...
        Ankle'],...
460         'FontSize',16);xlabel([num2str(percent_val) '% of Gait ...
                Cycle'],...
461         'FontSize',16);ylabel('Angle (Degrees)','FontSize',16);...
462         set(gca, 'XTickLabelMode', 'Manual');%set(gca, 'XTick', ...
                [])     ;
```

133

```matlab
463         end
464     end
465     end
466     hold off
467     if x_col_val == 1
468     filename_list = ['allstat_x' num2str(vals_x) '.xls'];
469     final_allstats_list = allstats_listx;
470     elseif y_col_val == 1
471     filename_list = ['allstat_y' num2str(vals_y) '.xls'];
472     final_allstats_list = allstats_listy;
473     elseif z_col_val == 1
474     filename_list = ['allstat_z' num2str(vals_z) '.xls'];
475     final_allstats_list = allstats_listz;
476     end
477     A = {'min';'max';'mean';'std';'mode';'q2p5';'q5';'q25';'q50';...
478         'q75';'q95';'q97p5';'kurt';'skew'};
479     xlswrite(filename_list,A);
480     if size(rr,1) == 2
481     xlswrite(filename_list,final_allstats_list,'B1:C14');
482     elseif size(rr,1) == 3
483     xlswrite(filename_list,final_allstats_list,'B1:D14');
484     elseif size(rr,1) == 4
485     xlswrite(filename_list,final_allstats_list,'B1:E14');
486     end
487
488
489     % ——— Executes on button press in load_csv.
490     function load_csv_Callback(hObject, eventdata, handles)
491     global org_dir2 pathname2 rr2
492     addpath('C:\Anum_Thesis')
493     org_dir2 = pwd;
494     pathname2 = uigetdir;
```

134

```matlab
495  cd(pathname2)
496  rr2 = dir('*Trial*.csv');
497  set(handles.textbox_for_csv_file,'string',pathname2);
498  set(handles.numer_of_csv,'string',size(rr2,1));
499  pause(0.05);
500  for csv_file_number = 1:size(rr2,1)
501      csv_filename = rr2(csv_file_number,1).name;
502      origin_fix(csv_filename,csv_file_number)
503  end
504
505
506  function textbox_for_csv_file_Callback(hObject, eventdata, handles)
507  % hObject    handle to textbox_for_csv_file (see GCBO)
508  % eventdata  reserved - to be defined in a future version of MATLAB
509  % handles    structure with handles and user data (see GUIDATA)
510
511  % Hints: get(hObject,'String') returns contents of
512  %textbox_for_csv_file as text
513  % str2double(get(hObject,'String')) returns contents of
514  %textbox_for_csv_file as a double
515
516
517  % --- Executes during object creation, after setting all properties.
518  function textbox_for_csv_file_CreateFcn(hObject, eventdata, handles)
519  % hObject    handle to textbox_for_csv_file (see GCBO)
520  % eventdata  reserved - to be defined in a future version of MATLAB
521  % handles    empty - handles not created until after all ...
         CreateFcns called
522
523  % Hint: edit controls usually have a white background on Windows.
524  %       See ISPC and COMPUTER.
525  if ispc && isequal(get(hObject,'BackgroundColor'),...
```

```matlab
526             get(0,'defaultUicontrolBackgroundColor'))
527        set(hObject,'BackgroundColor','white');
528  end
529
530  function numer_of_csv_Callback(hObject, eventdata, handles)
531  % hObject    handle to numer_of_csv (see GCBO)
532  % eventdata  reserved — to be defined in a future version of MATLAB
533  % handles    structure with handles and user data (see GUIDATA)
534
535  % Hints: get(hObject,'String') returns contents of numer_of_csv ...
            as text
536  %str2double(get(hObject,'String')) returns contents of numer_of_csv
537  %as a double
538
539  % ——— Executes during object creation, after setting all properties.
540  function numer_of_csv_CreateFcn(hObject, eventdata, handles)
541  % hObject    handle to numer_of_csv (see GCBO)
542  % eventdata  reserved — to be defined in a future version of MATLAB
543  % handles    empty — handles not created until after all ...
            CreateFcns called
544
545  % Hint: edit controls usually have a white background on Windows.
546  %        See ISPC and COMPUTER.
547  if ispc && isequal(get(hObject,'BackgroundColor'), ...
548             get(0,'defaultUicontrolBackgroundColor'))
549        set(hObject,'BackgroundColor','white');
550  end
551
552  function percent_values_Callback(hObject, eventdata, handles)
553  % hObject    handle to percent_values (see GCBO)
554  % eventdata  reserved — to be defined in a future version of MATLAB
555  % handles    structure with handles and user data (see GUIDATA)
```

```matlab
556
557 % Hints: get(hObject,'String') returns contents of percent_values ...
       as text
558 %str2double(get(hObject,'String')) returns contents of ...
       percent_values as
559 %a double
560
561 % ——— Executes during object creation, after setting all properties.
562 function percent_values_CreateFcn(hObject, eventdata, handles)
563 % hObject    handle to percent_values (see GCBO)
564 % eventdata  reserved — to be defined in a future version of MATLAB
565 % handles    empty — handles not created until after all ...
       CreateFcns called
566
567 % Hint: edit controls usually have a white background on Windows.
568 %       See ISPC and COMPUTER.
569 if ispc && isequal(get(hObject,'BackgroundColor'),...
570         get(0,'defaultUicontrolBackgroundColor'))
571     set(hObject,'BackgroundColor','white');
572 end
```

```matlab
1 % clc
2 % clear all
3 % close all
4 function origin_fix(csv_filename,csv_file_number)
5 filename = csv_filename;
6 fid=fopen(filename);
7 data_f1=textscan(fid,'%f %*f %*f %f %f %*f %f %f %*f %f %f %*f %f ...
      %f', ...
8     'delimiter',', ','headerlines',5);
```

```matlab
9  data_f1{1,2} = data_f1{1,2}*(-1);data_f1{1,4} = data_f1{1,4}*(-1);

10 data_f1{1,6} = data_f1{1,6}*(-1);data_f1{1,8} = data_f1{1,8}*(-1);

11 fclose(fid);

12 new_table = zeros(size(data_f1{1,1},1),size(data_f1,2)-1);

13 for i = 1:size(data_f1{1,1},1)

14     x_red = -data_f1{1,2}(i); z_red = -data_f1{1,3}(i);

15     for j = 1:size(data_f1,2)

16         v(1) = data_f1{1,2}(i)+x_red;

17         v(2) = data_f1{1,3}(i)+z_red;

18         v(3) = data_f1{1,4}(i)+x_red;

19         v(4) = data_f1{1,5}(i)+z_red;

20         v(5) = data_f1{1,6}(i)+x_red;

21         v(6) = data_f1{1,7}(i)+z_red;

22         v(7) = data_f1{1,8}(i)+x_red;

23         v(8) = data_f1{1,9}(i)+z_red;

24

25         new_table(i,:) = v;

26     end

27 end

28

29 xlswrite(strcat(filename(1:end-4),'_corrected.xls'),new_table)

30

31 %reads in segment values

32 segment = xlsread('segment.xlsx');

33 L1 = segment(:,1);L2 = segment(:,2);L3 = segment(:,3);

34 %change x to z and z to x....because I need to make sure the ...
       motion in in

35 %first quadrant

36

37 %defining markers where x1 = hip, x2 = knee, x3 = ankle, x4 = pinky

38 z1 = new_table(:,1);z2 = new_table(:,3);z3 = new_table(:,5);

39 z4 = new_table(:,7);
```

138

```matlab
40

41  %defining markers where z1 = hip, z2 = knee, z3 = ankle, z4 = pinky
42  x1 = new_table(:,2);x2 = new_table(:,4);x3 = new_table(:,6);
43  x4 = new_table(:,8);

44

45  x1 = abs(x1);x2 = abs(x2);x3 = abs(x3);x4 = abs(x4);
46  xlswrite(strcat(filename(1:end-4),'_corrected.xls'),new_table)
47  %plug into GB equations
48  %Let start with equation 6 to find for s1
49  s1 = (z2)./L1;

50

51  %Next, with equation 5, find c1
52  c1_squared = (-1).*((-L1.^2 + (z2).^2)./L1.^2);
53  c1_p = sqrt(c1_squared);
54  c1_n = c1_p.*(-1);

55

56  %Using equation 1 to find c3
57  c3_p = (-1).*(L1.*x4./(L2.*L3).*(c1_p) + (-0.5.*L1.^2 + ...
        0.5.*L2.^2 + ...
58      0.5.*L3.^2 - 0.5.*x4.^2 - 0.5.*z4.^2 + z4.*(z2))./(L2.*L3));
59  c3_n = (-1).*(L1.*x4./(L2.*L3).*(c1_n) + (-0.5.*L1.^2 + ...
        0.5.*L2.^2 +...
60      0.5.*L3.^2 - 0.5.*x4.^2 - 0.5.*z4.^2 + z4.*(z2))./(L2.*L3));

61

62

63  %Using equation 4 to find s2
64      %Looking at equation 4 we can see it is a quadratice ...
            equation, so let's
65      %set it up accordingly
66      B_p = ((-L1.^4.*z4 - L1.^2.*L2.^2.*z4 + L1.^2.*L3.^2.*z4 + ...
67          2.*L1.^2.*x4.^2.*z4 -2.*L1.^2.*z4.^3 +...
```

139

```
68        4.*L1.^2.*z4.^2.*(z2)-L2.^2.*x4.^2.*z4 + ...
             2.*L2.^2.*x4.^2.*(z2) -...

69        L2.^2.*z4.^3 + 2.*L2.^2.*z4.^2.*(z2) +...

70        L3.^2.*x4.^2.*z4 - 2.*L3.^2.*x4.^2.*(z2) + L3.^2.*z4.^3 - ...

71        2.*L3.^2.*z4.^2.*(z2) - x4.^4.*z4 - 2.*x4.^2.*z4.^3 ...

72        + 4.*x4.^2.*z4.^2.*(z2) - 4.*x4.^2.*z4.*(z2).^2 - z4.^5 + ...

73        4.*z4.^4.*(z2) - 4.*z4.^3.*(z2).^2)./(L1.^4.*L2 -...

74        2.*L1.^2.*L2.*x4.^2 + 2.*L1.^2.*L2.*z4.^2 -...

75        4.*L1.^2.*L2.*z4.*(z2) + L2.*x4.^4 + 2.*L2.*x4.^2.*z4.^2 -...

76        4.*L2.*x4.^2.*z4.*(z2) + 4.*L2.*x4.^2.*(z2).^2 + ...
             L2.*z4.^4 -...

77        4.*L2.*z4.^3.*(z2) + 4.*L2.*z4.^2.*(z2).^2).*(c1_p)...

78        + (L1.^4.*x4.*(z2) - 2.*L1.^2.*L2.^2.*x4.*z4 + ...
             L1.^2.*L2.^2.*...

79        x4.*(z2) + 2.*L1.^2.*L3.^2.*x4.*z4 -...

80        L1.^2.*L3.^2.*x4.*(z2) - 2.*L1.^2.*x4.^3.*(z2) + ...
             2.*L1.^2.*x4.*...

81        z4.^2.*(z2) - 4.*L1.^2.*x4.*z4.*(z2).^2 +...

82        L2.^2.*x4.^3.*(z2) +L2.^2.*x4.*z4.^2.*(z2) - ...
             L3.^2.*x4.^3.*(z2)-...

83        L3.^2.*x4.*z4.^2.*(z2) + x4.^5.*(z2) +...

84        2.*x4.^3.*z4.^2.*(z2)-4.*x4.^3.*z4.*(z2).^2 + ...
             4.*x4.^3.*(z2).^3 ...

85      + x4.*z4.^4.*(z2) - 4.*x4.*z4.^3.*(z2).^2 +...

86        4.*x4.*z4.^2.*(z2).^3)./(L1.^5.*L2 - 2.*L1.^3.*L2.*x4.^2 ...
             + ...

87        2.*L1.^3.*L2.*z4.^2 - 4.*L1.^3.*L2.*z4.*(z2) +...

88        L1.*L2.*x4.^4 + 2.*L1.*L2.*x4.^2.*z4.^2 - ...
             4.*L1.*L2.*x4.^2.*z4.*...

89        (z2) + 4.*L1.*L2.*x4.^2.*(z2).^2 +...

90       L1.*L2.*z4.^4 - 4.*L1.*L2.*z4.^3.*(z2) + ...
             4.*L1.*L2.*z4.^2.*(z2).^2));
```

```
 91    B_n = ((−L1.^4.*z4 −L1.^2.*L2.^2.*z4 + L1.^2.*L3.^2.*z4 + ...
         2.*L1.^2.*...
 92       x4.^2.*z4 − 2.*L1.^2.*z4.^3 +...
 93       4.*L1.^2.*z4.^2.*(z2) − L2.^2.*x4.^2.*z4 + ...
           2.*L2.^2.*x4.^2.*(z2)...
 94     − L2.^2.*z4.^3 + 2.*L2.^2.*z4.^2.*(z2) +...
 95     L3.^2.*x4.^2.*z4 − 2.*L3.^2.*x4.^2.*(z2) + L3.^2.*z4.^3 ...
 96     − 2.*L3.^2.*z4.^2.*(z2) − x4.^4.*z4 − 2.*x4.^2.*z4.^3 ...
 97     + 4.*x4.^2.*z4.^2.*(z2) − 4.*x4.^2.*z4.*(z2).^2 − z4.^5 ...
 98   + 4.*z4.^4.*(z2) − 4.*z4.^3.*(z2).^2)./(L1.^4.*L2 −...
 99       2.*L1.^2.*L2.*x4.^2 + 2.*L1.^2.*L2.*z4.^2 − ...
           4.*L1.^2.*L2.*z4.*...
100     (z2) + L2.*x4.^4 + 2.*L2.*x4.^2.*z4.^2 −...
101     4.*L2.*x4.^2.*z4.*(z2) + 4.*L2.*x4.^2.*(z2).^2 + ...
           L2.*z4.^4 − 4.*...
102     L2.*z4.^3.*(z2) + 4.*L2.*z4.^2.*(z2).^2).*(c1_n)...
103     + (L1.^4.*x4.*(z2) −2.*L1.^2.*L2.^2.*x4.*z4 + ...
           L1.^2.*L2.^2.*x4.*...
104     (z2) + 2.*L1.^2.*L3.^2.*x4.*z4 −...
105     L1.^2.*L3.^2.*x4.*(z2) − 2.*L1.^2.*x4.^3.*(z2) + ...
           2.*L1.^2.*x4.*...
106     z4.^2.*(z2) − 4.*L1.^2.*x4.*z4.*(z2).^2 +...
107     L2.^2.*x4.^3.*(z2) + L2.^2.*x4.*z4.^2.*(z2) − ...
           L3.^2.*x4.^3.*(z2)...
108     − L3.^2.*x4.*z4.^2.*(z2) + x4.^5.*(z2) +...
109     2.*x4.^3.*z4.^2.*(z2)−4.*x4.^3.*z4.*(z2).^2 + ...
           4.*x4.^3.*(z2).^3 ...
110     + x4.*z4.^4.*(z2) − 4.*x4.*z4.^3.*(z2).^2 +...
111     4.*x4.*z4.^2.*(z2).^3)./(L1.^5.*L2 − 2.*L1.^3.*L2.*x4.^2 ...
           + ...
112     2.*L1.^3.*L2.*z4.^2 − 4.*L1.^3.*L2.*z4.*(z2) +...
```

141

```
113    L1.*L2.*x4.^4 + 2.*L1.*L2.*x4.^2.*z4.^2 − ...
           4.*L1.*L2.*x4.^2.* ...
114    z4.*(z2) + 4.*L1.*L2.*x4.^2.*(z2).^2 +...
115     L1.*L2.*z4.^4 − 4.*L1.*L2.*z4.^3.*(z2) + ...
           4.*L1.*L2.*z4.^2.*(z2).^2));
116    C_p = (−0.5.*L1.^6.*x4 +...
117      L1.^4.*x4.^3 − L1.^4.*x4.*z4.^2 + 2.*L1.^4.*x4.*z4.*(z2) ...
           + 0.5.*...
118      L1.^2.*L2.^4.*x4 −...
119      L1.^2.*L2.^2.*L3.^2.*x4 +2.*L1.^2.*L2.^2.*x4.*z4.^2 − ...
           2.*L1.^2.*...
120      L2.^2.*x4.*z4.*(z2) +...
121      0.5.*L1.^2.*L3.^4.*x4 −0.5.*L1.^2.*x4.^5 − ...
           L1.^2.*x4.^3.*z4.^2 +...
122      2.*L1.^2.*x4.^3.*z4.*(z2) −...
123      2.*L1.^2.*x4.^3.*(z2).^2 −0.5.*L1.^2.*x4.*z4.^4 + ...
           2.*L1.^2.*x4.*...
124      z4.^3.*(z2) − 2.*L1.^2.*x4.*z4.^2.*(z2).^2 −...
125      2.*L2.^2.*x4.^3.*z4.*(z2) +2.*L2.^2.*x4.^3.*(z2).^2 − ...
           2.*L2.^2.*...
126      x4.*z4.^3.*(z2) +...
127      2.*L2.^2.*x4.*z4.^2.*(z2).^2)./(L1.^5.*L2.^2 − ...
           2.*L1.^3.*L2.^2.*...
128      x4.^2 + 2.*L1.^3.*L2.^2.*z4.^2 −...
129      4.*L1.^3.*L2.^2.*z4.*(z2) + L1.*L2.^2.*x4.^4 + ...
           2.*L1.*L2.^2.*...
130      x4.^2.*z4.^2 − 4.*L1.*L2.^2.*x4.^2.*z4.*(z2) +...
131      4.*L1.*L2.^2.*x4.^2.*(z2).^2 + L1.*L2.^2.*z4.^4 − ...
           4.*L1.*L2.^2.*...
132      z4.^3.*(z2) +...
133      4.*L1.*L2.^2.*z4.^2.*(z2).^2).*(c1_p) + (1./4.*L1.^8 − ...
           0.5.*...
```

```
134    L1.^6.*L2.^2 − 0.5.*L1.^6.*L3.^2 −...

135    1./4.*L1.^6.*x4.^2 + 3./4.*L1.^6.*z4.^2 − ...
           3./2.*L1.^6.*z4.*...

136    (z2) + 1./4.*L1.^4.*L2.^4 −...

137    0.5.*L1.^4.*L2.^2.*L3.^2 + L1.^4.*L2.^2.*x4.^2 + ...
           2.*L1.^4.*...

138    L2.^2.*z4.*(z2) + 1./4.*L1.^4.*L3.^4 +...

139    L1.^4.*L3.^2.*x4.^2 − L1.^4.*L3.^2.*z4.^2 + ...
           2.*L1.^4.*L3.^2.*...

140    z4.*(z2) − 1./4.*L1.^4.*x4.^4 +...

141    0.5.*L1.^4.*x4.^2.*z4.^2 − L1.^4.*x4.^2.*z4.*(z2) + ...
           L1.^4.*...

142    x4.^2.*(z2).^2 + 3./4.*L1.^4.*z4.^4 −...

143    3.*L1.^4.*z4.^3.*(z2) + 3.*L1.^4.*z4.^2.*(z2).^2 + ...
           1./4.*L1.^2.*...

144    L2.^4.*x4.^2 + 1./4.*L1.^2.*L2.^4.*z4.^2 −...

145    0.5.*L1.^2.*L2.^4.*z4.*(z2) − ...
           0.5.*L1.^2.*L2.^2.*L3.^2.*x4.^2 −...

146    0.5.*L1.^2.*L2.^2.*L3.^2.*z4.^2 +...

147    L1.^2.*L2.^2.*L3.^2.*z4.*(z2) − 0.5.*L1.^2.*L2.^2.*x4.^4 ...
           − 2.*...

148    L1.^2.*L2.^2.*x4.^2.*z4.*(z2) −...

149    L1.^2.*L2.^2.*x4.^2.*(z2).^2 + 0.5.*L1.^2.*L2.^2.*z4.^4 − ...
           3.*...

150    L1.^2.*L2.^2.*z4.^2.*(z2).^2 +...

151    1./4.*L1.^2.*L3.^4.*x4.^2 + 1./4.*L1.^2.*L3.^4.*z4.^2 − ...
           0.5.*...

152    L1.^2.*L3.^4.*z4.*(z2) −...

153    0.5.*L1.^2.*L3.^2.*x4.^4 − L1.^2.*L3.^2.*x4.^2.*z4.^2 + ...
           2.*...

154    L1.^2.*L3.^2.*x4.^2.*z4.*(z2) −...
```

```
155    2.*L1.^2.*L3.^2.*x4.^2.*(z2).^2 - ...
          0.5.*L1.^2.*L3.^2.*z4.^4 + 2.*...
156    L1.^2.*L3.^2.*z4.^3.*(z2) -...
157    2.*L1.^2.*L3.^2.*z4.^2.*(z2).^2 + 1./4.*L1.^2.*x4.^6 + ...
          3./4.*...
158    L1.^2.*x4.^4.*z4.^2 - 3./2.*L1.^2.*x4.^4.*z4.*(z2)...
159    + L1.^2.*x4.^4.*(z2).^2 + 3./4.*L1.^2.*x4.^2.*z4.^4 - 3.*...
160    L1.^2.*x4.^2.*z4.^3.*(z2) +...
161    4.*L1.^2.*x4.^2.*z4.^2.*(z2).^2 - 2.*L1.^2.*x4.^2.*z4.*...
162    (z2).^3 + 1./4.*L1.^2.*z4.^6 - 3./2.*L1.^2.*z4.^5.*(z2) +...
163    3.*L1.^2.*z4.^4.*(z2).^2 - 2.*L1.^2.*z4.^3.*(z2).^3 + ...
          L2.^2.*...
164    x4.^4.*(z2).^2 + 2.*L2.^2.*x4.^2.*z4.*(z2).^3 -...
165    L2.^2.*z4.^4.*(z2).^2 + ...
          2.*L2.^2.*z4.^3.*(z2).^3)./(L1.^6.*...
166    L2.^2 - 2.*L1.^4.*L2.^2.*x4.^2 +...
167    2.*L1.^4.*L2.^2.*z4.^2 - 4.*L1.^4.*L2.^2.*z4.*(z2) + ...
          L1.^2.*...
168    L2.^2.*x4.^4 + 2.*L1.^2.*L2.^2.*x4.^2.*z4.^2 ...
169    - 4.*L1.^2.*L2.^2.*x4.^2.*z4.*(z2) + ...
          4.*L1.^2.*L2.^2.*x4.^2.*...
170    (z2).^2 + L1.^2.*L2.^2.*z4.^4 -...
171    4.*L1.^2.*L2.^2.*z4.^3.*(z2) + ...
          4.*L1.^2.*L2.^2.*z4.^2.*(z2).^2);
172    C_n = (-0.5.*L1.^6.*x4 +...
173    L1.^4.*x4.^3 - L1.^4.*x4.*z4.^2 + 2.*L1.^4.*x4.*z4.*(z2) ...
          + 0.5.*...
174    L1.^2.*L2.^4.*x4 -...
175    L1.^2.*L2.^2.*L3.^2.*x4 +2.*L1.^2.*L2.^2.*x4.*z4.^2 - ...
          2.*L1.^2.*...
176    L2.^2.*x4.*z4.*(z2) +...
```

144

```
177  0.5.*L1.^2.*L3.^4.*x4 - 0.5.*L1.^2.*x4.^5 - ...
        L1.^2.*x4.^3.*z4.^2+...
178  2.*L1.^2.*x4.^3.*z4.*(z2) -...
179  2.*L1.^2.*x4.^3.*(z2).^2 - 0.5.*L1.^2.*x4.*z4.^4 + ...
        2.*L1.^2.*...
180  x4.*z4.^3.*(z2) - 2.*L1.^2.*x4.*z4.^2.*(z2).^2 -...
181  2.*L2.^2.*x4.^3.*z4.*(z2) + 2.*L2.^2.*x4.^3.*(z2).^2 - 2.*...
182  L2.^2.*x4.*z4.^3.*(z2) +...
183  2.*L2.^2.*x4.*z4.^2.*(z2).^2)./(L1.^5.*L2.^2 - 2.*L1.^3.*...
184  L2.^2.*x4.^2 + 2.*L1.^3.*L2.^2.*z4.^2 -...
185  4.*L1.^3.*L2.^2.*z4.*(z2) + L1.*L2.^2.*x4.^4 + ...
        2.*L1.*L2.^2.*...
186  x4.^2.*z4.^2 - 4.*L1.*L2.^2.*x4.^2.*z4.*(z2) +...
187  4.*L1.*L2.^2.*x4.^2.*(z2).^2 + L1.*L2.^2.*z4.^4 - ...
        4.*L1.*L2.^2.*...
188  z4.^3.*(z2) +...
189  4.*L1.*L2.^2.*z4.^2.*(z2).^2).*(c1_n) + (1./4.*L1.^8 - ...
        0.5.*...
190  L1.^6.*L2.^2 - 0.5.*L1.^6.*L3.^2 -...
191  1./4.*L1.^6.*x4.^2 + 3./4.*L1.^6.*z4.^2 - ...
        3./2.*L1.^6.*z4.*(z2)...
192  + 1./4.*L1.^4.*L2.^4 -...
193  0.5.*L1.^4.*L2.^2.*L3.^2 + L1.^4.*L2.^2.*x4.^2 + ...
        2.*L1.^4.*...
194  L2.^2.*z4.*(z2) + 1./4.*L1.^4.*L3.^4 +...
195  L1.^4.*L3.^2.*x4.^2 - L1.^4.*L3.^2.*z4.^2 + ...
        2.*L1.^4.*L3.^2.*...
196  z4.*(z2) - 1./4.*L1.^4.*x4.^4 +...
197  0.5.*L1.^4.*x4.^2.*z4.^2 - L1.^4.*x4.^2.*z4.*(z2) + ...
        L1.^4.*...
198  x4.^2.*(z2).^2 + 3./4.*L1.^4.*z4.^4 -...
199  3.*L1.^4.*z4.^3.*(z2) + 3.*L1.^4.*z4.^2.*(z2).^2 + 1./4.*...
```

```
200   L1.^2.*L2.^4.*x4.^2 + 1./4.*L1.^2.*L2.^4.*z4.^2 -...
201   0.5.*L1.^2.*L2.^4.*z4.*(z2) - 0.5.*L1.^2.*L2.^2.*L3.^2.*...
202   x4.^2 - 0.5.*L1.^2.*L2.^2.*L3.^2.*z4.^2 +...
203   L1.^2.*L2.^2.*L3.^2.*z4.*(z2) - 0.5.*L1.^2.*L2.^2.*x4.^4 ...
        - 2.*...
204   L1.^2.*L2.^2.*x4.^2.*z4.*(z2) -...
205   L1.^2.*L2.^2.*x4.^2.*(z2).^2 + 0.5.*L1.^2.*L2.^2.*z4.^4 - ...
        3.*...
206   L1.^2.*L2.^2.*z4.^2.*(z2).^2 +...
207   1./4.*L1.^2.*L3.^4.*x4.^2 + 1./4.*L1.^2.*L3.^4.*z4.^2 - ...
        0.5.*...
208   L1.^2.*L3.^4.*z4.*(z2) -...
209   0.5.*L1.^2.*L3.^2.*x4.^4 - L1.^2.*L3.^2.*x4.^2.*z4.^2 + ...
        2.*...
210   L1.^2.*L3.^2.*x4.^2.*z4.*(z2) -...
211   2.*L1.^2.*L3.^2.*x4.^2.*(z2).^2 - ...
        0.5.*L1.^2.*L3.^2.*z4.^4 + ...
212   2.*L1.^2.*L3.^2.*z4.^3.*(z2) -...
213   2.*L1.^2.*L3.^2.*z4.^2.*(z2).^2 + 1./4.*L1.^2.*x4.^6 + ...
        3./4.*...
214   L1.^2.*x4.^4.*z4.^2 - 3./2.*L1.^2.*x4.^4.*z4.*(z2)...
215   + L1.^2.*x4.^4.*(z2).^2 + 3./4.*L1.^2.*x4.^2.*z4.^4 - 3.*...
216   L1.^2.*x4.^2.*z4.^3.*(z2) +...
217   4.*L1.^2.*x4.^2.*z4.^2.*(z2).^2 - 2.*L1.^2.*x4.^2.*z4.*...
218   (z2).^3 + 1./4.*L1.^2.*z4.^6 - 3./2.*L1.^2.*z4.^5.*(z2) +...
219   3.*L1.^2.*z4.^4.*(z2).^2 - 2.*L1.^2.*z4.^3.*(z2).^3 + ...
        L2.^2.*...
220   x4.^4.*(z2).^2 + 2.*L2.^2.*x4.^2.*z4.*(z2).^3 -...
221   L2.^2.*z4.^4.*(z2).^2 + ...
        2.*L2.^2.*z4.^3.*(z2).^3)./(L1.^6.*...
222   L2.^2 - 2.*L1.^4.*L2.^2.*x4.^2 +...
```

146

```matlab
            2.*L1.^4.*L2.^2.*z4.^2 - 4.*L1.^4.*L2.^2.*z4.*(z2) + ...
                L1.^2.*...
            L2.^2.*x4.^4 + 2.*L1.^2.*L2.^2.*x4.^2.*z4.^2 ...
            - 4.*L1.^2.*L2.^2.*x4.^2.*z4.*(z2) + ...
                4.*L1.^2.*L2.^2.*x4.^2.*...
            (z2).^2 + L1.^2.*L2.^2.*z4.^4 -...
            4.*L1.^2.*L2.^2.*z4.^3.*(z2) + ...
                4.*L1.^2.*L2.^2.*z4.^2.*(z2).^2);


        %Putting in the quadratic formula

        %fnding the positive root while plugging in positive c1

        s2_1 = (-(B_p)+sqrt((B_p).^2-4.*(C_p)))./(2);

        %fnding the negative root while plugging in positive c1

        s2_2 = (-(B_p)-sqrt((B_p).^2-4.*(C_p)))./(2);

        %fnding the positive root while plugging in negative c1

        s2_3 = (-(B_n)+sqrt((B_n).^2-4.*(C_n)))./(2);

        %fnding the negative root while plugging in negative c1

        s2_4 = (-(B_n)-sqrt((B_n).^2-4.*(C_n)))./(2);


        %Note: All together, we now have 4 values for s2


         %Using equation 2 to find s3
        s3_1 = (-1)  .* ((L1.^4.*x4 - L1.^2.*x4.^3 - ...
            L1.^2.*x4.*(z4).^2)./...
            (L1.^4.*L3 - L1.^2.*L3.*x4.^2 - 2.*L1.^2.*L3.*(z4).*(z2)...
            + L3.*x4.^2.*(z2).^2 + ...
                L3.*(z4).^2.*(z2).^2).*(s2_1).*(c1_p) + ...
            (-L1.^5 + L1.^3.*x4.^2 - L1.^3.*(z4).^2 +...
            3.*L1.^3.*(z4).*(z2) + L1.*x4.^2.*(z4).*(z2) - ...
                2.*L1.*x4.^2.*...
            (z2).^2 + L1.*(z4).^3.*(z2) -...
```

```matlab
248    2.*L1.*(z4).^2.*(z2).^2)./(L1.^4.*L3 - L1.^2.*L3.*x4.^2 - ...
           2.*...
249    L1.^2.*L3.*(z4).*(z2) + L3.*x4.^2.*(z2).^2 +...
250    L3.*(z4).^2.*(z2).^2).*(s2_1) + (0.5.*L1.^5.*(z4) + ...
           0.5.*L1.^3.*...
251    L2.^2.*(z4) - 0.5.*L1.^3.*L3.^2.*(z4) -...
252    0.5.*L1.^3.*x4.^2.*(z4) + 0.5.*L1.^3.*x4.^2.*(z2) + ...
           0.5.*L1.^3.*...
253    (z4).^3 - 3./2.*L1.^3.*(z4).^2.*(z2) -...
254    0.5.*L1.*L2.^2.*x4.^2.*(z2) - ...
           0.5.*L1.*L2.^2.*(z4).^2.*(z2) + ...
255    0.5.*L1.*L3.^2.*x4.^2.*(z2) +...
256    0.5.*L1.*L3.^2.*(z4).^2.*(z2) - 0.5.*L1.*x4.^4.*(z2) - ...
           L1.*...
257    x4.^2.*(z4).^2.*(z2) + L1.*x4.^2.*(z4).*(z2).^2 -...
258    0.5.*L1.*(z4).^4.*(z2) + ...
           L1.*(z4).^3.*(z2).^2)./(L1.^4.*L2.*...
259    L3 - L1.^2.*L2.*L3.*x4.^2 -...
260    2.*L1.^2.*L2.*L3.*(z4).*(z2) + L2.*L3.*x4.^2.*(z2).^2 + ...
           L2.*L3.*...
261    (z4).^2.*(z2).^2).*(c1_p) + (-0.5.*L1.^4.*x4.*(z4) -...
262    0.5.*L1.^4.*x4.*(z2) + 0.5.*L1.^2.*L2.^2.*x4.*(z4) - 0.5.*...
263    L1.^2.*L2.^2.*x4.*(z2) - 0.5.*L1.^2.*L3.^2.*x4.*(z4)...
264    + 0.5.*L1.^2.*L3.^2.*x4.*(z2) + 0.5.*L1.^2.*x4.^3.*(z4) + ...
           0.5.*...
265    L1.^2.*x4.^3.*(z2) + 0.5.*L1.^2.*x4.*(z4).^3 -...
266    0.5.*L1.^2.*x4.*(z4).^2.*(z2) + ...
           2.*L1.^2.*x4.*(z4).*(z2).^2 ...
267    - x4.^3.*(z2).^3 - x4.*(z4).^2.*(z2).^3)./(L1.^4.*L2.*L3 -...
268    L1.^2.*L2.*L3.*x4.^2 - 2.*L1.^2.*L2.*L3.*(z4).*(z2) + ...
           L2.*L3.*...
269    x4.^2.*(z2).^2 + L2.*L3.*(z4).^2.*(z2).^2));
```

```
s3_2 = (-1) .* ((L1.^4.*x4 - L1.^2.*x4.^3 - ...
    L1.^2.*x4.*(z4).^2)./...
    (L1.^4.*L3 - L1.^2.*L3.*x4.^2 - 2.*L1.^2.*L3.*(z4).*(z2)...
    + L3.*x4.^2.*(z2).^2 + ...
        L3.*(z4).^2.*(z2).^2).*(s2_2).*(c1_p) + ...
    (-L1.^5 + L1.^3.*x4.^2 - L1.^3.*(z4).^2 +...
    3.*L1.^3.*(z4).*(z2) + L1.*x4.^2.*(z4).*(z2) - ...
        2.*L1.*x4.^2.*...
    (z2).^2 + L1.*(z4).^3.*(z2) -...
    2.*L1.*(z4).^2.*(z2).^2)./(L1.^4.*L3 - L1.^2.*L3.*x4.^2 - ...
        2.*...
    L1.^2.*L3.*(z4).*(z2) + L3.*x4.^2.*(z2).^2 +...
    L3.*(z4).^2.*(z2).^2).*(s2_2) + (0.5.*L1.^5.*(z4) + ...
        0.5.*L1.^3.*...
    L2.^2.*(z4) - 0.5.*L1.^3.*L3.^2.*(z4) -...
    0.5.*L1.^3.*x4.^2.*(z4) + 0.5.*L1.^3.*x4.^2.*(z2) + ...
        0.5.*L1.^3.*...
    (z4).^3 - 3./2.*L1.^3.*(z4).^2.*(z2) -...
    0.5.*L1.*L2.^2.*x4.^2.*(z2) - ...
        0.5.*L1.*L2.^2.*(z4).^2.*(z2) +...
    0.5.*L1.*L3.^2.*x4.^2.*(z2) +...
    0.5.*L1.*L3.^2.*(z4).^2.*(z2) - 0.5.*L1.*x4.^4.*(z2) - ...
        L1.*...
    x4.^2.*(z4).^2.*(z2) + L1.*x4.^2.*(z4).*(z2).^2 -...
    0.5.*L1.*(z4).^4.*(z2) + ...
        L1.*(z4).^3.*(z2).^2)./(L1.^4.*L2.*L3 ...
    - L1.^2.*L2.*L3.*x4.^2 -...
    2.*L1.^2.*L2.*L3.*(z4).*(z2) + L2.*L3.*x4.^2.*(z2).^2 + ...
        L2.*L3.*...
    (z4).^2.*(z2).^2).*(c1_p) + (-0.5.*L1.^4.*x4.*(z4) -...
    0.5.*L1.^4.*x4.*(z2) + 0.5.*L1.^2.*L2.^2.*x4.*(z4) - 0.5.*...
```

```
292      L1.^2.*L2.^2.*x4.*(z2) − 0.5.*L1.^2.*L3.^2.*x4.*(z4)...
293      + 0.5.*L1.^2.*L3.^2.*x4.*(z2) + 0.5.*L1.^2.*x4.^3.*(z4) + ...
             0.5.*...
294      L1.^2.*x4.^3.*(z2) + 0.5.*L1.^2.*x4.*(z4).^3 −...
295      0.5.*L1.^2.*x4.*(z4).^2.*(z2) + ...
             2.*L1.^2.*x4.*(z4).*(z2).^2 − ...
296      x4.^3.*(z2).^3 − x4.*(z4).^2.*(z2).^3)./(L1.^4.*L2.*L3 −...
297      L1.^2.*L2.*L3.*x4.^2 − 2.*L1.^2.*L2.*L3.*(z4).*(z2) + ...
             L2.*L3.*...
298      x4.^2.*(z2).^2 + L2.*L3.*(z4).^2.*(z2).^2));

299

300      s3_3 = (−1) .* ((L1.^4.*x4 − L1.^2.*x4.^3 − ...
             L1.^2.*x4.*(z4).^2)./...
301      (L1.^4.*L3 − L1.^2.*L3.*x4.^2 − 2.*L1.^2.*L3.*(z4).*(z2)...
302      + L3.*x4.^2.*(z2).^2 + ...
             L3.*(z4).^2.*(z2).^2).*(s2_3).*(c1_n) +...
303      (−L1.^5 + L1.^3.*x4.^2 − L1.^3.*(z4).^2 +...
304      3.*L1.^3.*(z4).*(z2) + L1.*x4.^2.*(z4).*(z2) − ...
             2.*L1.*x4.^2.*...
305      (z2).^2 + L1.*(z4).^3.*(z2) −...
306      2.*L1.*(z4).^2.*(z2).^2)./(L1.^4.*L3 − L1.^2.*L3.*x4.^2 − ...
             2.*...
307      L1.^2.*L3.*(z4).*(z2) + L3.*x4.^2.*(z2).^2 +...
308      L3.*(z4).^2.*(z2).^2).*(s2_3) + (0.5.*L1.^5.*(z4) + ...
             0.5.*L1.^3.*...
309      L2.^2.*(z4) − 0.5.*L1.^3.*L3.^2.*(z4) −...
310      0.5.*L1.^3.*x4.^2.*(z4) + 0.5.*L1.^3.*x4.^2.*(z2) + ...
             0.5.*L1.^3.*...
311      (z4).^3 − 3./2.*L1.^3.*(z4).^2.*(z2) −...
312      0.5.*L1.*L2.^2.*x4.^2.*(z2) − ...
             0.5.*L1.*L2.^2.*(z4).^2.*(z2) + ...
313      0.5.*L1.*L3.^2.*x4.^2.*(z2) +...
```

```
314    0.5.*L1.*L3.^2.*(z4).^2.*(z2) − 0.5.*L1.*x4.^4.*(z2) − ...
          L1.*...
315    x4.^2.*(z4).^2.*(z2) + L1.*x4.^2.*(z4).*(z2).^2 −...
316    0.5.*L1.*(z4).^4.*(z2) + ...
          L1.*(z4).^3.*(z2).^2)./(L1.^4.*L2.*L3 −...
317    L1.^2.*L2.*L3.*x4.^2 −...
318    2.*L1.^2.*L2.*L3.*(z4).*(z2) + L2.*L3.*x4.^2.*(z2).^2 + ...
          L2.*L3.*...
319    (z4).^2.*(z2).^2).*(c1_n) + (−0.5.*L1.^4.*x4.*(z4) −...
320    0.5.*L1.^4.*x4.*(z2) + 0.5.*L1.^2.*L2.^2.*x4.*(z4) − 0.5.*...
321    L1.^2.*L2.^2.*x4.*(z2) − 0.5.*L1.^2.*L3.^2.*x4.*(z4)...
322    + 0.5.*L1.^2.*L3.^2.*x4.*(z2) + 0.5.*L1.^2.*x4.^3.*(z4) + ...
          0.5.*...
323    L1.^2.*x4.^3.*(z2) + 0.5.*L1.^2.*x4.*(z4).^3 −...
324    0.5.*L1.^2.*x4.*(z4).^2.*(z2) + ...
          2.*L1.^2.*x4.*(z4).*(z2).^2 − ...
325    x4.^3.*(z2).^3 − x4.*(z4).^2.*(z2).^3)./(L1.^4.*L2.*L3 −...
326    L1.^2.*L2.*L3.*x4.^2 − 2.*L1.^2.*L2.*L3.*(z4).*(z2) + ...
          L2.*L3.*...
327    x4.^2.*(z2).^2 + L2.*L3.*(z4).^2.*(z2).^2));
328
329    s3_4 = (−1) .* ((L1.^4.*x4 − L1.^2.*x4.^3 − ...
          L1.^2.*x4.*(z4).^2)./...
330    (L1.^4.*L3 − L1.^2.*L3.*x4.^2 − 2.*L1.^2.*L3.*(z4).*(z2)...
331    + L3.*x4.^2.*(z2).^2 + ...
          L3.*(z4).^2.*(z2).^2).*(s2_4).*(c1_n) ...
332    + (−L1.^5 + L1.^3.*x4.^2 − L1.^3.*(z4).^2 +...
333    3.*L1.^3.*(z4).*(z2) + L1.*x4.^2.*(z4).*(z2) − ...
          2.*L1.*x4.^2.*...
334    (z2).^2 + L1.*(z4).^3.*(z2) −...
335    2.*L1.*(z4).^2.*(z2).^2)./(L1.^4.*L3 − L1.^2.*L3.*x4.^2 − ...
          2.*...
```

151

```
336    L1.^2.*L3.*(z4).*(z2) + L3.*x4.^2.*(z2).^2 +...

337    L3.*(z4).^2.*(z2).^2).*(s2_4) + (0.5.*L1.^5.*(z4) + 0.5.*...

338    L1.^3.*L2.^2.*(z4) − 0.5.*L1.^3.*L3.^2.*(z4) −...

339    0.5.*L1.^3.*x4.^2.*(z4) + 0.5.*L1.^3.*x4.^2.*(z2) + ...
          0.5.*L1.^3.*...

340    (z4).^3 − 3./2.*L1.^3.*(z4).^2.*(z2) −...

341    0.5.*L1.*L2.^2.*x4.^2.*(z2) − ...
          0.5.*L1.*L2.^2.*(z4).^2.*(z2) +...

342    0.5.*L1.*L3.^2.*x4.^2.*(z2) +...

343    0.5.*L1.*L3.^2.*(z4).^2.*(z2) − 0.5.*L1.*x4.^4.*(z2) − ...
          L1.*...

344    x4.^2.*(z4).^2.*(z2) + L1.*x4.^2.*(z4).*(z2).^2 −...

345    0.5.*L1.*(z4).^4.*(z2) + L1.*(z4).^3.*(z2).^2)./(L1.^4.*...

346    L2.*L3 − L1.^2.*L2.*L3.*x4.^2 −...

347    2.*L1.^2.*L2.*L3.*(z4).*(z2) + L2.*L3.*x4.^2.*(z2).^2 + ...
          L2.*...

348    L3.*(z4).^2.*(z2).^2).*(c1_n) + (−0.5.*L1.^4.*x4.*(z4) −...

349    0.5.*L1.^4.*x4.*(z2) + 0.5.*L1.^2.*L2.^2.*x4.*(z4) − 0.5.*...

350    L1.^2.*L2.^2.*x4.*(z2) − 0.5.*L1.^2.*L3.^2.*x4.*(z4)...

351    + 0.5.*L1.^2.*L3.^2.*x4.*(z2) + 0.5.*L1.^2.*x4.^3.*(z4) + ...
          0.5.*...

352    L1.^2.*x4.^3.*(z2) + 0.5.*L1.^2.*x4.*(z4).^3 −...

353    0.5.*L1.^2.*x4.*(z4).^2.*(z2) + ...
          2.*L1.^2.*x4.*(z4).*(z2).^2 − ...

354    x4.^3.*(z2).^3 − x4.*(z4).^2.*(z2).^3)./(L1.^4.*L2.*L3 −...

355    L1.^2.*L2.*L3.*x4.^2 − 2.*L1.^2.*L2.*L3.*(z4).*(z2) + ...
          L2.*L3.*...

356    x4.^2.*(z2).^2 + L2.*L3.*(z4).^2.*(z2).^2));

357

358    s3_1 = abs(s3_1);

359    s3_2 = abs(s3_2);

360    s3_3 = abs(s3_3);
```

152

```matlab
s3_4 = abs(s3_4);


%Using equation 3 to find c2
c2_1 = (-1) .* ((-L1.^3.*z4 + L1.*x4.^2.*(z2) + ...
    L1.*z4.^2.*(z2))./...
    (L1.^4 - L1.^2.*x4.^2 - 2.*L1.^2.*z4.*(z2) + ...
        x4.^2.*(z2).^2 ...
    +z4.^2.*(z2).^2).*(s2_1).*(c1_p) + (-L1.^2.*x4.*z4 + ...
        L1.^2.*x4.*...
    (z2))./(L1.^4 - L1.^2.*x4.^2 - 2.*L1.^2.*z4.*(z2)...
    + x4.^2.*(z2).^2 + z4.^2.*(z2).^2).*(s2_1) + ...
        (-0.5.*L1.^4.*...
    x4 + 0.5.*L1.^2.*L2.^2.*x4 -...
    0.5.*L1.^2.*L3.^2.*x4 + 0.5.*L1.^2.*x4.^3 + ...
        0.5.*L1.^2.*x4.*...
    z4.^2)./(L1.^4.*L2 - L1.^2.*L2.*x4.^2 ...
    - 2.*L1.^2.*L2.*z4.*(z2) + L2.*x4.^2.*(z2).^2 + ...
        L2.*z4.^2.*...
    (z2).^2).*(c1_p) + (0.5.*L1.^5 +...
    0.5.*L1.^3.*L2.^2 - 0.5.*L1.^3.*L3.^2 - 0.5.*L1.^3.*x4.^2 ...
        +...
    0.5.*L1.^3.*z4.^2 -...
    3./2.*L1.^3.*z4.*(z2) - 0.5.*L1.*L2.^2.*z4.*(z2) + ...
        0.5.*L1.*...
    L3.^2.*z4.*(z2) - 0.5.*L1.*x4.^2.*z4.*(z2) +...
    L1.*x4.^2.*(z2).^2 - 0.5.*L1.*z4.^3.*(z2) + L1.*z4.^2.*...
    (z2).^2)./(L1.^4.*L2 - L1.^2.*L2.*x4.^2 -...
    2.*L1.^2.*L2.*z4.*(z2) + L2.*x4.^2.*(z2).^2 + ...
        L2.*z4.^2.*(z2).^2));


c2_2 = (-1) .* ((-L1.^3.*z4 + L1.*x4.^2.*(z2) + ...
    L1.*z4.^2.*(z2))./...
```

```
383        (L1.^4 − L1.^2.*x4.^2 − 2.*L1.^2.*z4.*(z2) + ...
               x4.^2.*(z2).^2 ...

384        + z4.^2.*(z2).^2).*(s2_2).*(c1_p) + (−L1.^2.*x4.*z4 + ...
               L1.^2.*...

385        x4.*(z2))./(L1.^4 − L1.^2.*x4.^2 − 2.*L1.^2.*z4.*(z2)...

386        + x4.^2.*(z2).^2 + z4.^2.*(z2).^2).*(s2_2) + ...
               (−0.5.*L1.^4.*x4...

387        + 0.5.*L1.^2.*L2.^2.*x4 −...

388        0.5.*L1.^2.*L3.^2.*x4 + 0.5.*L1.^2.*x4.^3 + ...
               0.5.*L1.^2.*x4.*...

389        z4.^2)./(L1.^4.*L2 − L1.^2.*L2.*x4.^2 ...

390        − 2.*L1.^2.*L2.*z4.*(z2) + L2.*x4.^2.*(z2).^2 + ...
               L2.*z4.^2.*...

391        (z2).^2).*(c1_p) + (0.5.*L1.^5 +...

392        0.5.*L1.^3.*L2.^2 − 0.5.*L1.^3.*L3.^2 − 0.5.*L1.^3.*x4.^2 ...
               +...

393        0.5.*L1.^3.*z4.^2 −...

394        3./2.*L1.^3.*z4.*(z2) − 0.5.*L1.*L2.^2.*z4.*(z2) + ...
               0.5.*L1.*...

395        L3.^2.*z4.*(z2) − 0.5.*L1.*x4.^2.*z4.*(z2) +...

396        L1.*x4.^2.*(z2).^2 − 0.5.*L1.*z4.^3.*(z2) + ...
               L1.*z4.^2.*(z2).^...

397        2)./(L1.^4.*L2 − L1.^2.*L2.*x4.^2 −...

398        2.*L1.^2.*L2.*z4.*(z2) + L2.*x4.^2.*(z2).^2 + ...
               L2.*z4.^2.*(z2).^2));

399

400    c2_3 = (−1) .* ((−L1.^3.*z4 + L1.*x4.^2.*(z2) + ...
               L1.*z4.^2.*(z2))./...

401        (L1.^4 − L1.^2.*x4.^2 − 2.*L1.^2.*z4.*(z2) + ...
               x4.^2.*(z2).^2 ...

402        + z4.^2.*(z2).^2).*(s2_3).*(c1_n) + (−L1.^2.*x4.*z4 + ...
               L1.^2.*...
```

```
403    x4.*(z2))./(L1.^4 − L1.^2.*x4.^2 − 2.*L1.^2.*z4.*(z2)...

404    + x4.^2.*(z2).^2 + z4.^2.*(z2).^2).*(s2_3) + ...

           (−0.5.*L1.^4.*x4 ...

405    + 0.5.*L1.^2.*L2.^2.*x4 −...

406    0.5.*L1.^2.*L3.^2.*x4 + 0.5.*L1.^2.*x4.^3 + ...

           0.5.*L1.^2.*x4.*...

407    z4.^2)./(L1.^4.*L2 − L1.^2.*L2.*x4.^2 ...

408    − 2.*L1.^2.*L2.*z4.*(z2) + L2.*x4.^2.*(z2).^2 + ...

           L2.*z4.^2.*...

409    (z2).^2).*(c1_n) + (0.5.*L1.^5 +...

410    0.5.*L1.^3.*L2.^2 − 0.5.*L1.^3.*L3.^2 − 0.5.*L1.^3.*x4.^2 ...

           + ...

411    0.5.*L1.^3.*z4.^2 −...

412    3./2.*L1.^3.*z4.*(z2) − 0.5.*L1.*L2.^2.*z4.*(z2) + ...

           0.5.*L1.*...

413    L3.^2.*z4.*(z2) − 0.5.*L1.*x4.^2.*z4.*(z2) +...

414    L1.*x4.^2.*(z2).^2 − 0.5.*L1.*z4.^3.*(z2) + L1.*z4.^2.*...

415    (z2).^2)./(L1.^4.*L2 − L1.^2.*L2.*x4.^2 −...

416    2.*L1.^2.*L2.*z4.*(z2) + L2.*x4.^2.*(z2).^2 + ...

           L2.*z4.^2.*(z2).^2));


417

418    c2_4 = (−1) .* ((−L1.^3.*z4 + L1.*x4.^2.*(z2) + ...

           L1.*z4.^2.*(z2))./...

419    (L1.^4 − L1.^2.*x4.^2 − 2.*L1.^2.*z4.*(z2) + ...

           x4.^2.*(z2).^2 ...

420    + z4.^2.*(z2).^2).*(s2_4).*(c1_n) + (−L1.^2.*x4.*z4 + ...

           L1.^2.*...

421    x4.*(z2))./(L1.^4 − L1.^2.*x4.^2 − 2.*L1.^2.*z4.*(z2)...

422    + x4.^2.*(z2).^2 + z4.^2.*(z2).^2).*(s2_4) + ...

           (−0.5.*L1.^4.*...

423    x4 + 0.5.*L1.^2.*L2.^2.*x4 −...
```

```matlab
424          0.5.*L1.^2.*L3.^2.*x4 + 0.5.*L1.^2.*x4.^3 + ...
                 0.5.*L1.^2.*x4.*...
425          z4.^2)./(L1.^4.*L2 − L1.^2.*L2.*x4.^2 ...
426          − 2.*L1.^2.*L2.*z4.*(z2) + L2.*x4.^2.*(z2).^2 + ...
                 L2.*z4.^2.*...
427          (z2).^2).*(c1_n) + (0.5.*L1.^5 +...
428          0.5.*L1.^3.*L2.^2 − 0.5.*L1.^3.*L3.^2 − 0.5.*L1.^3.*x4.^2 ...
                 +...
429          0.5.*L1.^3.*z4.^2 −...
430          3./2.*L1.^3.*z4.*(z2) − 0.5.*L1.*L2.^2.*z4.*(z2) + ...
                 0.5.*L1.*...
431          L3.^2.*z4.*(z2) − 0.5.*L1.*x4.^2.*z4.*(z2) +...
432          L1.*x4.^2.*(z2).^2 − 0.5.*L1.*z4.^3.*(z2) + L1.*z4.^2.*...
433          (z2).^2)./(L1.^4.*L2 − L1.^2.*L2.*x4.^2 −...
434          2.*L1.^2.*L2.*z4.*(z2) + L2.*x4.^2.*(z2).^2 + ...
                 L2.*z4.^2.*(z2).^2));

435

436

437      %Now that I have obtained the values for all ...
                 sin[theta1,theta2,theta3]
438      %and cos[theta1,theta2,theta3], lets take inverse of those ...
                 values to
439      %get the angles
440      %note: c1p, c1p, c1n, c1n

441

442  theta1_1 = (atan(s1./c1_p)).*(180./pi);
443  theta1_3 = (−1).*(atan(s1./c1_n)).*(180./pi);
444  theta2_1 = (atan(s2_1./c2_1)).*(180./pi);
445  theta2_2 = (−1).*(atan(s2_2./c2_2)).*(180./pi);
446  theta2_3 = (atan(s2_3./c2_3)).*(180./pi);
447  theta2_4 = (atan(s2_4./c2_4)).*(180./pi);
448  theta3_1 = ((atan(s3_1./c3_p)).*(180./pi));
```

```matlab
449  theta3_2 = ((atan(s3_2./c3_p)).*(180./pi));

450  theta3_2 = (-1).*(90-abs(theta3_2));

451  theta3_3 = ((atan(s3_3./c3_n)).*(180./pi));

452  theta3_4 = ((atan(s3_4./c3_n)).*(180./pi));

453  headers1 = {'theta1_1','theta2_2','theta3_2'};

454  data1 = [theta1_1,theta2_2,theta3_2];

455  xlswrite(['Predicted Angles' num2str(csv_file_number) ...
         '.xls'],headers1);

456  xlswrite(['Predicted Angles' num2str(csv_file_number) '.xls'],data1);
```

Bibliography

1. Gait analysis marker set. Unpublished manuscript

2. Iraq body count. Retrieved 02/04, 2013, from http://www.iraqbodycount.org/database/

3. Lower-limb orthotics. new york, ny, new york university postgraduate medical school, prosthetics and orthotics, 1981.

4. Normal and pathological gait syllabus. downey, ca, professional staff association of rancho los amigos hospital inc, 1978.

5. Pirates & revolutionaries: The sympathy of sensation: Rhythm and body in merleau-ponty and deleuze.

6. Plug in gait. From http://wweb.uta.edu/faculty/ricard/Classes/KINE-5350/PIGManualver1.pdf

7. Vicon motion capture systems. Retrieved 03/06, from www.vicon.com

8. Pro-form, 2013. from http://www.proform.com

9. Shelley Bampton. *A guide to the visual examination of pathological gait.* Temple University, Rehabilitation Research and Training Center, 1979.

10. J Bobet and RW Norman. Effects of load placement on back muscle activity in load carriage. *European journal of applied physiology and occupational physiology*, 53(1):71–75, 1984.

11. Christoph C. Borel, David J. Bunker, Ronald F. Tuttle, Anum Barki, and G. Charmaine Gilbreath. Multimodal gait signatures and motion studies. In *Proceedings of the 2012 Military Sensing Symposia (MSS) Specialty Group On BAMS*, 2012.

12. N. A. Borghese, L. Bianchi, and F. Lacquaniti. Kinematic determinants of human locomotion. *The Journal of physiology*, 494(Pt 3):863–879, 1996.

13. Bruno Buchberger. Gröbner bases: A short introduction for systems theorists. *Computer Aided Systems TheoryEUROCAST 2001*, pages 1–19, 2001.

14. S. R. Buss. Introduction to inverse kinematics with jacobian transpose, pseudoinverse and damped least squares methods. *University of California, San Diego, Typeset manuscript, available from http://math.ucsd.edu/ sbuss/ResearchWeb*, 2004.

15. Emine Can. Normal gait cycle, 2007. Unpublished manuscript

16. Sara Cuccurullo. *Physical medicine and rehabilitation board review.* Demos Medical Publishing, 2004.

17. Hubert de Bruin, Dianne J. Russell, John E. Latter, and JT Sadler. Angle-angle diagrams in monitoring and quantification of gait patterns for children with cerebral palsy. *American Journal of Physical Medicine*, 61(4):176, 1982.

18. Wikipedia Foundation. Inverse kinematics, 2013. Unpublished manuscript

19. G MU Ghori and RG Luckwill. Responses of the lower limb to load carrying in walking man. *European journal of applied physiology and occupational physiology*, 54(2):145–150, 1985.

20. G. H. Golub and C. Reinsch. Singular value decomposition and least squares solutions. *Numerische Mathematik*, 14(5):403–420, 1970.

21. Robert Goodkin and Leonard Diller. Reliability among physical therapists in diagnosis and treatment of gait deviations in hemiplegics. *Perceptual and motor skills*, 37(3):727–734, 1973.

22. Ralph Gross and Jianbo Shi. The cmu motion of body (mobo) database, 2001.

23. Susan J. Hall. *Basic biomechanics*. McGraw-Hill, New York, NY, 2012. ID: 436028191.

24. M. H. R. Hicks, H. Dardagan, P. M. Bagnall, M. Spagat, and J. A. Sloboda. Casualties in civilians and coalition soldiers from suicide bombings in iraq, 200310: a descriptive study. *The Lancet*, 378(9794):906–914, 2011.

25. G. Greneker III. Very low cost stand-off suicide bomber detection system using human gait analysis to screen potential bomb carrying individuals. In *Defense and Security*, pages 46–56. International Society for Optics and Photonics, 2005.

26. T. Isobe, K. Nagasaka, and S. Yamamoto. A new approach to kinematic control of simple manipulators. *Systems, Man and Cybernetics, IEEE Transactions on*, 22(5):1116–1124, 1992. ID: 1.

27. MP Kadaba, HK Ramakrishnan, ME Wootten, J. Gainey, G. Gorton, and GVB Cochran. Repeatability of kinematic, kinetic, and electromyographic data in normal adult gait. *Journal of Orthopaedic Research*, 7(6):849–860, 2005.

28. Kimberly Kendricks. Solving the inverse kinematic robotics problem: A comparison study of the denavit-hartenberg matrix and groebner basis theory, 2007.

29. Kimberly D. Kendricks, Adam M. Fullenkamp, Robert McGrellis, Jonathan Juhl, and Ronald F. Tuttle. An inverse kinematic mathematical model using groebner basis theory for arm swing movement in the gait cycle, 2010.

30. Kimberly D. Kendricks, Anthony Taylor, and Ronald F. Tuttle. Predicting shoulder flexion and extension angles over a complete gait cycle using measured kinematics. *Journal of Biomechanics*.

31. H. Kinoshita. Effects of different loads and carrying systems on selected biomechanical parameters describing walking gait. *Ergonomics*, 28(9):1347–1362, 1985.

32. Joseph Knapik, Everett Harman, and Katy Reynolds. Load carriage using packs: A review of physiological, biomechanical and medical aspects. *Applied Ergonomics*, 27(3):207–216, 1996.

33. D. E. Krebs, J. E. Edelstein, and S. Fishman. Reliability of observational kinematic gait analysis. *Physical Therapy*, 65(7):1027–1033, 1985.

34. American Academy of Orthopaedic Surgeons. Joint motion: Methods of measuring and recording, 1965.

35. University of South Florida. Baseline algorithm and performance for gait based human id challenge problem, 2004.

36. P. O. Riley, G. Paolini, U. Della Croce, K. W. Paylo, and D. C. Kerrigan. A kinematic and kinetic comparison of overground and treadmill walking in healthy subjects. *Gait and posture*, 26(1):17–24, 2007.

37. Greece Samos. Introduction to grobner bases.

38. Tim Sell. Vicon nesus, 2011.

39. Douglas G. Smith, John W. Michael, and John H. Bowker. *Atlas of Amputations and Limb Deficiencies - Surgical, Prosthetic, and Rehabilitation Principles.* American Academy of Orthopaedic Surgeons, Rosemont, IL, 3 edition, 2004.

40. Anthony Taylor. Motion in matlab. *Central State University's Undergraduate Research Journal*, 2011.

41. D. C. Tilbury-Davis and R. H. Hooper. The kinetic and kinematic effects of increasing load carriage upon the lower limb. *Human Movement Science*, 18(5):693–700, 1999.

42. Deepak Tolani, Ambarish Goswami, and Norman I. Badler. Real-time inverse kinematics techniques for anthropomorphic limbs. *Graphical Models*, 62(5):353–388, 9 2000.

43. C. W. Wampler. Manipulator inverse kinematic solutions based on vector formulations and damped least-squares methods. *Systems, Man and Cybernetics, IEEE Transactions on*, 16(1):93–101, 1986.

44. L. C T. Wang and C. C. Chen. A combined optimization method for solving the inverse kinematics problems of mechanical manipulators. *Robotics and Automation, IEEE Transactions on*, 7(4):489–499, 1991. ID: 1.

45. J. R. Watt, J. R. Franz, K. Jackson, J. Dicharry, P. O. Riley, and D. C. Kerrigan. A three-dimensional kinematic and kinetic comparison of overground and treadmill walking in healthy elderly subjects. *Clinical Biomechanics*, 25(5):444–449, 2010.

46. M. Wenz and H. Worn. Solving the inverse kinematics problem symbolically by means of knowledge-based and linear algebra-based methods. In *Emerging Technologies and Factory Automation, 2007. ETFA. IEEE Conference on*, pages 1346–1353, 2007. ID: 1.

47. Daniel E. Whitney. Resolved motion rate control of manipulators and human prostheses. *Man-Machine Systems, IEEE Transactions on*, 10(2):47–53, 1969.

48. M. G. Wittman, J. M. Ward, and P. J. Flynn. Visual analysis of the effects of load carriage on gait. In *Defense and Security*, pages 15–22. International Society for Optics and Photonics, 2005.

49. A. K. Yegian. The roles of muscles in arm swing and thoracic rotation during walking. 2012.

50. Rong Zhang, Christian Vogler, and Dimitris Metaxas. Human gait recognition at sagittal plane. *Image and Vision Computing*, 25(3):321–330, 3 2007.

Vita

Anum Barki was born in Lahore, Pakistan which is located in the province of Punjab. She moved to the United States with her parents and her brother at the age of ten. After graduating from Beavercreek High School in 2006, she studied Biomedical Engineering at Wright State University in Ohio. While she was a senior in college, she obtained a research assistant position at the Air Force Instititue of Technology (AFIT) at Wright Patterson Air Force Base. She graduated with a Bachelor of Science Degree in Biomedical Engineering - Pre Medicine Track in June 2011. During the following months, she continued on to pursue her higher education at AFIT in the Graduate Optical Science and Engineering program to obtain a Master's Degree with a strong interest in remote sensing.

REPORT DOCUMENTATION PAGE

1. REPORT DATE *(DD–MM–YYYY)*	2. REPORT TYPE	3. DATES COVERED *(From — To)*
21–03–2013	Master's Thesis	Oct 2011 — Mar 2013

4. TITLE AND SUBTITLE

An Inverse Kinematic Approach Using Groebner Basis Theory Applied to Gait Cycle Analysis

5a. CONTRACT NUMBER

MIPR N0017312MP00112

5b. GRANT NUMBER

5c. PROGRAM ELEMENT NUMBER

6. AUTHOR(S)

Barki, Anum

5d. PROJECT NUMBER

5e. TASK NUMBER

5f. WORK UNIT NUMBER

7. PERFORMING ORGANIZATION NAME(S) AND ADDRESS(ES)

Air Force Institute of Technology
Graduate School of Engineering and Management (AFIT/EN)
2950 Hobson Way
WPAFB OH 45433-7765

8. PERFORMING ORGANIZATION REPORT NUMBER

AFIT-ENP-13-M-02

9. SPONSORING / MONITORING AGENCY NAME(S) AND ADDRESS(ES)

Dr. Charmaine Gilbreath
Naval Research Laboratory
4555 Overlook Ave., SW
Washington, DC 20375-5320

10. SPONSOR/MONITOR'S ACRONYM(S)

NRL

11. SPONSOR/MONITOR'S REPORT NUMBER(S)

12. DISTRIBUTION / AVAILABILITY STATEMENT

APPROVED FOR PUBLIC RELEASE; DISTRIBUTION UNLIMITED.

13. SUPPLEMENTARY NOTES

14. ABSTRACT   Kinematics of the human body was researched for the purposes of this study. The force protection issues of today was the motivation to research pattern recognition in the human gait cycle to identify individuals carrying a concealed load on their body. The goal of this research was to identify gait signatures of human subjects and distinguish between subjects carrying a concealed load to subjects without load. Thus, this research was focused on studying the human gait cycle as well as methods used in identifying gait signatures. The main focus hearin is concerned with the movement of the lower extremities, in particular, the placement of the foot and how the joint angles are affected with carrying extra load on the body. A method of Inverse Kinematics (IK) using Groebner Basis (GB) Theory is developed to a model of the lower extremities to determine all the solutions of the joint angles, given the position and orientation of the foot. The human gait cycle was captured and analyzed using an VICON Motion capture system. This research highlights the results obtained from applying the method of IK, using GB, to the lower limbs of a human gait cycle to extract and identify gait signatures.

15. SUBJECT TERMS

Gait Analysis, Groebner Basis, Inverse Kinematics, Lower extremity joints angles, Load influenced gait, Vicon Motion Capture gait, Biometrics, Sagittal plan lower extremity motion, Treadmil influenced gait

16. SECURITY CLASSIFICATION OF:			17. LIMITATION OF ABSTRACT	18. NUMBER OF PAGES	19a. NAME OF RESPONSIBLE PERSON
a. REPORT	b. ABSTRACT	c. THIS PAGE			Dr. Ronald F. Tuttle, AFIT/ENP
U	U	U	U	176	19b. TELEPHONE NUMBER *(include area code)* (937) 255-6565, x4536; ronald.tuttle@afit.edu